Universidade Estadual de Campinas
Faculdade de Engenharia Elétrica e de Computação

Rodrigo Mologni Gonçalves dos Santos

Contribuições ao Planejamento Virtual Tridimensional de Cirurgia Ortognática

Campinas
2018

Rodrigo Mologni Gonçalves dos Santos

Contribuições ao Planejamento Virtual Tridimensional de Cirurgia Ortognática

Tese de doutorado apresentada ao Programa de Pós-Graduação em Engenharia Elétrica da Faculdade de Engenharia Elétrica e de Computação da Universidade Estadual de Campinas, como parte dos requisitos exigidos para a obtenção do título de Doutor em Engenharia Elétrica, na área de Engenharia de Computação.

Orientação de
Prof. Dr. José Mario De Martino

Coorientação de
Prof. Dr. Luis Augusto Passeri

Este exemplar corresponde à versão final da tese defendida pelo aluno
Rodrigo Mologni Gonçalves dos Santos e orientada pelo Prof. Dr. José Mario De Martino.

Campinas
2018

Agência(s) de fomento e nº(s) de processo(s): CAPES
ORCID: http://orcid.org/0000-0002-7006-1621

Ficha catalográfica
Universidade Estadual de Campinas
Biblioteca da Área de Engenharia e Arquitetura
Luciana Pietrosanto Milla - CRB 8/8129

Sa59c

Santos, Rodrigo Mologni Gonçalves, 1985-
Contribuições ao planejamento virtual tridimensional de cirurgia ortognática / Rodrigo Mologni Gonçalves dos Santos. – Campinas, SP : [s.n.], 2018.

Orientador: José Mario De Martino.
Coorientador: Luis Augusto Passeri.
Tese (doutorado) – Universidade Estadual de Campinas, Faculdade de Engenharia Elétrica e de Computação.

1. Cirurgia ortognática. 2. Cefalometria. 3. Computação gráfica. 4. Automação. I. De Martino, José Mario, 1958-. II. Passeri, Luis Augusto, 1957-. III. Universidade Estadual de Campinas. Faculdade de Engenharia Elétrica e de Computação. IV. Título.

Informações para Biblioteca Digital

Título em outro idioma: Contributions to the three-dimensional virtual treatment planning of orthognathic surgery
Palavras-chave em inglês:
Orthognathic surgery
Cephalometry
Computer graphics
Automation
Área de concentração: Engenharia de Computação
Titulação: Doutor em Engenharia Elétrica
Banca examinadora:
José Mario De Martino [Orientador]
Carla Maria Dal Sasso Freitas
Guilherme Cardinali Barreiro
Léo Pini Magalhães
Mário Francisco Real Gabrielli
Data de defesa: 20-02-2018
Programa de Pós-Graduação: Engenharia Elétrica

COMISSÃO JULGADORA - TESE DE DOUTORADO

Canditato: Rodrigo Mologni Gonçalves dos Santos RA: 046327
Data da Defesa: 20 de fevereiro de 2018

Título da Tese: “Contribuições ao Planejamento Virtual Tridimensional de Cirurgia Ortognática”.

Prof. Dr. José Mario De Martino (Presidente, FEEC/UNICAMP)
Prof.ª Dr.ª Carla Maria Dal Sasso Freitas (INF/UFRGS)
Prof. Dr. Guilherme Cardinali Barreiro (FCM/UNICAMP)
Prof. Dr. Léo Pini Magalhães (FEEC/UNICAMP)
Prof. Dr. Mário Francisco Real Gabrielli (FOAr/UNESP)

A ata de defesa, com as respectivas assinaturas dos membros da Comissão Julgadora, encontra-se no processo de vida acadêmica do aluno.

Esta tese é dedicada à minha mãe, Zilda Mologni, pois sem seu apoio, hoje eu certamente não estaria me tornando um doutor.

Agradecimentos

Ao *Prof. Dr. José Mario De Martino* e ao *Prof. Dr. Luis Augusto Passeri*, docente da Faculdade de Ciências Médicas, pelas orientações, disponibilidade, dedicação e contribuições significativas no desenvolvimento deste trabalho de doutorado.

Ao *Prof. Dr. Francisco Haiter Neto*, docente da Faculdade de Odontologia de Piracicaba, pelo acesso à base de imagens de tomografia computadorizada da Área de Radiologia Odontológica desta faculdade, sem a qual não teria sido possível desenvolver o trabalho apresentado nesta tese; e pelas contribuições nos artigos científicos publicados.

Ao *Prof. Dr. Romis Ribeiro de Faissol Attux*, docente da Faculdade de Engenharia Elétrica e de Computação, pelos ensinamentos em Otimização Evolutiva Multiobjetivo e pela contribuição em um dos artigos científicos publicados.

À *Prof.ª Dr.ª Paula Dornhofer Paro Costa*, docente da Faculdade de Engenharia Elétrica e de Computação, pelos ensinamentos em Métodos Estatísticos e Análise de Dados.

À *Coordenação de Aperfeiçoamento de Pessoal de Nível Superior* pela bolsa de doutorado concedida, sem a qual eu não poderia ter me dedicado integralmente aos estudos.

À *Faculdade de Engenharia Elétrica e de Computação* e ao *Departamento de Engenharia de Computação e Automação Industrial*, desta mesma faculdade, pela infraestrutura disponibilizada.

Resumo

A tecnologia mais recente à disposição da Cirurgia Ortognática possibilita que o diagnóstico e o planejamento do tratamento das deformidades dentofaciais sejam realizados sob uma representação virtual tridimensional (3D) da cabeça do paciente. Com o propósito de contribuir para o aperfeiçoamento desta tecnologia, o trabalho apresentado nesta tese identificou e tratou quatro problemas. A primeira contribuição consistiu na verificação da validade da hipótese de que a mudança de definição do plano horizontal de Frankfort não produz diferenças de medição clinicamente relevantes quando sob indivíduos cujos crânios são consideravelmente simétricos. Os resultados da análise realizada no contexto deste tese indicam que, ao contrário do que se presumia, a hipótese é falsa. A segunda contribuição consistiu na extensão do método de análise cefalométrica de McNamara para que ele pudesse produzir valores 3D. Ao contrário de outros métodos de análise cefalométrica 3D, a extensão criada produz valores verdadeiramente 3D, não perde as informações do método original e preserva as definições geométricas originais das linhas e planos cefalométricos. A terceira contribuição consistiu *a*) no estabelecimento de normas cefalométricas para brasileiros adultos de ascendência europeia, a partir de imagens de tomografia computadorizada de feixe cônico, que produz uma imagem craniofacial mais precisa e confiável do que a telerradiografia; e *b*) na avaliação de dimorfismo sexual, para a identificação de características anatômicas diferenciadas entre homens e mulheres desta população. A quarta e última contribuição consistiu na automatização da principal etapa da tecnologia em questão, na qual o cirurgião executa o reposicionamento dos segmentos ósseos maxilares no crânio. O método criado é capaz de corrigir automaticamente os problemas dentofaciais mais comuns tratados pela Cirurgia Ortognática, que envolvem maloclusão esquelética, assimetria facial e discrepância de maxilares. Todas as contribuições deste trabalho foram publicadas em periódicos internacionais do campo da Odontologia e afins.

Abstract

The latest technology available for orthognathic surgery allows the diagnosis and treatment planning of dentofacial deformities based on a three-dimensional (3D) virtual representation of the patient's head. In order to contribute to the improvement of this technology, the work presented in this thesis identified and treated four problems. The first contribution consisted in testing the validity of the hypothesis that changing the definition of the Frankfort horizontal plane does not produce clinically relevant measurement differences for subjects whose skulls are considerably symmetrical. The results of the analysis performed in this thesis indicate that, contrary to what was presumed, the hypothesis is false. The second contribution is an extension of the McNamara's method of cephalometric analysis to produce 3D values. Unlike other methods of 3D cephalometric analysis, the extension produces true 3D values, does not lose information captured by the original method, and preserves the original geometric definitions of the cephalometric lines and planes. The third contribution consisted in a) establishing cephalometric norms for Brazilian adults of European descent, based on images from cone-beam computed tomography, which produce a more accurate and reliable craniofacial image than cephalometric radiography; and b) evaluating sexual dimorphism, for the identification of distinct anatomic features between males and females of this population. The fourth contribution consisted in automating the main stage of the technology in question, in which the surgeon performs the positioning of jaw bone segments in the skull. The created method is able to automatically correct the most common dentofacial problems treated by orthognathic surgery, which involves skeletal malocclusion, facial asymmetry, and jaw discrepancy. The contributions of this work were published in international journals of the field of Dentistry and related.

Sumário

Capítulo 1

Introdução

A Cirurgia Ortognática é o ramo da Cirurgia e Traumatologia Bucomaxilofacial que trata as deformidades dentofaciais que não são passíveis de correção apenas pela Ortodontia ou Ortopedia Funcional dos Maxilares, pois dependem do reposicionamento ósseo dos maxilares no crânio (PROFFIT; R. P. WHITE; SARVER, 2003). Ela é formada por um conjunto de técnicas de osteotomias executadas no sistema mastigatório, com o propósito de restabelecer o equilíbrio entre o crânio e a face e, por conseguinte, beneficiar a estética facial e as funções mastigatória, fonatória, respiratória e da articulação temporomandibular (ver Figura 1.1).

A preparação da Cirurgia Ortognática é um procedimento artesanal e trabalhoso, baseado em diagnóstico e planejamento de tratamento considerando a documentação ortodôntica do paciente, que contém pelo menos uma telerradiografia em norma lateral, uma radiografia panorâmica, fotografias intrabucais e extrabucais, e um modelo de gesso das arcadas dentárias (ver Figura 1.3). A tecnologia mais recente à disposição da Cirurgia Ortognática — conhecida como planejamento virtual tridimensional (3D) de cirurgia ortognática (SWENNEN; SCHUTYSER, 2007; SWENNEN; MOLLEMANS; SCHUTYSER, 2009; CEVIDANES; TUCKER et al., 2010; POPAT; RICHMOND, 2010; CEVIDANES; STYNER et al., 2013; EDWARDS; CONLEY, 2014) — possibilita que o diagnóstico e o planejamento do tratamento sejam realizados em ambiente virtual, explorando as vantagens do computador e fazendo uso de uma representação 3D da cabeça do paciente, fidedigna à real (ver Figura 1.2).

Devido aos inúmeros benefícios propiciados pelo planejamento virtual 3D de cirurgia ortognática, as perspectivas indicam que no futuro esta tecnologia substituirá o planejamento convencional da Cirurgia Ortognática. Acreditando no seu potencial, esta tese de doutorado busca contribuir para o aprimoramento desta tecnologia e difusão efetiva do seu uso.

Figura 1.1. Antes e depois de uma paciente tratada pela Cirurgia Ortognática. Fotografia adquirida de http://www.drantipov.com/ (30 jan. 2018).

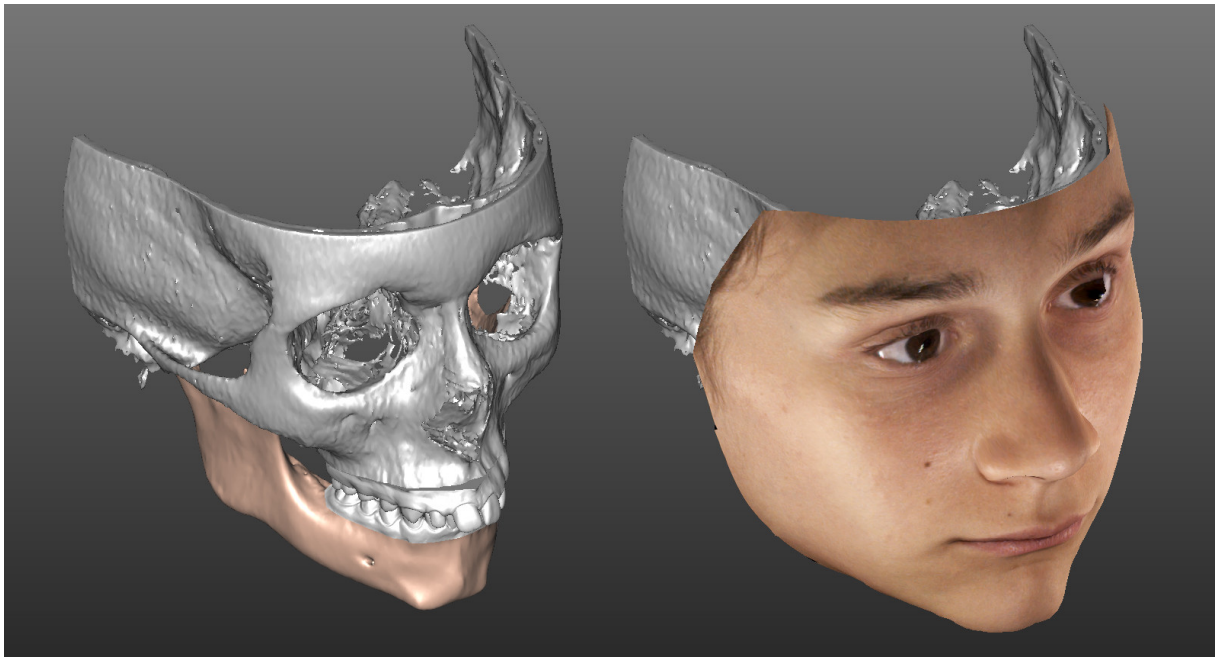

Figura 1.2. Exemplo de cabeça virtual usada no planejamento virtual 3D de cirurgia ortognática. Imagem adquirida de Santos, De Martino, Passeri et al. (2017).

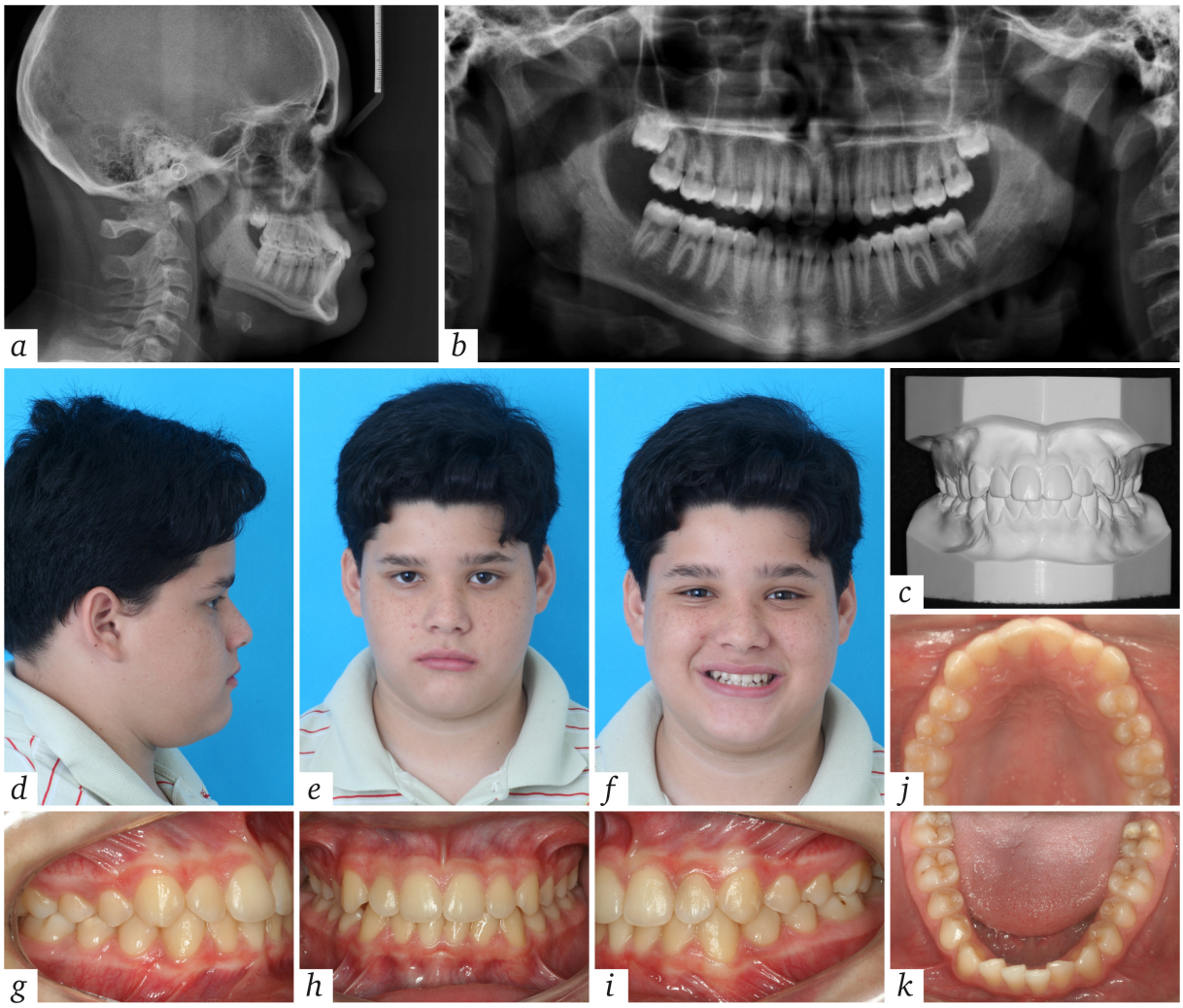

Figura 1.3. Exemplo de documentação ortodôntica: *a*) telerradiografia em norma lateral; *b*) radiografia panorâmica; *c*) modelos de gesso das arcadas dentárias superior e inferior; *d–f*) fotografias extrabucais de perfil, frontal e frontal com sorriso; *g–k*) fotografias intrabucais lateral direita, frontal, lateral esquerda, oclusal superior e oclusal inferior. Fotografias adquiridas de http://www.faceimagem.com.br/ e http://www.radimagemdigital.com.br/ (11 dez. 2016).

1.1 Visão Geral

No planejamento virtual 3D de cirurgia ortognática são realizadas, em geral, as seguintes etapas (SWENNEN; SCHUTYSER, 2007; SWENNEN; MOLLEMANS; SCHUTYSER, 2009; CEVIDANES; TUCKER et al., 2010; POPAT; RICHMOND, 2010; CEVIDANES; STYNER et al., 2013; EDWARDS; CONLEY, 2014):

Reconstrução da cabeça do paciente. Cria-se a representação virtual 3D da cabeça do paciente, constituída por modelos geométricos das superfícies de seu crânio, de suas arcadas dentárias e de sua face. O modelo do crânio é criado a partir de imagens craniofaciais adquiridas por tomografia computadorizada de feixe cônico (TCFC). Os modelos das arcadas dentárias e do rosto também podem ser produzidos a partir destas mesmas imagens. Contudo, por questões de maior precisão e realismo, outras tecnologias são eventualmente utilizadas neste processo, como dispositivos de escaneamento 3D a laser e fotogrametria.

Reorientação da cabeça. Reorienta-se a cabeça virtual do paciente no espaço 3D para que ela fique na posição padrão da Cefalometria (detalhada adiante). A reorientação é feita girando-se a cabeça ou, preferencialmente, criando-se um sistema de coordenadas Cartesiano 3D a partir do plano horizontal de Frankfort — que cruza o ponto mais inferior sobre a margem da órbita (orbital) e o ponto mais superior do meato acústico externo (pório) — e do plano sagital mediano — que é perpendicular ao plano anterior e divide a cabeça em duas metades consideravelmente simétricas. Estes dois planos definem a posição padrão em questão.

Análise cefalométrica. Aplica-se um método de análise cefalométrica, que consiste: *a*) na identificação de pontos cefalométricos na cabeça virtual; *b*) na criação de linhas e planos cefalométricos; e, por fim, *c*) na realização de medidas cefalométricas, definidas a partir dos pontos, linhas e planos cefalométricos.

Simulação da cirurgia ortognática. Simula-se a cirurgia ortognática, que consiste: *a*) na execução das osteotomias, isto é, da segmentação dos ossos maxilares que serão reposicionados no crânio; *b*) no reposicionamento de segmentos ósseos maxilares no crânio, para fins de correção dos problemas dentofaciais apresentados pelo paciente; e *c*) na simulação da deformação natural do tecido mole de revestimento da face em reflexo à movimentação dos segmentos ósseos maxilares.

Confecção das guias cirúrgicas. Confecciona-se, por prototipagem rápida, as guias cirúrgicas que serão usadas para conduzir os segmentos ósseos maxilares para suas novas posições no crânio durante a execução da cirurgia ortognática.

A seguir são apresentadas as quatro contribuições deste trabalho ao planejamento virtual 3D de cirurgia ortognática. A Contribuição I concentra-se na etapa de reorientação da cabeça. A Contribuição II concentra-se na etapa de análise cefalométrica. A Contribuições III e IV concentram-se na etapa de simulação da cirurgia ortognática, ou mais especificamente na etapa de reposicionamento de segmentos ósseos maxilares no crânio.

1.2 Contribuição 1

A posição padrão da Cefalometria foi estabelecida originalmente para a aquisição de imagens craniofaciais por telerradiografia (BROADBENT, 1931). Consiste em colocar o paciente sentado, com sua cabeça fixada no cefalostato, um dispositivo que mantém a cabeça orientada os planos horizontal de Frankfort e sagital mediano, de modo que o primeiro plano fique paralelo ao solo e o segundo plano fique paralelo (ou perpendicular) ao detector de raios-x (ver Figuras 1.4 e 1.5). O objetivo do posicionamento padrão da cabeça, do ponto de vista clínico, é viabilizar a comparação das medidas cefalométricas de um paciente com um padrão cefalométrico — para o diagnóstico de problemas craniofaciais do paciente — ou dele mesmo em momentos distintos — para o acompanhamento do crescimento e desenvolvimento craniofacial do paciente. É importante salientar que quanto maior a precisão do posicionamento da cabeça, maior também é a confiança na execução e comparação das medidas cefalométricas.

Embora as imagens craniofaciais por TCFC sejam eventualmente adquiridas com o paciente já na posição padrão da Cefalometria, a etapa de reorientação da cabeça (ver Seção 1.1) possibilita que a cabeça seja disposta com maior precisão, pois o cirurgião pode visualizar o crânio do paciente, que é justamente onde se encontram os pontos cefalométricos que definem os planos horizontal de Frankfort e sagital mediano usados na posição padrão da Cefalometria. Embora, a etapa de reorientação da cabeça solucione o problema técnico de imprecisão decorrente do posicionamento real da cabeça do paciente na posição padrão da Cefalometria, em contrapartida, ela cria um novo problema de imprecisão, desta vez conceitual, apresentado abaixo.

O plano horizontal de Frankfort é definido como o plano que intersecta os pórios esquerdo e direito e o orbital esquerdo (GARSON, 1885; SPENCER, 1997; T. D. WHITE; BLACK; FOLKENS, 2012). Apesar desta definição ser uma convenção, outras seis definições envolvendo estes três pontos cefalométricos e o orbital direito também são usadas por pesquisadores (BAYOME; J. H. PARK; KOOK, 2013; SWENNEN; SCHUTYSER; BARTH et al., 2006; S.-H. PARK et al., 2006; SWENNEN; SCHUTYSER; HAUSAMEN, 2006; TERAJIMA et al., 2009; CENTENERO; HERNÁNDEZ-ALFARO, 2012; CHEUNG et

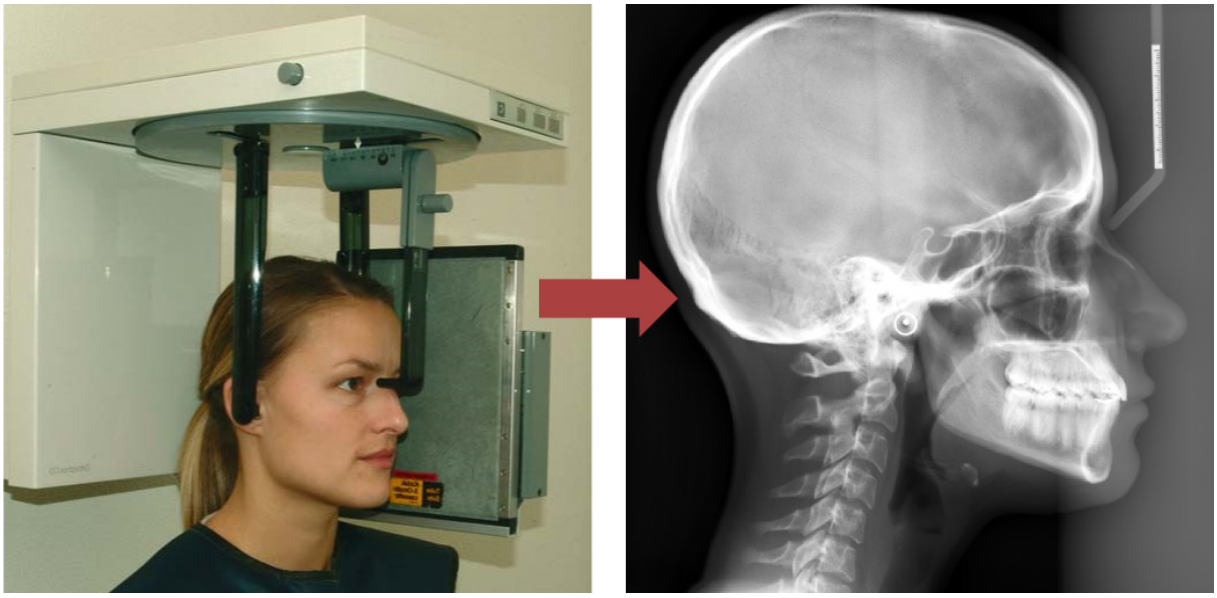

Figura 1.4. Cabeça de uma paciente fixada em um cefalostato para aquisição de uma imagem craniofacial por telerradiografia. Imagens adquiridas e adaptadas de Swennen, Schutyser e Hausamen (2006) e http://drgstoothpix.com/ (26 jan. 2018).

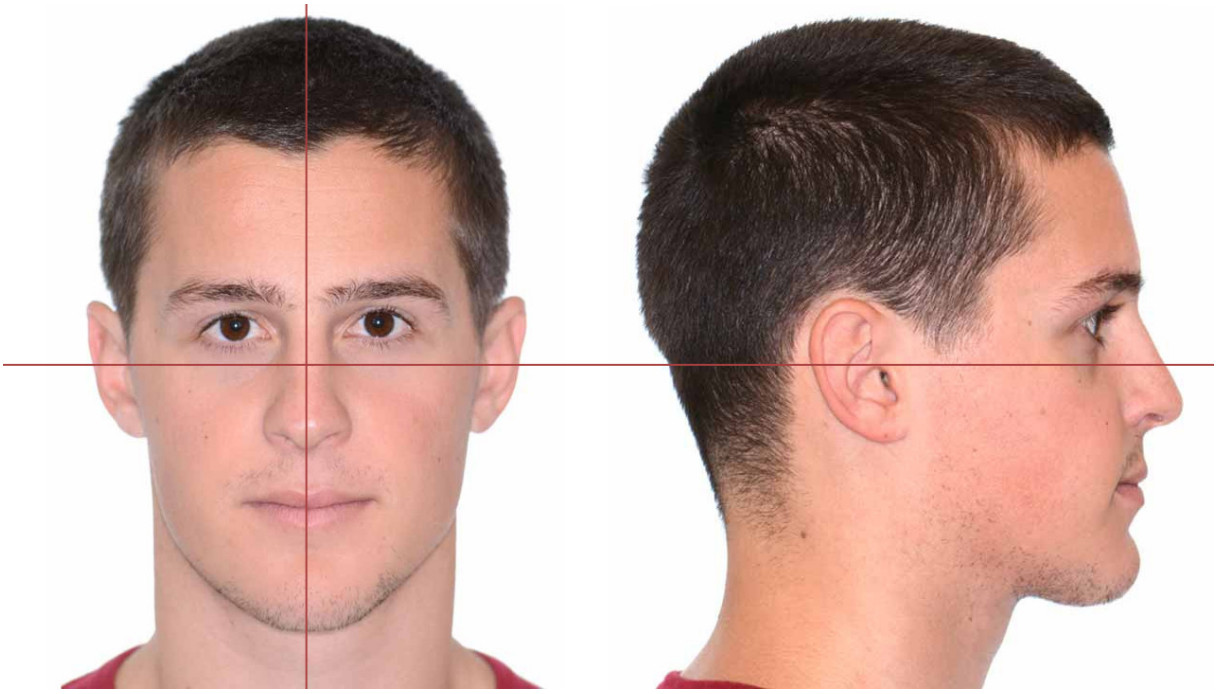

Figura 1.5. Representação do plano horizontal de Frankfort (linha horizontal) e do plano sagital mediano (linha vertical). Fotografia adquirida e adaptada de http://www.drantipov.com/ (3 fev. 2018).

al., 2011; DAMSTRA; FOURIE et al., 2011; GATENO; XIA; TEICHGRAEBER, 2011; E.-J. KIM et al., 2011; Y.-I. KIM et al., 2011; WONG; CHAU; HÄGG, 2011; OH et al., 2013; S.-B. PARK et al., 2013; SONG et al., 2013). Estas outras definições são usadas por desconhecimento da existência de uma definição padrão — que é antiga e originada da Craniometria — ou como alternativa para casos em que a definição padrão produz um plano horizontal de Frankfort destoante do normal — ocorrência comum em indivíduos com assimetria craniofacial. Independentemente da definição adotada, os pesquisadores consideram que elas não produzem diferenças de medição clinicamente relevantes de indivíduos normais, cujos crânios são consideravelmente simétricos. Entretanto, esta afirmação é uma hipótese que nunca foi validada na sua integralidade.

Com o propósito de validar a hipótese em questão, um estudo foi realizado no contexto deste trabalho de doutorado. Os resultados do estudo indicam que a hipótese é falsa, ou seja, que ao contrário do que se presumia, a mudança de definição do plano horizontal de Frankfort pode sim produzir diferenças de medição clinicamente relevantes mesmo para indivíduos normais. O estudo completo é apresentado no artigo intitulado "*Influence of Different Setups of the Frankfort Horizontal Plane on 3-Dimensional Cephalometric Measurements*", publicado em agosto de 2017 na *American Journal of Orthodontics and Dentofacial Orthopedics*. O Capítulo 2 desta tese contém uma cópia da versão final do artigo, autorizada pela editora Elsevier.

1.3 Contribuição 2

Os métodos de análise cefalométrica são fundamentalmente usados na Ortodontia, Ortopedia Funcional dos Maxilares e Cirurgia e Traumatologia Bucomaxilofacial, pois fornecem informações que ajudam os especialistas a diagnosticar problemas dentofaciais, elaborar planos de tratamento e avaliar tratamentos. Estes métodos são constituídos essencialmente por medidas cefalométricas e seus valores ideais. As medidas cefalométricas são definidas, direta ou indiretamente, a partir de pontos cefalométricos identificados originalmente em imagens craniofaciais de telerradiografia. Estas medidas são bidimensionais (2Ds) e incorporam erros de precisão decorrentes das limitações da telerradiografia — tais como: sobreposição e deformação de tamanho e forma dos tecidos (KAPILA, 2014). No planejamento virtual 3D de cirurgia ortognática, os pontos cefalométricos são identificados na cabeça virtual do paciente. Consequentemente, as medidas cefalométricas são precisas, confiáveis e ainda podem produzir valores 3D.

Métodos de análise cefalométrica 3D têm sido criados com o propósito de explorar a tridimensionalidade da geometria da cabeça (S.-H. PARK et al., 2006; SWENNEN; SCHUTYSER; HAUSAMEN, 2006; CHEUNG et al., 2011; DAMSTRA; FOURIE et al.,

2011; GATENO; XIA; TEICHGRAEBER, 2011; WONG; CHAU; HÄGG, 2011; BAYOME; J. H. PARK; KOOK, 2013; DEVANNA, 2015). Estes métodos são compostos por medidas cefalométricas originalmente 3D e, principalmente, por medidas cefalométricas 2D convencionais, porém com suas definições geométricas adaptadas para produzir valores 3D. Uma análise comparativa das adaptações presentes nos principais métodos de análise cefalométrica 3D relevou que há diferentes adaptações para uma mesma medida cefalométrica 2D convencional. Consequentemente, elas produzem diferentes valores 3D. Além disso, a comparação também mostrou que há adaptações que não produzem valores verdadeiramente 3D, ocasionam em perda de informação e alteram as definições geométricas de linhas e planos cefalométricos.

Buscando sanar os problemas mencionados acima, uma adaptação 3D do método de análise cefalométrica elaborado por McNamara (1984) foi desenvolvida como parte deste trabalho de doutorado. Em comparação com os métodos de análise cefalométrica 3D citados acima, o novo método supera os problemas identificados e apresenta uma nova forma para cálculo das medidas cefalométricas de distância orientada entre um ponto e uma linha cefalométrica. O novo método é apresentado no artigo intitulado "*Cone-Beam Computed Tomography-Based Three-Dimensional McNamara Cephalometric Analysis*", pré-publicado em janeiro de 2018 na *Journal of Craniofacial Surgery*. O Capítulo 2 apresenta uma cópia da versão aceita para publicação do artigo, autorizada pela editora Wolters Kluwer.

1.4 Contribuição 3

Como mencionado acima, os métodos de análise cefalométrica são compostos essencialmente por medidas cefalométricas e seus valores ideais, que juntos auxiliam o cirurgião no diagnóstico e planejamento do tratamento de deformidades dentofaciais. Os valores ideais ajudam nestes processos, pois servem de referencial para o cirurgião. Entretanto, nem sempre os valores ideais presentes nos próprios métodos de análise cefalométrica podem ser utilizados. Esses valores ideais podem servir de referência para determinados pacientes, mas não para outros, pois indivíduos de diferentes grupos étnicos tem suas próprias características físicas, e elas precisam e devem ser respeitadas pelo cirurgião. É aí que entram as normas cefalométricas, que contém os valores ideais das medidas cefalométricas para indivíduos de uma população específica.

Assim como os métodos de análise cefalométrica, as normas cefalométricas foram estabelecidas originalmente a partir de imagens craniofaciais de telerradiografia. Portanto, elas também incorporam os erros de precisão decorrentes das limitações da telerradiografia. Como as imagens de TCFC são mais precisas e confiáveis do que as imagens

de telerradiografia, têm-se estabelecido normas cefalométricas por meio dessas imagens para diferentes populações. Normas cefalométricas baseadas nestas imagens já foram estabelecidas para a população chinesa, indiana, coreana, turca, porém nenhuma para a população brasileira (CHEUNG et al., 2011; WONG; CHAU; HÄGG, 2011; LIANG et al., 2014; DEVANNA, 2015; BAYOME; J. H. PARK; KOOK, 2013; VAHDETTIN et al., 2016). Estas normas seriam clinicamente relevantes para o tratamento de pacientes da Cirurgia Ortognática no Brasil.

Com o propósito de contribuir com a comunidade científica, normas cefalométricas para adultos brasileiros de ascendência europeia foram estabelecidas como parte deste trabalho de doutorado. Além disso, dimorfismo sexual também foi avaliado. Os resultados desta avaliação indicam que os homens têm os maxilares maiores do que as mulheres, apesar de ambos apresentarem a mesma morfologia craniofacial. As normas e os resultados da avaliação são apresentados no artigo intitulado "*Cone Beam Computed Tomography-Based Cephalometric Norms for Brazilian Adults*", publicado em janeiro de 2018 na *International Journal of Oral and Maxillofacial Surgery*. O Capítulo 2 contém uma cópia da versão final do artigo, autorizada pela editora Elsevier.

1.5 Contribuição 4

Uma das vantagens do uso do computador como ferramenta de apoio ao diagnóstico e planejamento de cirurgias é a possibilidade de usá-lo na automatização de procedimentos, visando a redução significativa do tempo gasto pelos cirurgiões na execução de tarefas, principalmente daquelas monótonas, complexas ou demoradas. Neste contexto, pesquisadores têm contribuído com métodos para a automatização, completa ou parcial, das etapas do planejamento virtual 3D de cirurgia ortognática. São exemplos, os métodos desenvolvidos para registro automático de modelos do crânio, das arcadas dentárias e da face (RANGEL et al., 2012); identificação automática de pontos cefalométricos e de planos de referência, como os planos horizontal de Frankfort e sagital mediano (CHENG; LEOW; LIM, 2012; CAUTER et al., 2010; GUPTA et al., 2015; KEUSTERMANS; SMEETS et al., 2011; MAKRAM; KAMEL, 2012; SHAHIDI et al., 2014); segmentação automática dos maxilares e dos dentes (BRANDARIZ et al., 2014; CHANG; XIA; YUAN et al., 2013; GOLLMER; BUZUG, 2012; KAINMUELLER et al., 2009; WANG et al., 2014; DUY et al., 2012; GAO; CHAE, 2010; JI; ONG; FOONG, 2014; KEUSTERMANS; VANDERMEULEN; SUETENS, 2012; S. S. NAUMOVICH; S. A. NAUMOVICH; GONCHARENKO, 2015; ZHANG; CHEN et al., 2016); entre outros métodos (H. KIM; JÜRGENS; REYES, 2011; MAZZA; BARBARINO, 2011; MOLLEMANS et al., 2007; PAN et al., 2012; ZHANG; TANG et al., 2015).

Dentre todas as etapas do planejamento virtual 3D de cirurgia ortognática, a etapa de reposicionamento de segmentos ósseos maxilares no crânio (ver Seção 1.1) pode ser considerada a principal delas, porque é justamente nela que o cirurgião estabelece a estratégia de correção dos problemas dentofaciais do paciente. Apesar da importância desta etapa, apenas um método de automatização aplicável a ela foi identificado na revisão da literatura. Este método promove o restabelecimento da oclusão dentária a partir do posicionamento das arcadas dentárias superior e inferior em máxima intercuspidação (CHANG; XIA; GATENO et al., 2010; XIA et al., 2010). Porém, a etapa de reposicionamento de segmentos ósseos maxilares no crânio vai além disto. Ela também envolve a correção de assimetrias faciais e discrepâncias de maxilares. Para esta última classe de problemas, por exemplo, o cirurgião movimenta um ou mais segmentos ósseos maxilares sobre o perfil craniofacial, até que ele consiga aproximar o máximo possível as medidas cefalométricas do paciente de seus valores ideais. Como essas medidas são muitas vezes correlacionadas, a mudança de uma delas compromete outras. Isto torna esta tarefa de correção complexa e demorada. O desenvolvimento de um método para a automatização completa da etapa de reposicionamento de segmentos ósseos maxilares no crânio seria, portanto, de grande valia ao agilizar e, consequentemente, reduzir o custo do planejamento cirúrgico.

Com o propósito de agilizar a etapa de reposicionamento de segmentos ósseos maxilares no crânio, um método de automatização foi desenvolvido como parte deste trabalho de doutorado. Os resultados mostraram que o método é eficaz no tratamento de pacientes com deformidades dentofaciais passíveis de correção cirúrgica por meio do reposicionamento ósseo da maxila, da mandíbula e do mento. O método é apresentado no artigo intitulado "*Automatic Repositioning of Jaw Segments for Three-Dimensional Virtual Treatment Planning of Orthognathic Surgery*", publicado em setembro de 2017 na *Journal of Cranio-Maxillo-Facial Surgery*. O Capítulo 2 contém uma cópia da versão final do artigo, autorizada pela editora Elsevier. Ainda associado a esta contribuição, um pedido de patente foi devidamente depositado junto ao Instituto Nacional da Propriedade Industrial, em 2 de março de 2017 (nº BR 10.2017.004146-8).

1.6 Aprovação Ética da Pesquisa

O trabalho apresentado nesta tese foi conduzido em acordo com as diretrizes e normas regulamentadoras de pesquisas envolvendo seres humanos exigidas pelo Conselho Nacional de Saúde (Resolução nº 466, de 12 de dezembro de 2012). Os aspectos éticos do trabalho foram analisados e aprovados pelo Comitê de Ética em Pesquisa da Universidade Estadual de Campinas, em 25 de março de 2015. O projeto de pesquisa referente

ao trabalho encontra-se registrado sob o protocolo de número 27917314.0.0000.5404.

1.7 Organização da Tese

Esta tese é apresentada no formato de coletânea de publicações aceito pela Universidade Estadual de Campinas. O texto da tese está organizado em consonância com as normas vigentes para elaboração de dissertações e teses (Informação CCPG/001/2015), da seguinte maneira: o Capítulo 2 contém cópia dos quatro artigos citados acima; o Capítulo 3 discute sinteticamente os resultados do trabalho, ressaltando suas relevâncias; o Capítulo 4 apresenta as conclusões do trabalho, assim como suas contribuições, limitações e perspectivas de trabalhos futuros; o Apêndice A apresenta as permissões das editoras Elsevier e Wolters Klumer para a inclusão dos artigos na tese; e, por fim, o Apêndice B contém cópia dos pareceres consubstanciados emitidos pelo Comitê de Ética em Pesquisa da Universidade.

Capítulo 2

Publicações

Este capítulo contém cópia dos quatro artigos citados no Capítulo 1 e referenciados abaixo. As permissões concedidas pelas editoras para a inclusão das cópias na tese são apresentadas no Apêndice A. Por questões de direitos de reprodução, a cópia do segundo artigo corresponde à versão aceita para publicação e não à versão final publicada.

1. SANTOS, R. M. G.; DE MARTINO, J. M.; HAITER NETO, F. et al. Influence of different setups of the Frankfort horizontal plane on 3-dimensional cephalometric measurements. **American Journal of Orthodontics and Dentofacial Orthopedics**, v. 152, n. 2, p. 242–249, ago. 2017. DOI: 10.1016/j.ajodo.2016.12.023.
2. SANTOS, R. M. G.; DE MARTINO, J. M.; HAITER NETO, F. et al. Cone-beam computed tomography-based three-dimensional McNamara cephalometric analysis. **Journal of Craniofacial Surgery**, jan. 2018. Pré-publicado. DOI: 10.1097/SCS.0000000000004248.
3. SANTOS, R. M. G.; DE MARTINO, J. M.; HAITER NETO, F. et al. Cone beam computed tomography-based cephalometric norms for Brazilian adults. **International Journal of Oral and Maxillofacial Surgery**, v. 47, n. 1, p. 64–71, jan. 2018. DOI: 10.1016/j.ijom.2017.06.030.
4. SANTOS, R. M. G.; DE MARTINO, J. M.; PASSERI, L. A. et al. Automatic repositioning of jaw segments for three-dimensional virtual treatment planning of orthognathic surgery. **Journal of Cranio-Maxillo-Facial Surgery**, v. 45, n. 9, p. 1399–1407, set. 2017. DOI: 10.1016/j.jcms.2017.06.017.

2.1 Publicação 1

Influence of Different Setups of the Frankfort Horizontal Plane on 3-Dimensional Cephalometric Measurements

Rodrigo Mologni Gonçalves dos Santos
José Mario De Martino
Francisco Haiter Neto
Luis Augusto Passeri

American Journal of Orthodontics and Dentofacial Orthopedics

Agosto de 2017

ORIGINAL ARTICLE AJO-DO

Influence of different setups of the Frankfort horizontal plane on 3-dimensional cephalometric measurements

Rodrigo Mologni Gonçalves dos Santos,[a] José Mario De Martino,[b] Francisco Haiter Neto,[c] and Luis Augusto Passeri[d]
Campinas and Piracicaba, São Paulo, Brazil

Introduction: The Frankfort horizontal (FH) is a plane that intersects both porions and the left orbitale. However, other combinations of points have also been used to define this plane in 3-dimensional cephalometry. These variations are based on the hypothesis that they do not affect the cephalometric analysis. We investigated the validity of this hypothesis. **Methods:** The material included cone-beam computed tomography data sets of 82 adult subjects with Class I molar relationship. A third-party method of cone-beam computed tomography-based 3-dimensional cephalometry was performed using 7 setups of the FH plane. Six lateral cephalometric hard tissue measurements relative to the FH plane were carried out for each setup. Measurement differences were calculated for each pair of setups of the FH plane. The number of occurrences of differences greater than the limits of agreement was counted for each of the 6 measurements. **Results:** Only 3 of 21 pairs of setups had no occurrences for the 6 measurements. No measurement had no occurrences for the 21 pairs of setups. Setups based on left or right porion and both orbitales had the greatest number of occurrences for the 6 measurements. **Conclusions:** This investigation showed that significant and undesirable measurement differences can be produced by varying the definition of the FH plane. (Am J Orthod Dentofacial Orthop 2017;152:242-9)

The Frankfort horizontal (FH) is an imaginary cranial reference plane used in orienting the skull for standardizing and unifying the cephalometric and craniometric measurements. Previously called the "German horizontal," it was renamed in the Frankfort Craniometric Agreement established in the 13th General Congress of the German Anthropological Society held in Frankfort in August 1882. According to the agreement, the FH plane is defined by 2 lines, one on either side of the skull, connecting the uppermost point on the margin of the external acoustic meatus (porion) with the lowermost point on the orbital margin (orbitale). Since 2 lines are coplanar solely when they are either parallel or intersecting, this definition of the FH plane is not formally consistent from a purely mathematical point of view. After the inconsistency was identified, the definition was modified to the mathematically correct definition of a plane as uniquely determined by 3 noncollinear points. In this definition, the FH plane is determined by both porions and the left orbitale.[1-3]

Despite the agreement, other combinations of craniometric points have often been used to set up the FH plane by dental researchers. For example, just 1 porion and both orbitales were used in the studies of Bayome et al[4] and Swennen et al.[5] The left porion was used in

[a]Department of Computer Engineering and Industrial Automation, School of Electrical and Computer Engineering, University of Campinas, Campinas, São Paulo, Brazil.
[b]Department of Computer Engineering and Industrial Automation, School of Electrical and Computer Engineering, University of Campinas, Campinas, São Paulo, Brazil; Universidade Estadual de Campinas, Faculdade de Engenharia Elétrica e de Computação, Cidade Universitária "Zeferino Vaz," Campinas, São Paulo, Brazil.
[c]Department of Oral Diagnosis, Piracicaba Dental School, University of Campinas, Piracicaba, São Paulo, Brazil.
[d]Department of Surgery, School of Medical Sciences, University of Campinas, Campinas, São Paulo, Brazil.
All authors have completed and submitted the ICMJE Form for Disclosure of Potential Conflicts of Interest, and none were reported.
Support to the first author from the Coordination for the Improvement of Higher Education Personnel, Ministry of Education, Brazil.
Address correspondence to: José Mario De Martino, Av. Albert Einstein 400, Cidade Universitária, Campinas, SP, Brazil, 13083-852; e-mail, martino@fee.unicamp.br.
Submitted, January 2016; revised and accepted, December 2016.
0889-5406/$36.00

http://dx.doi.org/10.1016/j.ajodo.2016.12.023

the first study, and the right porion was used in the second study. Compiling other related studies, we found that 6 points have been used for setting up the FH plane: 4 points representing anatomic structures of the skull (anatomic points) and 2 points secondarily obtained from these points (constructed points).[4-18] The left porion (PoL), right porion (PoR), left orbitale (OrL), and right orbitale (OrR) points are the 4 anatomic points. The midpoint between both the porions (PoC) and the midpoint between the orbitales (OrC) are the 2 constructed points. As a result, there are 7 acceptable possibilities for connecting these points to set up the FH plane: (1) PoL, PoR, and OrL[6,12,13]; (2) PoL, PoR, and OrR[12-14,17]; (3) PoL, PoR, and OrC[8,12,18]; (4) PoL, OrL, and OrR[4,12,15,16]; (5) PoR, OrL, and OrR[5,7,8,12,15,16]; (6) PoC, OrL, and OrR[7,9-12]; and (7) PoL, PoR, OrL, and OrR (by least-squares plane fitting).[12] Considering the large number of studies based on different setups of the FH plane, we supposed that these variations do not impact the cephalometric measurements for subjects with craniofacial symmetry. To check this hypothesis is the purpose of this study.

Cephalometric measurement values are used by surgeons and orthodontists for diagnosis, treatment planning, and treatment evaluation of orthodontic and orthognathic surgery patients. The greater the accuracy of these values, the lower the probability of disparate or erroneous clinical outcomes. For this reason, validating this hypothesis is of paramount importance. To the best of our knowledge, no study has been published to confirm specifically this hypothesis. A literature review showed 3 related studies. Oh et al[16] investigated the influence of different horizontal reference planes for evaluating occlusal cant. They used distances based on teeth. Yoon et al[19] analyzed the influence of different reference systems for evaluating facial asymmetry. They used horizontal and vertical deviations of landmarks. Lin et al[20] evaluated the influence of different horizontal reference planes in analyzing patients with facial symmetry or asymmetry. They also used distances based on teeth. Our study is based on cephalometric hard tissue measurements originally performed on lateral cephalometric radiography and frequently used by surgeons.

Our goal in this article was to evaluate whether variations in the FH plane impact cephalometric analysis.

MATERIAL AND METHODS

This study was conducted in accordance with the ethical guidelines for biomedical research involving human subjects from the National Health Council of Brazil. It was approved by the Human Research Ethics Committee of the School of Medical Sciences at the University of Campinas (protocol number: 27917314.0.0000.5404).

Out of a total of 135, 82 cone-beam computed tomography (CBCT) data sets acquired from living subjects (27 men, 55 women) were selected from the Division of Oral Radiology's archive at the Piracicaba Dental School at the University of Campinas in Brazil. The eligibility criteria were based not only on the subjects' features, but also on the quality of the CBCT data sets. The inclusion criteria were the following: subjects with Class I molar relationship, subjects aged 18 to 32 years, CBCT data sets with a large field of view (diameter, 16 cm; height, 13-22 cm), and CBCT data sets with a voxel size of 0.4 mm^3 or less. The exclusion criteria were subjects with craniofacial asymmetry or deformity, subjects who had surgery of the facial bones, and CBCT data sets with severe noise.

A custom software toolkit for visualizing and interacting with the CBCT data sets was developed by the first author using Python (version 2.7.7; Python Software Foundation; Beaverton, Ore)[21] programming environment and NumPy (version 1.7.1; NumFOCUS; Austin, Tex),[22] PyQt (version 4.11; Riverbank Computing; Wimborne, Dorset, United Kingdom),[23] and VTK (version 6.1.0; Kitware; Clifton Park, NY)[24] extension packages. The marching cubes algorithm was applied on each CBCT data set to build a high-resolution 3-dimensional (3D) geometric model representing the hard tissue surface of the skull, producing a reconstructed skull.[24,25]

The method of CBCT-based 3D cephalometry described by Swennen et al[7] was adopted for this study. It provided a suitable procedure to accurately evaluate the hypothesis. The method has 4 stages: (1) setting up the 3D cephalometric reference system (semiautomatic); (2) identifying the 3D cephalometric hard tissue landmarks (manual); (3) setting up the 3D cephalometric planes (automatic); and (4) performing the 3D cephalometric hard tissue measurements (automatic). These stages were sequentially performed for each of the 82 reconstructed skulls. The technical terms adopted by Swennen et al were followed in our study.

In stage 1, 5 tasks were carried out to set up a 3D cephalometric reference system based on the anterior cranial base, called the sella-nasion plane; this is required to standardize the 3D cephalometric hard tissue measurements. The first task was to position the reconstructed skull to the FH and median planes (Fig 1). In the anterior view, the skull is symmetrically placed facing forward, with the horizontal line in the screen crossing the OrL and OrR points, and the vertical line crossing the point where the frontonasal and internasal sutures intersect (nasion). In right lateral view, the skull is positioned so that the horizontal line intersects the PoR and OrR points. Horizontal and vertical lines are mutually orthogonal and represent the FH and median planes, respectively.

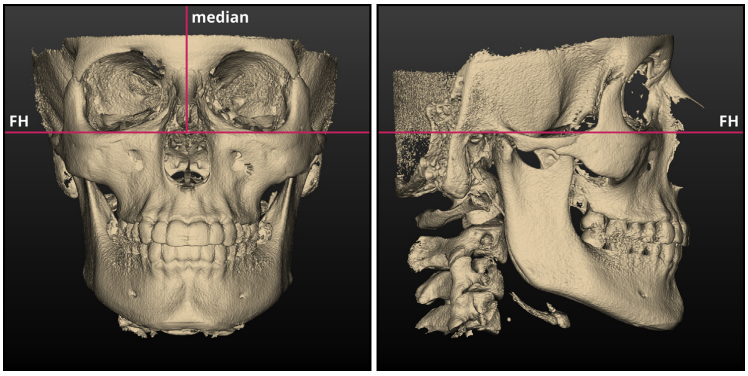

Fig 1. Frontal and right lateral views of a reconstructed skull oriented to the FH and median planes.

Orthogonal projection is required in this task. The second task was to generate the simulated lateral and posteroanterior cephalometric radiographs (Fig 2). An image-order volume-rendering algorithm is used on the CBCT data set to build both radiographs.[24] The third task was to identify nasion (N) and sella (S) 3D cephalometric hard tissue landmarks (Fig 3). The S landmark is situated in the center of the hypophyseal fossa. The fourth task was to set up the sella-nasion 3D cephalometric plane, which intersects the S and N landmarks and is orthogonal to lateral radiography (Fig 2). The fifth task was to set up the horizontal, vertical, and median 3D cephalometric reference planes (Fig 2). The horizontal plane is generated by rotating the sella-nasion plane 6° clockwise around the S landmark on the lateral radiography. The vertical plane intersects the S landmark and is orthogonal to the lateral radiography and to the horizontal plane. The median plane intersects the S landmark and is orthogonal to both planes.

In stage 2, a total of 12 3D cephalometric hard tissue landmarks were identified on the reconstructed skull: 4 landmarks located in the median plane (unpaired landmarks) and 8 landmarks on either side of this plane (paired landmarks). The 4 unpaired landmarks were A-point (A), the most posterior point on the intermaxillary suture; pogonion (Pog), the most anterior point on the mandibular symphysis; menton (Me), the lowermost point on the mandibular symphysis; and gnathion (Gn), the most anteroinferior point on the mandibular symphysis. The 8 paired landmarks were PoL and PoR; OrL and OrR; left gonion (GoL) and right gonion (GoR), the points where the line bisecting the angle formed by extending the posterior ramus border and the inferior body border intersect the gonial angle of each mandibular ramus in the lateral view; and left upper incisor (UIL) and right upper incisors (U1R), the most mesial points on the cusp of each maxillary central incisor. These landmarks are shown in the Figure 3. The simulated cephalometric radiographs help the observer in the 3D positioning of the landmarks.

In stage 3, the facial, y-axis, mandibular, and FH 3D cephalometric planes were set up on the reconstructed skull (Fig 4). The facial plane intersects the N and Pog 3D cephalometric hard tissue landmarks and is orthogonal to the median 3D cephalometric reference plane. The y-axis plane intersects the S and Gn landmarks and is orthogonal to the median plane. The mandibular plane intersects the GoL, GoR, and Me landmarks. As already mentioned, there are 7 possible definitions for the FH plane. Therefore, the FH 3D cephalometric plane can be FH1, the plane that intersects the PoL, PoR, and OrL landmarks; FH2, the plane that intersects the PoL, PoR, and OrR landmarks; FH3, the plane that intersects the PoL, PoR, and OrC landmarks; FH4, the plane that intersects the PoL, OrL, and OrR landmarks; FH5, the plane that intersects the PoR, OrL, and OrR landmarks; FH6, the plane that intersects the PoC, OrL, and OrR landmarks; or FH7, the least-squares best-fit plane[26,27] to the PoL, PoR, OrL, and OrR landmarks (ie, the plane with the lowest square sum of the shortest distances from each landmark to the plane itself).

In stage 4, a total of 6 3D cephalometric hard tissue measurements related to the FH plane were performed on the reconstructed skull: 3 linear projective measurements and 3 angular projective measurements. These measurements were denoted projective because they were performed on the median 3D cephalometric reference plane using the orthogonal projections of the A, N, Pog, UIL, and UIR 3D cephalometric landmarks

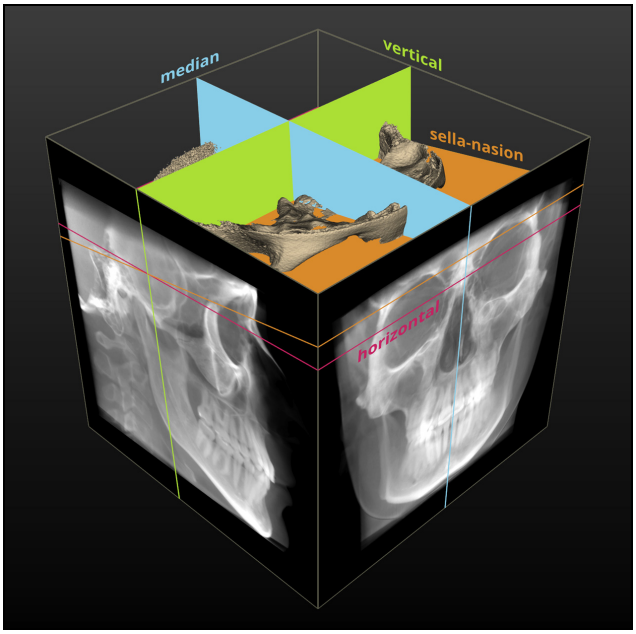

Fig 2. Simulated lateral and posteroanterior cephalometric radiographs and the reconstructed skull created from the same CBCT data set. The sella-nasion 3D cephalometric plane used to generate the horizontal plane. The horizontal, vertical, and median 3D cephalometric reference planes used to set up a 3D cephalometric reference system based on the anterior cranial base.

onto this plane and the lines where the facial, y-axis, mandibular, and FH 3D cephalometric planes intersect the median plane. The 3 linear projective measurements were A-point to nasion perpendicular (A-Np), the distance from A-point to the line that intersects N and is orthogonal to the FH line (nasion perpendicular); pogonion to nasion perpendicular (Pog-Np), the distance from Pog to nasion perpendicular; and upper incisor to A-point vertical (UI-Av), the distance from the midpoint between the UIL and UIR points to the line that intersects A-point and is orthogonal to the FH line. The negative sign was used to indicate that the point was more posteriorly positioned than the reference line. The 3 angular projective measurements were facial angle (FA), the inferoposterior angle between the FH and the facial lines; y-axis angle (YAA), the inferoanterior angle between the FH and the y-axis lines; and mandibular plane angle (MPA), the inferoanterior angle between the FH and themandibular lines. The lines and points used in these measurements are shown in Figure 5. The linear and angular measurements are expressed in millimeters and degrees, respectively. The 6 measurements were performed 7 times, one for each setup of the FH plane. They were chosen because they were originally performed on lateral cephalometric radiography and are usually performed by surgeons.

For estimating the measurement variability introduced by an observer, stages 2 to 4 were performed twice by the same observer (R.M.G.S.). The second observation was done almost 2 years after the first observation. In the second observation, the 3D cephalometric hard tissue measurements (stage 4) were performed only for the FH6 3D cephalometric plane, which is the set up used by Swennen et al.[7]

Statistical analysis

Intraobserver variability is described by 2 values: the mean (bias) and the standard deviation of the measurement differences between 2 observations.[28] Based on the Bland-Altman analysis,[28-30] these values were used to calculate the limits of agreement, with 95%

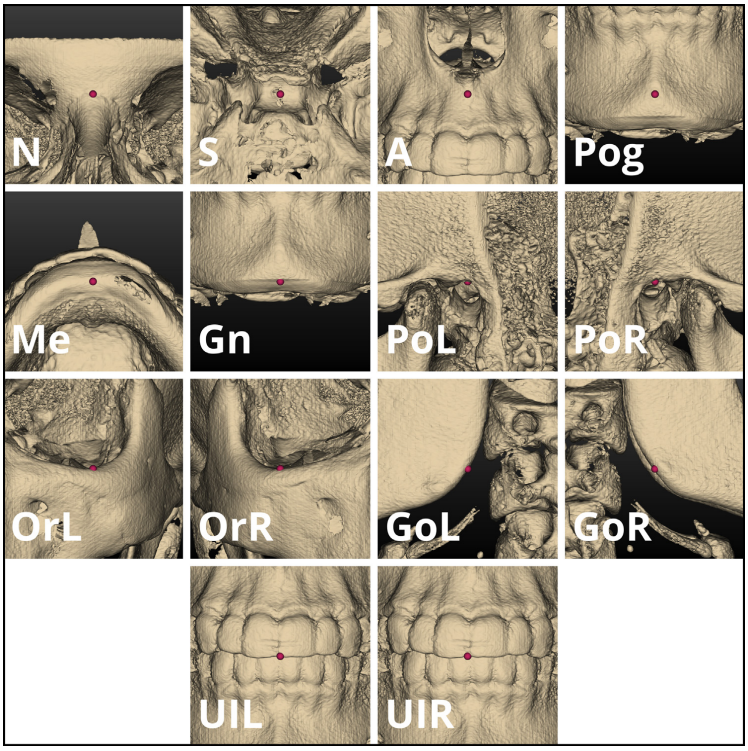

Fig 3. The 14 3D cephalometric hard tissue landmarks identified on a reconstructed skull. The land marks are represented by a sphere with a radius of 1 mm.

confidence intervals around the limits, for each 3D cephalometric hard tissue measurement. The numbers of occurrences in which the measurement differences between 2 setups of the FH plane were greater than the limits of agreement were counted. This was done for all pairwise comparisons of setups of the FH plane, for a total of 21 pairwise comparisons. The R (version 3.1.0; R Foundation for Statistical Computing; Vienna, Austria)[31] statistical computing environment was used for this statistical evaluation.

RESULTS

A total of 3936 (82 subjects × 6 measurements × 7 setups + 82 subjects × 6 measurements × 1 setup) 3D cephalometric hard tissue measurements were performed for this study: 1968 linear projective measurements and 1968 angular projective measurements. Intraobserver variability of the 3D cephalometric hard tissue measurements is shown in Table I. The numbers and percentages of occurrences in which the measurement differences between pairwise comparisons of setups of the FH plane were greater than the limits of agreement are presented in Table II. The FH3-FH6, FH3-FH7, and FH6-FH7 pairwise comparisons were the only ones with no occurrences for all 3D cephalometric hard tissue measurements. No 3D cephalometric hard tissue measurement had no occurrences for all pairwise comparisons. The FH4-FH5 pairwise comparison had the greatest number of occurrences for all the 3D cephalometric hard tissue measurements.

DISCUSSION

Although there is a standard definition for the FH plane, other definitions have also been used by clinicians and researchers.[4-18] We investigated whether the change in the setup of the FH plane can impact the

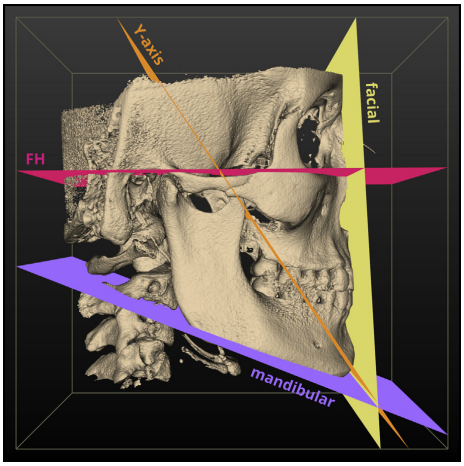

Fig 4. The facial, y-axis, mandibular, and FH 3D cephalometric planes.

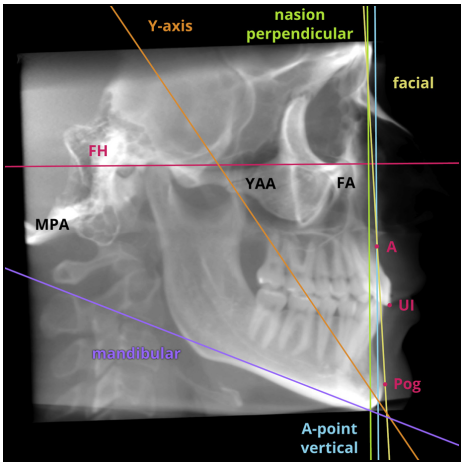

Fig 5. The lines and points in the median 3D cephalometric plane used as references for the projective 3D cephalometric hard tissue measurements.

cephalometric analysis. The hypothesis was that it does not significantly modify the cephalometric measurements performed on subjects with craniofacial symmetry. A total of 82 CBCT data sets were used for this study. The numbers of occurrences in which different setups of the FH plane impact the cephalometric measurement values were calculated. The results presented in Table II allowed us to state that this hypothesis is not true. Only the FH3-FH6, FH3-FH7, and FH6-FH7 pairwise comparisons had no occurrences for all the 3D cephalometric hard tissue measurements. This means that to replace FH3 by FH6 or vice versa will not produce significantly different values. The same is true for the other pairwise comparisons.

Table I. Intraobserver variability of the 3D cephalometric hard tissue measurements

	Bias	*SD*	*LOA*
A-Np (mm)	−0.02	0.20	−0.50, 0.45
Pog-Np (mm)	−0.01	0.11	−0.26, 0.25
UI-Av (mm)	0.01	0.22	−0.51, 0.53
FA (°)	0.01	0.04	−0.09, 0.11
YAA (°)	0.14	0.36	−0.70, 0.98
MPA (°)	−0.12	0.50	−1.28, 1.04

Bias, Mean of the differences; *LOA*, limits of agreement with 95% confidence intervals of the limits.

In the method of Swennen et al,[7] the definition of FH5 was used to orient the reconstructed skull (stage 1; Fig 1), and the definition of FH6 was used to set up the FH 3D cephalometric plane (stage 3; Fig 4). Therefore, the best choice would have been to keep the same definition for both and preferably to have used the agreed-upon definition (FH1).

The definition of FH7 is conceptually similar to the original definition of the FH plane in the Frankfort Craniometric Agreement.[1,2] The FH plane created from this definition rarely intersects the PoL, PoR, OrL, and OrR landmarks, but it is closest to them. Considering the results presented in Table II, the best choice would have been to use the definitions of FH3 or FH6, because the number of occurrences was equal to zero for all 3D cephalometric hard tissue measurements.

In Table II, note that the number of occurrences is growing for the linear and angular projective measurements: UI-Av ≤A-Np ≤Pog-Np and MPA ≤YAA ≤FA. This observation suggests that (1) when the distance between 2 landmarks is used to calculate a linear projective measurement, the number of occurrences is greater; and (2) the longer the line segment used to calculate an angular projective measurement, the lower the number of occurrences.

Oh et al[16] identified which horizontal reference planes have the greatest correlation with a clinical evaluation of occlusal cant. A total of 7 horizontal planes were analyzed in their study. The FH4 and FH5 planes were 2 of them. The differences between 2 bilateral distances were used. They concluded that both FH planes are the most

Table II. Numbers (and percentages) of occurrences in which the measurement differences between pairwise comparisons of setups of the FH plane were greater than the limits of agreement

	A-NP	*Pog-Np*	*UI-Av*	*FA*	*YAA*	*MPA*
FH1-FH2	42 (51.2)	67 (81.7)	4 (4.9)	67 (81.7)	27 (32.9)	19 (23.2)
FH1-FH3	16 (19.5)	56 (68.3)	0 (0)	57 (69.5)	7 (8.5)	1 (1.2)
FH1-FH4	4 (4.9)	35 (42.7)	0 (0)	39 (47.6)	0 (0)	0 (0)
FH1-FH5	50 (61)	69 (84.1)	11 (13.4)	71 (86.6)	36 (43.9)	27 (32.9)
FH1-FH6	19 (23.2)	56 (68.3)	0 (0)	57 (69.5)	9 (11)	1 (1.2)
FH1-FH7	18 (22)	56 (68.3)	0 (0)	57 (69.5)	8 (9.8)	1 (1.2)
FH2-FH3	18 (22)	54 (65.9)	0 (0)	57 (69.5)	3 (3.7)	2 (2.4)
FH2-FH4	49 (59.8)	69 (84.1)	11 (13.4)	71 (86.6)	34 (41.5)	24 (29.3)
FH2-FH5	5 (6.1)	35 (42.7)	0 (0)	40 (48.8)	1 (1.2)	0 (0)
FH2-FH6	14 (17.1)	54 (65.9)	0 (0)	55 (67.1)	2 (2.4)	1 (1.2)
FH2-FH7	17 (20.7)	54 (65.9)	0 (0)	57 (69.5)	3 (3.7)	1 (1.2)
FH3-FH4	33 (40.2)	63 (76.8)	1 (1.2)	65 (79.3)	17 (20.7)	6 (7.3)
FH3-FH5	33 (40.2)	63 (76.8)	1 (1.2)	65 (79.3)	17 (20.7)	10 (12.2)
FH3-FH6	0 (0)	0 (0)	0 (0)	0 (0)	0 (0)	0 (0)
FH3-FH7	0 (0)	0 (0)	0 (0)	0 (0)	0 (0)	0 (0)
FH4-FH5	55 (67.1)	71 (86.6)	18 (22)	71 (86.6)	38 (46.3)	29 (35.4)
FH4-FH6	33 (40.2)	63 (76.8)	1 (1.2)	66 (80.5)	18 (22)	6 (7.3)
FH4-FH7	33 (40.2)	63 (76.8)	1 (1.2)	66 (80.5)	16 (19.5)	6 (7.3)
FH5-FH6	33 (40.2)	63 (76.8)	1 (1.2)	66 (80.5)	19 (23.2)	6 (7.3)
FH5-FH7	34 (41.5)	63 (76.8)	1 (1.2)	66 (80.5)	19 (23.2)	9 (11)
FH6-FH7	0 (0)	0 (0)	0 (0)	0 (0)	0 (0)	0 (0)

appropriate horizontal planes for this propose. Yoon et al[19] measured the deviations of cephalometric landmarks from horizontal and median reference planes. A total of 3 horizontal planes were analyzed in their study. The FH1 and FH4 planes were 2 of them. The positioning of the landmarks was analyzed. They concluded that deviations of landmarks could vary depending on the reference plane. Lin et al[20] investigated whether there is any systematic difference between horizontal reference planes. A total of 5 horizontal planes were analyzed in their study. The FH3, FH4, FH5, and FH6 planes were 4 of them. The differences between 4 bilateral distances were used. They concluded that the horizontal planes have no statistically significant difference. Contrary to these studies, in our investigation, we used cephalometric hard tissue measurements originally performed on lateral cephalometric radiography and frequently used by surgeons; all 7 possible variations of the FH plane were compared.

The Bland-Altman[29,30] analysis also was applied by Swennen et al[7] to estimate the measurement variability of their 3D cephalometric hard tissue measurements. Standard deviations of the measurement differences between the 2 observations performed by a same observer were used to quantify intraobserver variability. Standard deviations of the measurement differences between the averages of the 2 observations performed by each of the 2 observers were used to quantify the interobserver variability. Intraobserver and interobserver variability were verified by them. However, they did not report which linear and angular projective measurements they performed or how much were the intraobserver and interobserver variability values of each of their measurements. They reported only the highest intraobserver and interobserver variability values, without bias. For this reason, we did not use their measurement variability values. The procedure we used for estimating the intraobserver variability was based on the study of Swennen et al.

It is important to observe that just 1 observer was involved in this study to calculate the interobserver variability because of operational limitations. However, since the period between the 2 observations was quite long, and since measurement variability tends to increase over time, we considered that the observations were independent. Moreover, an evaluation of the method based on measurements performed twice by 2 observers is not statistically powerful. Multiple observers and multiple observations by observers would improve the statistical power. However, measurement involving multiple observations and observers is a laborious and time-consuming task. For this study, the statistical analysis performed was enough. If the results had shown that the hypothesis was true, then a powerful statistical evaluation would be not required. Since it did not happen, we suggest that future studies should analyze the variance of the measurements performed many times by multiple observers. The aim is to verify the statistical significance of the different setups of the FH plane.

CONCLUSIONS

This study shows that (1) the hypothesis analyzed is not true: ie, the variation in the setup of the FH plane does produce different cephalometric measurement values; and (2) the standard definition of the FH plane should be used to increase the accuracy of 3D cephalometric measurement values and to reduce the probability of disparate or erroneous clinical outcomes.

REFERENCES

1. Garson JG. The Frankfort Craniometric Agreement, with critical remarks thereon. J Anthropol Inst Gt Britain Irel 1885;14:64-83.
2. Spencer F, editor. History of physical anthropology: an encyclopedia1. New York: Garland Publishing; 1997.
3. White TD, Black MT, Folkens PA. Human osteology. 3rd ed. Burlington, Mass: Elsevier Academic Press; 2012.
4. Bayome M, Park JH, Kook YA. New three-dimensional cephalometric analyses among adults with a skeletal Class I pattern and normal occlusion. Korean J Orthod 2013;43:62-73.
5. Swennen GR, Schutyser F, Barth EL, De Groeve P, De Mey A. A new method of 3-D cephalometry. Part I: the anatomic Cartesian 3-D reference system. J Craniofac Surg 2006;17:314-25.
6. Park SH, Yu HS, Kim KD, Lee KJ, Baik HS. A proposal for a new analysis of craniofacial morphology by 3-dimensional computed tomography. Am J Orthod Dentofacial Orthop 2006;129:600.e23-34.
7. Swennen GR, Schutyser F, Hausamen JE, editors. Three-dimensional cephalometry: a color atlas and manual. Berlin, Germany: Springer-Verlag; 2006.
8. Terajima M, Nakasima A, Aoki Y, Goto TK, Tokumori K, Mori N, et al. A 3-dimensional method for analyzing the morphology of patients with maxillofacial deformities. Am J Orthod Dentofacial Orthop 2009;136:857-67.
9. Centenero SA, Hernández-Alfaro F. 3D planning in orthognathic surgery: CAD/CAM surgical splints and prediction of the soft and hard tissues results—our experience in 16 cases. J Craniomaxillofac Surg 2012;40:162-8.
10. Cheung LK, Chan YM, Jayaratne YS, Lo J. Three-dimensional cephalometric norms of Chinese adults in Hong Kong with balanced facial profile. Oral Surg Oral Med Oral Pathol Oral Radiol Endod 2011;112:e56-73.
11. Damstra J, Fourie Z, Slater JJ, Ren Y. Reliability and the smallest detectable difference of measurements on 3-dimensional cone-beam computed tomography images. Am J Orthod Dentofacial Orthop 2011;140:e107-14.
12. Gateno J, Xia JJ, Teichgraeber JF. New 3-dimensional cephalometric analysis for orthognathic surgery. J Oral Maxillofac Surg 2011;69:606-22.
13. Kim EJ, Palomo JM, Kim SS, Lim HJ, Lee KM, Hwang HS. Maxillofacial characteristics affecting chin deviation between mandibular retrusion and prognathism patients. Angle Orthod 2011;81:988-93.
14. Kim YI, Cho BH, Jung YH, Son WS, Park SB. Cone-beam computerized tomography evaluation of condylar changes and stability following two-jaw surgery: Le Fort I osteotomy and mandibular setback surgery with rigid fixation. Oral Surg Oral Med Oral Pathol Oral Radiol Endod 2011;111:681-7.
15. Wong RW, Chau AC, Hägg U. 3D CBCT McNamara's cephalometric analysis in an adult Southern Chinese population. Int J Oral Maxillofac Surg 2011;40:920-5.
16. Oh S, Ahn J, Nam KU, Paeng JY, Hong J. Frankfort horizontal plane is an appropriate three-dimensional reference in the evaluation of clinical and skeletal cant. J Korean Assoc Oral Maxillofac Surg 2013;39:71-6.
17. Park SB, Kim YI, Hwang DS, Lee JY. Midfacial soft-tissue changes after mandibular setback surgery with or without paranasal augmentation: cone-beam computed tomography (CBCT) volume superimposition. J Craniomaxillofac Surg 2013;41:119-23.
18. Song WW, Kim SS, Sándor GK, Kim YD. Maxillary yaw as the primary predictor of maxillary dental midline deviation: 3D analysis using cone-beam computed tomography. J Oral Maxillofac Surg 2013;71:752-62.
19. Yoon KW, Yoon SJ, Kang BC, Kim YH, Kook MS, Lee JS, et al. Deviation of landmarks in accordance with methods of establishing reference planes in three-dimensional facial CT evaluation. Imaging Sci Dent 2014;44:207-12.
20. Lin HH, Chuang YF, Weng JL, Lo LJ. Comparative validity and reproducibility study of various landmark-oriented reference planes in 3-dimensional computed tomographic analysis for patients receiving orthognathic surgery. PLoS ONE 2015;10:1-16.
21. Rossum G. The Python language reference manual: revised and updated for Python 3.2. In: Drake FL Jr., editor. Eastbourne, United Kingdom: Network Theory; 2011.
22. Walt S, Colbert SC, Varoquaux G. The NumPy array: a structure for efficient numerical computation. Comput Sci Eng 2011;13:22-30.
23. Summerfield M. Rapid GUI programming with Python and Qt: the definitive guide to PyQt programming. Upper Saddle River, NJ: Pearson Education; 2007.
24. Schroeder W, Martin K, Lorensen B. The Visualization toolkit: an object-oriented approach to 3D graphics. 4th ed. Clifton Park, NY: Kitware; 2006.
25. Lorensen WE, Cline HE. Marching cubes: a high resolution 3D surface construction algorithm. Comp Graph 1987;21:163-9.
26. Pearson K. On lines and planes of closest fit to systems of points in space. Philos Mag 1901;2:559-72.
27. Ahn SJ. Least squares orthogonal distance fitting of curves and surfaces in space. Berlin, Germany: Springer-Verlag; 2004.
28. Sardanelli F, Di Leo G. Biostatistics for radiologists: planning, performing, and writing a radiologic study. Milan, Italy: Springer-Verlag; 2009.
29. Bland JM, Altman DG. Statistical methods for assessing agreement between two methods of clinical measurement. Lancet 1986;1:307-10.
30. Bland JM, Altman DG. Measuring agreement in method comparison studies. Stat Methods Med Res 1999;8:135-60.
31. R Development Core Team. R: a language and environment for statistical computing. Vienna, Austria: R Foundation for Statistical Computing; 2014.

2.2 Publicação 2

Cone-Beam Computed Tomography-Based Three-Dimensional McNamara Cephalometric Analysis

Rodrigo Mologni Gonçalves dos Santos
José Mario De Martino
Francisco Haiter Neto
Luis Augusto Passeri

Journal of Craniofacial Surgery

Janeiro de 2018
(pré-publicação)

Cone-beam computed tomography-based 3-dimensional McNamara's cephalometric analysis

Rodrigo Mologni Gonçalves dos Santos[a], José Mario De Martino[a,*], Francisco Haiter Neto[b], Luis Augusto Passeri[c]

[a]*Department of Computer Engineering and Industrial Automation, School of Electrical and Computer Engineering, University of Campinas, Campinas, SP, Brazil*
[b]*Department of Oral Diagnosis, Piracicaba Dental School, University of Campinas, Piracicaba, SP, Brazil*
[c]*Department of Surgery, School of Medical Sciences, University of Campinas, Campinas, SP, Brazil*

Abstract

This paper introduces a method that extends the McNamara's cephalometric analysis to produce 3-dimensional (3D) measurement values from cone-beam computed tomography images. In the extended method, the cephalometric landmarks are represented by 3D points; the bilateral cephalometric landmarks are identified on both sides of the skull; the cephalometric lines, with the exception of the *facial axis*, are represented by 3D lines; the cephalometric planes, with the exception of the *facial plane*, are represented by planes; the *effective mandibular length*, the *effective midfacial length*, and the *lower anterior facial height* are measured as 3D point-to-point distances; the *nasion perpendicular to point A*, the *pogonion to nasion perpendicular*, the *upper incisor to point A vertical*, and the *lower incisor to point A-pogonion line* are measured each as components of a vector; the *facial axis angle* is measured as a line-to-plane angle; and the *mandibular plane angle* is measured as a plane-to-plane angle. As a result, the method provide real effective lengths of the maxilla and mandible on both sides of the skull; real height of the lower anterior face; directed distances from the *point A* to the *nasion perpendicular*, from the *pogonion* to the *nasion perpendicular*, from the left and right *upper incisor* to the *point A vertical*, and from the left and right *lower incisor* to the *point A-pogonion line* for both the lateral and posteroanterior views of the skull; and real angles of the *facial axis* and the *mandibular plane*. Additionality, the method enables the identification of craniofacial asymmetries.

Keywords: three-dimensional cephalometry, three-dimensional cephalometric analysis, cone-beam computed tomography, three-dimensional cephalometric measurements, McNamara's cephalometric analysis

*Address: Universidade Estadual de Campinas, Faculdade de Engenharia Elétrica e de Computação, Av. Albert Einstein 400, Cidade Universitária "Zeferino Vaz", Barão Geraldo, Campinas, SP, Brazil, CEP 13083-852. Phone: +55 19 3521-3794. Fax: +55 19 3521-3845. E-mail: martino@dca.fee.unicamp.br.

This is a non-final version of an article published in final form in "Santos RMG, De Martino JM, Haiter Neto F, Passeri LA. Cone-beam computed tomography-based three-dimensional McNamara cephalometric analysis [published online ahead of print January 19, 2018]. *J Craniofac Surg* 2018. doi:10.1097/SCS.0000000000004248". Journal of Craniofacial Surgery is available online in http://journals.lww.com/jcraniofacialsurgery/.

1. Introduction

Before the application of cone-beam computed tomography (CBCT) in craniofacial imaging, 3-dimensional (3D) cephalometric analyses were performed by means of medical CT or combining cephalograms.[1,2] Medical CT provides 3D information about the craniofacial anatomy of the patient, enabling clinicians to perform accurate and reliable cephalometric measurements. However, medical CT scanner, besides being bulky, exposes the patients to a higher radiation dose, and requires them to be lying down, not in the standard position of cephalometry. The methods of 3D cephalometric analysis based on combining cephalograms are laborious, provide crude estimates of 3D information, and suffer from inherent undesirable effects of radiography, such as shape and size distortions of anatomical structures. Therefore, 3D cephalometric analyses based on medical CT or combining cephalograms were only clinically used for evaluation of patients with severe craniofacial problems. CBCT overcomes the limitations of the previous techniques. Compared to medical CT, CBCT scanner is compact, can be installed in dental offices, and provides 3D information using a lower radiation dose, with the patient in the standard position of cephalometry. These advantages have triggered the development of new CBCT-based methods of 3D cephalometric analysis.[3–10]

Clinicians and researchers have used CBCT to reconstruct the patient's skull in a 3D virtual space, to create cephalometric planes in a 3D space, to identify bilateral cephalometric landmarks on the left and right sides of the skull, to obtain 3D coordinates of cephalometric landmarks, to perform traditional cephalometric measurements on both sides of the skull, and to perform 3D cephalometric measurements.[3–10] The latter activity has practical relevance since it allows clinicians to analyze 3D measurement values, which are impossible or difficult to be obtained using traditional cephalometry. Researchers have usually taken 3D cephalometric measurements essentially considering 2-dimensional (2D) information available on lateral or posteroanterior cephalograms.[3–10] In general, researchers have not explored the three-dimensionality of CBCT in its full extent to produce 3D measurement values taking into account precise original geometric definitions of cephalometric lines and planes. Moreover, researchers also have defined a same 3D cephalometric measurement in different ways. The lack of standardization produces different results and invalidate the comparison of normative standards.

Among the existing CBCT-based methods of 3D cephalometric analysis, we highlight the study published by Gateno et al.[7] These authors present how to perform traditional cephalometric measurements to produce 3D values. The study is based on fundamentals of analytical geometry in 3D space, particularly in point-to-point distance, point-to-line distance, line-to-line angle, line-to-plane angle, and plane-to-plane angle. Inspired by this study, we extend the definitions of the cephalometric measurements performed by McNamara[11] to obtain 3D cephalometric measurements. McNamara describes a method of cephalometric analysis originally performed on lateral cephalograms. His method of analysis is well-known and usually applied by surgeons in clinical routine practices for the evaluation and treatment planning of orthodontic and orthognathic surgery patients. In contrast to studies published to date, our method explores the three-dimensionality of CBCT in its full extent, and con-

forms to original geometric definitions of the cephalometric lines and planes by McNamara.

2. Material and Methods

Our method, the CBCT-based 3D McNamara's cephalometric analysis, has 6 steps. In step 1, a 3D virtual representation of the patient's skull including the teeth (virtual skull) is created by applying the marching cubes algorithm[12,13] on CBCT images (Fig. 1). In step 2, the virtual skull is placed into the standard position of cephalometry. The virtual skull is horizontally and vertically aligned to the right *anatomic porion*, *nasion*, and left and right *orbitale* using the right lateral view and the frontal view of the virtual skull in parallel projection (Fig. 1).[4] In step 3, a coordinate system for the virtual skull is established. The cephalometric landmarks mentioned above and the left *anatomic porion* and *basion* are identified on the virtual skull (Fig. 2) to create the following cephalometric planes: the *Frankfort horizontal plane*, which is the least-squares best-fit plane[14,15] to the left and right *anatomic porion* and *orbitale*[7]; the *midsagittal plane*, which is a plane intersecting the *basion* and *nasion* and is orthogonal to the *Frankfort horizontal plane*; and the *transporionic plane*, which is a plane intersecting the midpoint between the left and right *anatomic porion* and is orthogonal to the *Frankfort horizontal plane* and *midsagittal plane*. These 3 planes inherently produces a 3D Cartesian coordinate system, whose origin is the point of intersection between them, and whose axes are on the lines where the planes intersect one another. We have established that the x-axis points to the left, the y-axis points forward, and the z-axis points down (Fig. 3). In step 4, the remaining cephalometric landmarks of the McNamara's analysis are identified on the virtual skull. The 3D definitions of the cephalometric landmarks are presented in Table 1 (Fig. 2).[4,16,17] In step 5, the cephalometric lines and planes of the McNamara's analysis are created in accordance with the 3D definitions presented in Table 2 (Fig. 4). Finally, in step 6, the cephalometric measurements of the McNamara's analysis are performed in accordance with the 3D definitions presented in Table 2 (Fig. 4).

3. Results

In our method, CBCT images are used instead of a lateral cephalometric radiography. Accordingly, the cephalometric analysis is performed on a virtual skull instead of on a cephalometric tracing. Nonetheless, the virtual skull is precisely placed into the standard position of cephalometry (steps 2 and 3). Compared to the McNamara's analysis, our method has the following differences: a) the cephalometric landmarks are represented by points with 3 coordinates (3D points) instead of points with 2 coordinates (2D points); b) the bilateral cephalometric landmarks are identified twice, one of each side of the virtual skull; c) the *nasion perpendicular*, the *point A vertical*, the *point A-pogonion line*, and the *facial plane* are represented by lines defined in a 3D space (3D lines) instead of lines defined in a 2D space (2D lines); d) the *Frankfort horizontal plane*, the *mandibular plane*, and the *facial axis* are represented by planes (which are intrinsically 3D) instead of 2D lines; e) the *effective mandibular length*, the *effective midfacial length*, and the *lower anterior facial height* are measured as distances between two 3D points (3D point-to-point distances) instead of

distances between two 2D points (2D point-to-point distances); f) the *nasion perpendicular to point A*, the *pogonion to nasion perpendicular*, the *upper incisor to point A vertical*, and the *lower incisor to point A-pogonion line* are measured as components of a vector instead of a directed distance from a 2D point to a 2D line (2D point-to-line distance); g) the *facial axis angle* is measured by as an angle between a 3D line and a plane (line-to-plane angle) instead of an angle between two 2D lines (2D line-to-line angle); h) the *mandibular plane angle* is measured as an angle between two planes (plane-to-plane angle) instead of a 2D line-to-line angle; and i) the *effective mandibular length*, the *effective midfacial length*, the *upper incisor to point A vertical*, and the *lower incisor to point A-pogonion line* are calculated for both sides of the virtual skull.

4. Discussion

This paper presents a new method, denoted CBCT-based 3D McNamara's cephalometric analysis, that extends the McNamara's cephalometric analysis.[11] The main contribution of our method is the establishment of a new way to perform cephalometric measurements taking full advantage of 3D information provided by CBCT imagery. In the following paragraphs, we contrast our method with related proposals that also consider CBCT-based 3D cephalometric measurements.

The *effective mandibular length*, the *effective midfacial length*, and the *lower anterior facial height* involve the calculation of the distance between 2 cephalometric landmarks.[11] In our method, this distance is measured as a 3D point-to-point distance instead of a 2D point-to-point distance since the cephalometric landmarks are 3D points instead of 2D points. Moreover, since the bilateral cephalometric landmarks are identified on both sides of the virtual skull, the *effective mandibular length* and the *effective midfacial length* are measured twice, one using the left *condylion* and other using the right *condylion* (Table 2). Among the related studies,[3–10] Cheung et al.[5], Damstra et al.[6], Swennen et al.[4], and Wong et al.[8] perform the *effective mandibular length*, the *effective midfacial length*, and the *lower anterior facial height* (Table 3). In all these studies, with the exception of Damstra et al., these 3 cephalometric measurements are performed in the same way as we do. On the other hand, Damstra et al. identify the left and right condylion on the virtual skull, but perform only the right *effective mandibular length* and the right *effective midfacial length*.

The *nasion perpendicular to point A*, the *pogonion to nasion perpendicular*, the *upper incisor to point A vertical*, and the *lower incisor to point A-pogonion line* involve the calculation of the directed distance from a cephalometric landmark to a cephalometric line, i.e. the absolute distance between both complemented by the landmark positioning in relation to the line.[11] In the McNamara's analysis, the directed distance is measured as a 2D point-to-line distance since the cephalometric landmarks are 2D points and the cephalometric lines are 2D lines. In our method, although the cephalometric landmarks are 3D points and the cephalometric lines are 3D lines, the distance in question is not measured as a 3D point-to-line distance because 3D point-to-line distance does not offer an easy, unambiguous way to obtain the directed distance from a 3D point to a 3D line. Therefore, we used a vector connecting orthogonally the line 3D to the 3D point and having the z-component parallel to

the 3D line. As a result, each of the 4 cephalometric measurements above provide 2 directed distances, one for the lateral view of the virtual skull, given by the x-component of the vector, and other for the posteroanterior view of the virtual skull, given by the y-component of the vector. Additionally in our method, the *upper incisor to point A vertical* and the *lower incisor to point A-pogonion line* are performed for the left and right sides of the virtual skull (Table 2).

Park et al.[3] and Wong et al.[8] perform the *nasion perpendicular to point A*, the *pogonion to nasion perpendicular*, the *upper incisor to point A vertical*, and the *lower incisor to point A-pogonion line* with a different approach (Table 3). The first 3 cephalometric measurements are calculated as point-to-plane distances, and the last cephalometric measurement is calculated as a 3D point-to-line distance. Although the original definitions of the cephalometric lines produce 3D lines in CBCT-based 3D cephalometry, only the *point A-pogonion line* is represent this way by Park et al. and Wong et al. The *nasion perpendicular* and the *point A vertical* are represented by planes orthogonal to the *midsagittal plane*. This restriction is required because there is not a single plane orthogonally intersecting the *Frankfort horizontal plane* from the *nasion* or the *point A*. However, the *nasion perpendicular to point A*, the *pogonion to nasion perpendicular*, and the *upper incisor to point A vertical* measured as point-plane distances produce the same results as 2D point-to-line distances. Consequently, the 3-dimensionality of CBCT is not truly explored.

The *facial axis angle* involves the calculation of the angle between 2 cephalometric lines, the *basion-nasion line* and the *facial axis*, and the *mandibular plane angle* involves the calculation of the angle between 2 cephalometric planes, the *mandibular plane* and the *Frankfort horizontal plane*.[11] These 2 cephalometric measurements are originally measured as a 2D line-to-line angle because both the cephalometric lines and planes are represented by 2D lines. In our method, the *facial axis angle* is measured as a line-to-plane angle and the *mandibular plane angle* is measured as a plane-to-plane angle because the *basion-nasion line* is represented by a 3D line and the *facial axis*, the *mandibular plane*, and the *Frankfort horizontal plane* are represented by planes.

In the McNamara's analysis, the *facial axis* is a line that connects the *pterygomaxillary fissure* to the *constructed gnathion*, and the *facial plane*, required to define the *constructed gnathion*, is a line that connects the *nasion* to the *pogonion*.[11] In our method, although the *facial axis* is a cephalometric line, it is represented by a plane instead of a 3D line because a 3D line alone is not able to intersect the left and right *pterygomaxillary fissure* and the *constructed gnathion*. Similarly, although the *facial plane* is a cephalometric plane, it is represented in our method by a 3D line instead of a plane because 2 cephalometric landmarks, the *nasion* and the *pogonion*, do not define a plane. In this context, Wong et al.[8] measure the *facial axis angle* as a 3D line-to-line angle (Table 3). In their method, both the *basion-nasion line* and the *facial axis* are 3D lines, and there are left and right *facial axis*. Compared to our method, Wong et al. also produce 3D values for the *facial axis angle*. However, their method is not appropriate for the studying the shape of the skull since the *facial axis angle* varies with the width and length of the mandible.

Concerning the *mandibular plane angle*, Cheung et al.[5], Park et al.[3], Swennen et al.[4], and Wong et al.[8] perform this cephalometric measurement (Table 3). We calculate the

mandibular plane angle in the same manner as Cheung et al. and Park et al. In contrast, Swennen et al. measure the *mandibular plane angle* as a 2D line-to-line angle, using the lines defined by the intersections of the *mandibular plane* and the *Frankfort horizontal plane* with the *midsagittal plane*. On the other hand, Wong et al. measure the *mandibular plane angle* as a line-to-plane angle. In their method, the *mandibular plane* is a 3D line, the *Frankfort horizontal plane* is a plane, and there are left and right mandibular plane. Compared to our method, Wong et al. also produce 3D values for the *mandibular plane angle*. However, their method is not appropriate for the studying the shape of the skull since the *mandibular plane angle* varies with the width and length of the mandible.

As already mentioned, our method is based on the study of Gateno et al.[7] Considering this study, we measured the *effective mandibular length*, the *effective midfacial length*, and the *lower anterior face height* as 3D point-to-point distances; the *facial axis angle* as a line-plane angle; and the *mandibular plane angle* as a plane-plane angle. However, unlike Gateno et al., we did not measure the *nasion perpendicular to point A*, the *pogonion to nasion perpendicular*, the *upper incisor to point A vertical*, and the *pogonion to point A-pogonion line* as 3D point-to-line distances. As explained above, 3D point-to-line distance does not allow the calculation of the directed distance from a 3D point to a 3D line. In our method, we use vectors for these 4 cephalometric measurements.

In short, our method provide a) real effective lengths of the maxilla and mandible on both sides of the skull; b) real height of the lower anterior face; c) directed distances from the *point A* to the *nasion perpendicular*, from the *pogonion* to the *nasion perpendicular*, from the left and right *upper incisor* to the *point A vertical*, and from the left and right *lower incisor* to the *point A-pogonion line* for both the lateral and posteroanterior views of the skull; and d) real angles of the *facial axis* and the *mandibular plane*. Moreover, the left and right *effective mandibular length*, the left and right *effective midfacial length*, the x-component of the *nasion perpendicular to point A*, and the x-component of the *pogonion to nasion perpendicular* allow the identification of craniofacial asymmetries.

Acknowledgments

This work was supported by the Coordination for the Improvement of Higher Education Personnel (CAPES), a foundation within the Ministry of Education in Brazil.

References

1. Grayson B, Cutting C, Bookstein FL, Kim H, McCarthy JG. The three-dimensional cephalogram: Theory, techniques, and clinical application. *Am J Orthod Dentofacial Orthop* 1988;94(4):327–337. doi:10.1016/0889-5406(88)90058-3.
2. Haffner CL, Pessa JE, Zadoo VP, Garza JR. A technique for three-dimensional cephalometric analysis as an aid in evaluating changes in the craniofacial skeleton. *Angle Orthod* 1999;69(4):345–348. doi:10.1043/0003-3219(1999)069<0345:ATFTDC>2.3.CO;2.
3. Park SH, Yu HS, Kim KD, Lee KJ, Baik HS. A proposal for a new analysis of craniofacial morphology by 3-dimensional computed tomography. *Am J Orthod Dentofacial Orthop* 2006;129(5):600.e23–600.e34. doi:10.1016/j.ajodo.2005.11.032.

4. Swennen GRJ, Schutyser F, Hausamen JE, eds. Three-Dimensional Cephalometry: A Color Atlas and Manual. Springer; 2006. ISBN 978-3-540-25440-9.
5. Cheung LK, Chan YM, Jayaratne YSN, Lo J. Three-dimensional cephalometric norms of Chinese adults in Hong Kong with balanced facial profile. *Oral Surg Oral Med Oral Pathol Oral Radiol* 2011;112(2):e56–e73. doi:10.1016/j.tripleo.2011.02.045.
6. Damstra J, Fourie Z, Slater JJRH, Ren Y. Reliability and the smallest detectable difference of measurements on 3-dimensional cone-beam computed tomography images. *Am J Orthod Dentofacial Orthop* 2011;140(3):e107–e114. doi:10.1016/j.ajodo.2011.02.020.
7. Gateno J, Xia JJ, Teichgraeber JF. New 3-dimensional cephalometric analysis for orthognathic surgery. *J Oral Maxillofac Surg* 2011;69(3):606–622. doi:10.1016/j.joms.2010.09.010.
8. Wong RWK, Chau ACM, Hägg U. 3D CBCT McNamara's cephalometric analysis in an adult southern Chinese population. *Int J Oral Maxillofac Surg* 2011;40(9):920–925. doi:10.1016/j.ijom.2011.03.011.
9. Bayome M, Park JH, Kook YA. New three-dimensional cephalometric analyses among adults with a skeletal Class I pattern and normal occlusion. *Korean J Orthod* 2013;43(2):62–73. doi:10.4041/kjod.2013.43.2.62.
10. Devanna R. Two-dimensional to three-dimensional: A new three-dimensional cone-beam computed tomography cephalometric analysis. *J Orthod Res* 2015;3(1):30–37. doi:10.4103/2321-3825.146356.
11. McNamara JAJ. A method of cephalometric evaluation. *Am J Orthod* 1984;86(6):449–469. doi:10.1016/s0002-9416(84)90352-x.
12. Lorensen WE, Cline HE. Marching cubes: A high resolution 3D surface construction algorithm. *Comput Graph* 1987;21(4):163–169. doi:10.1145/37402.37422.
13. Schroeder W, Martin K, Lorensen B. The Visualization Toolkit: An Object-Oriented Approach to 3D Graphics. 4 ed.; Kitware; 2006. ISBN 978-1-930934-19-1. URL: http://www.kitware.com/products/books/VTKTextbook.pdf.
14. Pearson K. On lines and planes of closest fit to systems of points in space. *Philos Mag* 1901;2(11):559–572. doi:10.1080/14786440109462720.
15. Ahn SJ. Least Squares Orthogonal Distance Fitting of Curves and Surfaces in Space. No. 3151 in Lecture Notes in Computer Science; Springer; 2004. ISBN 978-3-540-23966-6.
16. White TD, Black MT, Folkens PA. Human Osteology. 3 ed.; Elsevier; 2012. ISBN 978-0-12-374134-9.
17. Phulari BS. An Atlas on Cephalometric Landmarks. Jaypee Brothers Medical Publishers; 2008. ISBN 978-93-5090-324-7.

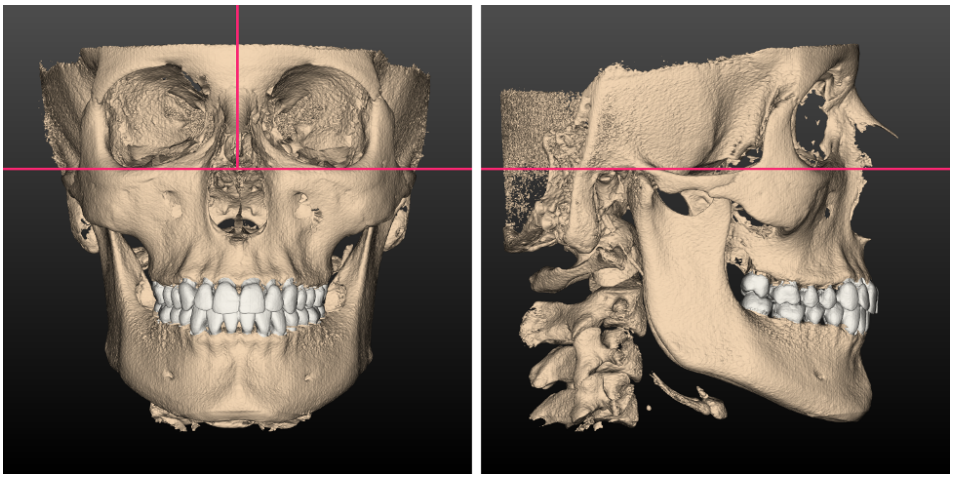

Figure 1. A virtual skull horizontally and vertically oriented to the right *anatomic porion*, *nasion*, and left and right *orbitale*.

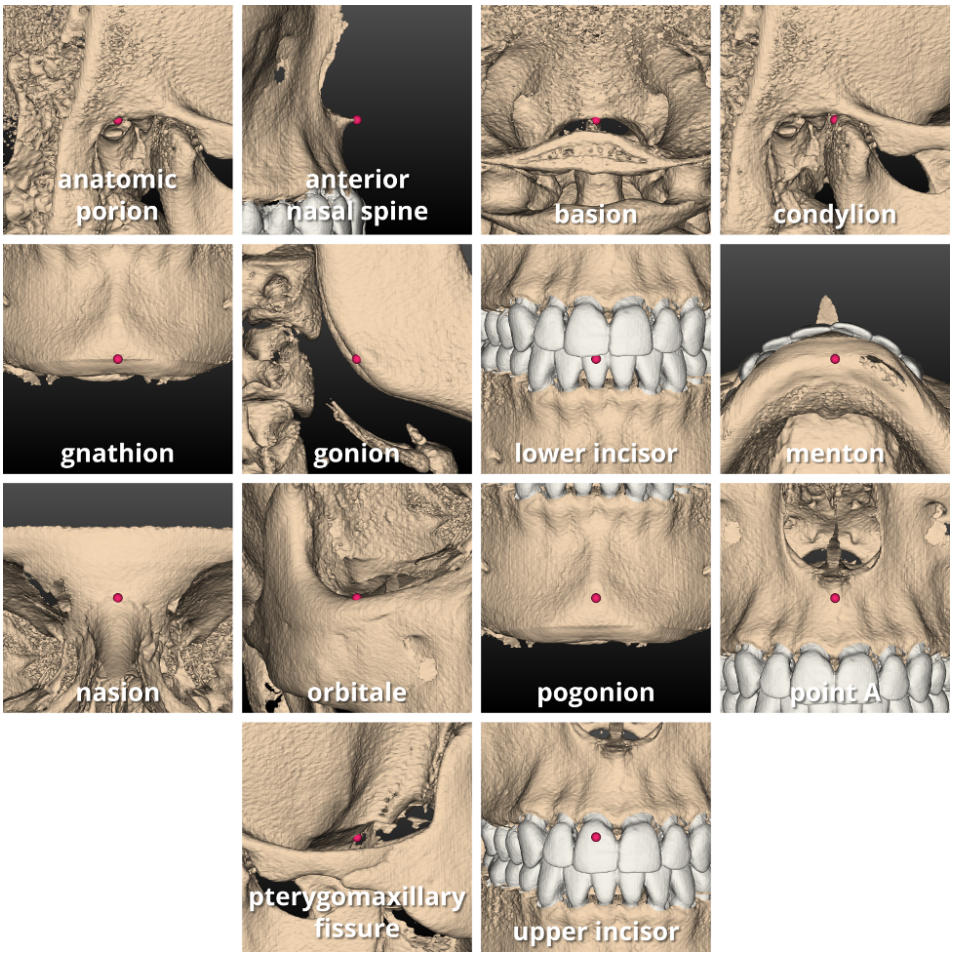

Figure 2. The cephalometric landmarks of the McNamara's analysis identified on a same virtual skull. Only the bilateral cephalometric landmarks on the right side of the virtual skull are shown.

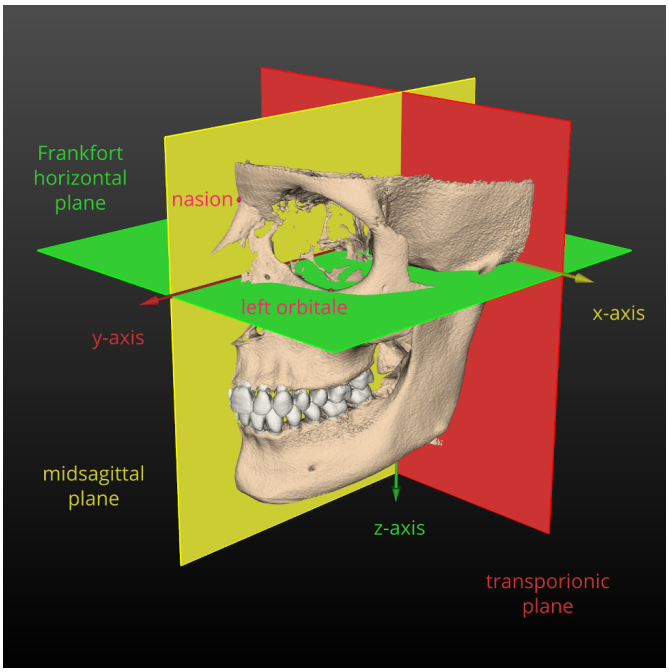

Figure 3. The 3D Cartesian coordinate system established for a virtual skull from the *Frankfort horizontal plane*, the *midsagittal plane*, and the *transporionic plane*. The axes of the coordinate system are not normalized in this picture.

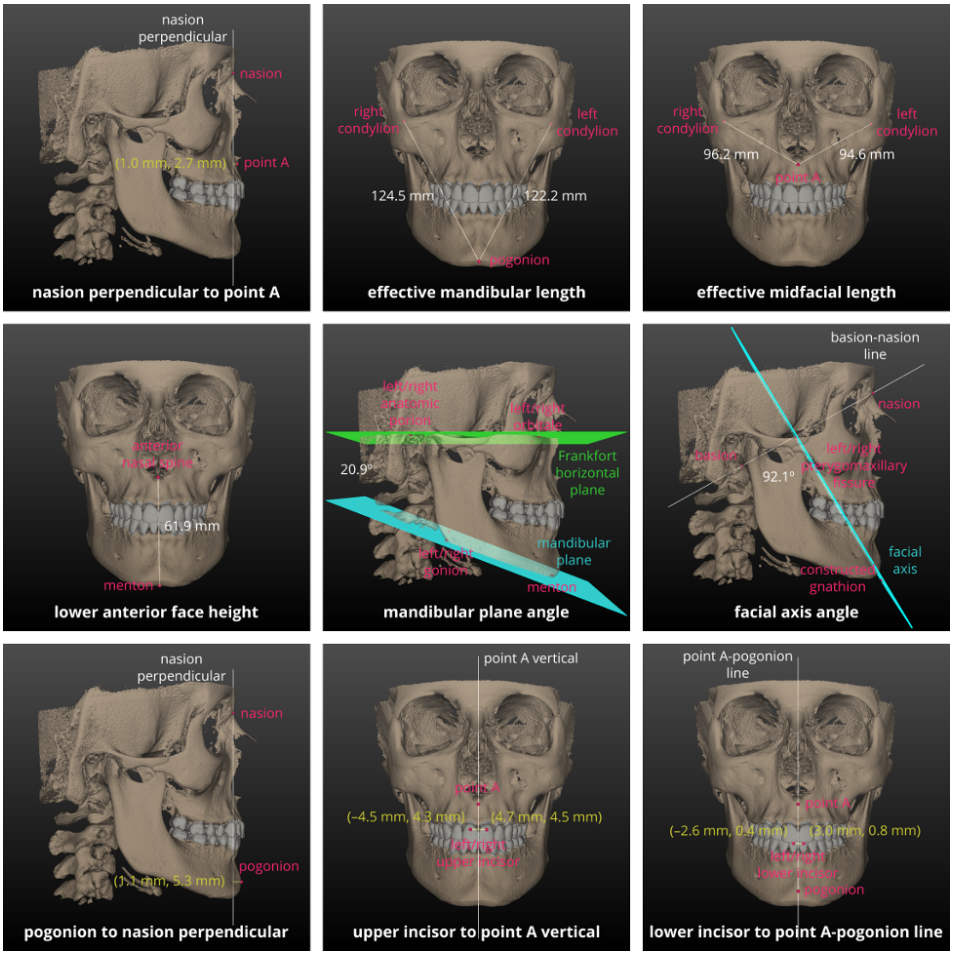

Figure 4. The CBCT-based 3D McNamara's cephalometric analysis performed on a same virtual skull.

Table 1. Three-dimensional definitions of the cephalometric landmarks of the McNamara's analysis.

Unilateral
Anterior nasal spine. The point on the tip of the anterior nasal spine.
Basion. The lowermost point on the midline of the anterior rim of the foramen magnum.
Gnathion. The most anteroinferior point on the mandibular symphysis.
Menton. The lowermost point on the mandibular symphysis.
Nasion. The point where the frontonasal and internasal sutures intersect.
Pogonion. The most anterior point on the mandibular symphysis.
Point A. The most posterior point on the intermaxillary suture.
Bilateral
Anatomic porion. The uppermost point on the margin of the left/right external acoustic meatus.
Condylion. The most posterosuperior point on the midline of the left/right mandibular condyle.
Gonion. The point where the line bisecting the angle formed by extending the posterior ramus border and the inferior body border intersect the gonial angle of the left/right mandibular ramus.
Lower incisor. The most anterior point on the midline of the labial surface of the left/right lower central incisor.
Orbitale. The lowermost point on the margin of the left/right orbital.
Pterygomaxillary fissure. The most posterosuperior point on the margin of the left/right pterygomaxillary fissure.
Upper incisor. The most anterior point on the midline of the labial surface of the left/right upper central incisor.

Table 2. Three-dimensional definitions of the cephalometric lines, planes, and measurements of the McNamara's analysis.

Maxilla to cranial base
Nasion perpendicular to point A. The vector connecting orthogonally the *nasion perpendicular* to the *point A*. The *nasion perpendicular* is a line intersecting orthogonally the *Frankfort horizontal plane* from the *nasion*.
Mandible to maxilla
Effective mandibular length. The distances between the *gnathion* and the left and right *condylion*.
Effective midfacial length. The distances between the *point A* and the left and right *condylion*.
Maxillomandibular differential. The differences between the *effective mandibular length* and *effective midfacial length* of the left and right side of the skull.
Lower anterior facial height. The distance between the *anterior nasal spine* and the *menton*.
Mandibular plane angle. The anteroinferior angle between the *mandibular plane* and *Frankfort horizontal plane*. The *mandibular plane* is a plane intersecting the left and right *gonion* and the *menton*.
Facial axis angle. The posteroinferior angle between the *basion-nasion line* and *facial axis*. The *basion-nasion line* is a line intersecting the *basion* and *nasion*. The *facial axis* is a plane intersecting the left and right *pterygomaxillary fissure* and the *constructed gnathion*. The *constructed gnathion* is the point where the *facial plane* and *mandibular plane* intersect. The *facial plane* is a line intersecting the *nasion* and *pogonion*.
Mandible to cranial base
Pogonion to nasion perpendicular. The vector connecting orthogonally the *nasion perpendicular* to the *pogonion*.
Dentition
Upper incisor to point A vertical. The vectors connecting orthogonally the *point A vertical* to the left and right *upper incisor*. The *point A vertical* is a line intersecting orthogonally the *Frankfurt horizontal plane* from the *point A*.
Lower incisor to point A-pogonion line. The vectors connecting orthogonally the *point A-pogonion line* to the left and right *lower incisor*. The *point A-pogonion line* is a line intersecting the *point A* and *pogonion*. Since this line is not necessarily parallel to the z-axis of the coordinate system, the following procedure is required to zero the z-components of the vectors: to rotate the vectors and the *point A-pogonion line* around an arbitrary axis mutually perpendicular to the z-axis and the *point A-pogonion line* until these two are parallel.

Table 3. How the cephalometric measurements of the McNamara's analysis are performed by other researchers in CBCT-based 3D cephalometry.

	Bayome et al. [9]	Cheung et al. [5]	Damstra et al. [6]	Devanna [10]	Gateno et al. [7]	Park et al. [3]	Swennen et al. [4]	Wong et al. [8]
effective mandibular length	–	3D point-to-point distance**	3D point-to-point distance	–	–	–	3D point-to-point distance	3D point-to-point distance
effective midfacial length	–	–	3D point-to-point distance	–	–	–	–	3D point-to-point distance
lower anterior facial height	*	3D point-to-point distance	3D point-to-point distance	–	–	–	*	3D point-to-point distance
nasion perpendicular to point A	–	–	–	–	–	point-to-plane distance	–	point-to-plane distance
pogonion to nasion perpendicular	–	–	–	–	–	point-to-plane distance	–	point-to-plane distance
upper incisor to point A vertical	–	–	–	–	–	–	–	point-to-plane distance
lower incisor to point A-pogonion line	–	–	–	–	–	–	–	3D point-to-line distance
facial axis angle	–	–	–	–	–	–	–	3D line-to-line angle***
mandibular plane angle	–	plane-to-plane angle	–	–	–	plane-to-plane angle	2D line-to-line angle	line-to-plane angle

* We did not consider the *lower anterior facial height* performed by Bayome et al. and Swennen et al. because the authors based on an other cephalometric definition of this measurement: the 'vertical' distance between the *anterior nasal spine* and *menton*. ** Cheung et al. use the *menton* instead of the *gnathion* for calculating the *effective mandibular length*. *** Wong et al. use the *gnathion* instead of the *constructed gnathion* for setting up the *facial axis*.

2.3 Publicação 3

Cone Beam Computed Tomography-Based Cephalometric Norms for Brazilian Adults

Rodrigo Mologni Gonçalves dos Santos
José Mario De Martino
Francisco Haiter Neto
Luis Augusto Passeri

International Journal of Oral and Maxillofacial Surgery

Janeiro de 2018

Int. J. Oral Maxillofac. Surg. 2018; 47: 64–71
http://dx.doi.org/10.1016/j.ijom.2017.06.030, available online at http://www.sciencedirect.com

International Journal of Oral & Maxillofacial Surgery

Clinical Paper
Orthognathic Surgery

Cone beam computed tomography-based cephalometric norms for Brazilian adults

R. M. G. Santos[1], J. M. De Martino[1], F. Haiter Neto[2], L. A. Passeri[3]
[1]Department of Computer Engineering and Industrial Automation, School of Electrical and Computer Engineering, University of Campinas, Campinas, SP, Brazil; [2]Department of Oral Diagnosis, Piracicaba Dental School, University of Campinas, Piracicaba, SP, Brazil; [3]Department of Surgery, School of Medical Sciences, University of Campinas, Campinas, SP, Brazil

R. M. G. Santos, J. M. De Martino, F. Haiter Neto, L. A. Passeri: Cone beam computed tomography-based cephalometric norms for Brazilian adults. Int. J. Oral Maxillofac. Surg. 2018; 47: 64–71.

Abstract. This study established cone beam computed tomography (CBCT)-based cephalometric norms for Brazilian adults, including the assessment of sexual dimorphism. An observer performed McNamara's cephalometric analysis twice on 60 CBCT datasets acquired from patients with a normal dental occlusion, divided equally into two groups by sex. Welch's *t*-test was applied to assess differences between the sexes in hard tissue cephalometric measurements, and Dahlberg's formula was used to calculate measurement error introduced by the observer. The cephalometric measurements of effective mandibular length, effective midfacial length, maxillomandibular differential, and lower anterior facial height presented sexual dimorphism. Linear measurements had error $\leq$0.78 mm, and angular measurements had error $\leq$1.24°. The results show that (1) the CBCT-based cephalometric norms established in this study are reliable for use by researchers and clinicians, and (2) Brazilian adult males and females have similar craniofacial morphology, with males possessing larger jaws than females.

Key words: orthodontics; cephalometry; three-dimensional imaging; dental occlusion; reference values.

Accepted for publication 6 June 2017
Available online 11 August 2017

Since its introduction by Broadbent in 1931, cephalometric radiography has been the standard craniofacial imaging technique used by clinicians for evaluating and planning the treatment of orthodontic and orthognathic surgery patients[1]. However, its position has been increasingly challenged by cone beam computed tomography (CBCT), the state-of-the-art imaging technique in the field of oral and maxillofacial surgery, introduced by Mozzo et al. in 1998[2]. CBCT has been gaining acceptance over radiography, since the latter produces undesirable effects inherently related to perspective projection, such as size and shape distortion, superimposition, and misrepresentation of anatomical structures, which can jeopardize cephalometric analysis[3]. These effects affect cephalometric measurement outcomes, mainly because they amplify values and distort the correct location of cephalometric landmarks[4,5]. Besides overcoming these problems, CBCT provides an accurate and reliable three-dimensional (3D) image of the patient's skull[5–7]. Among other advantages, CBCT allows clinicians to virtually orient the head after the image acquisition process, obtain the 3D position of cephalometric landmarks

0901-5027/01064 + 08

virtually identified on anatomical structures of the head, and perform 3D cephalometric measurements[8].

Prior studies have shown that cephalometric measurements performed on craniofacial images acquired from cephalometric radiography and CBCT present statistically significant and clinically relevant differences[9–11]. Consequently, cephalometric norms derived from the traditional radiographic analyses are not adequate for CBCT-based cephalometric analyses. Additionally, the ever-increasing use of CBCT imagery in routine clinical practice has also pushed the need for cephalometric norms based on CBCT technology[12].

Cephalometric norms are of paramount importance from a clinical point of view, as they provide useful guidelines for clinicians in planning orthodontic and surgical treatments. CBCT-based cephalometric norms have been established for Chinese[13–15], Indian[16], Korean[17], and Turkish[18] populations. However, CBCT-based cephalometric norms for Brazilians appear to be lacking. This study aimed to contribute to the establishment of such norms. In summary, the well-known method of cephalometric analysis developed by McNamara in 1984 was applied to a database of CBCT images acquired from adult male and female Brazilian subjects[19]. Furthermore, sexual dimorphism was assessed statistically.

Materials and methods

This study conformed to the ethical standards and procedures for biomedical research involving human subjects of the National Health Council of Brazil. The study was reviewed and approved by the Human Research Ethics Committee of the School of Medical Science at the University of Campinas.

Data collection

A total of 60 CBCT datasets acquired from Brazilian adults of European descent (30 male and 30 female) were obtained from the clinical archive of the Division of Oral Radiology, Piracicaba Dental School, University of Campinas. Inclusion criteria were the following: CBCT datasets from patients with a normal dental occlusion, age 18–35 years, and presence of all teeth (wearing or not dental braces or implants); the CBCT datasets had to have a large field of view (16 cm in diameter and 13–22 cm in height) and voxel size $\leq$0.4 mm^3. The following exclusion criteria were applied: CBCT datasets from patients who had undergone surgery of the facial bones or who had an abnormal facial asymmetry, and CBCT datasets with severe noise.

Procedure

The four steps described below were performed on each CBCT dataset by one observer. The last two steps were performed twice for the estimation of the technical error of measurement (TEM)[20]. The second observation was done almost 2 years after the first observation. A graphics software toolkit was developed by the first author specifically for these steps. The Python programming environment (version 2.7.7; Python Software Foundation, Beaverton, OR, USA) and its NumPy (version 1.7.1; NumFOCUS, Austin, TX, USA), PyQt (version 4.11; Riverbank Computing Ltd, Wimborne, Dorset, UK), and VTK (version 6.1.0; Kitware Inc., Clifton Park, NY, USA) extension packages were used to produce the toolkit.

In step 1, the patient's skull was virtually reconstructed (Fig. 1). The marching cubes algorithm was applied to the CBCT dataset to build a high-resolution 3D geometric model representing the hard tissue surface of the head[21]. For greater precision, different contour values were considered for bones and teeth since both have different radiodensitiy values.

In step 2, the reconstructed skull was precisely placed in a standardized position oriented to the Frankfort horizontal (FH) and midsagittal reference planes (Fig. 1). To accomplish this, the left and right porion, left and right orbitale, basion, and nasion hard tissue cephalometric landmarks were first marked on the reconstructed skull (Table 1, Fig. 2). Next, the FH, midsagittal, and transporionic planes were created (Fig. 1). The FH is the least-squares best-fit plane to the left and right porion and left and right orbitale[22]. The midsagittal plane intersects the basion and nasion landmarks and is orthogonal to the FH plane. The transporionic plane intersects the midpoint between the left and right porion, and is mutually orthogonal to the other two planes. Finally, the three planes were used to set up a 3D Cartesian coordinate system, where the origin is the intersection point between these planes. The *x*-axis is a leftward vector normal to the midsagittal plane, the *y*-axis is a frontward vector normal to the transporionic plane, and the *z*-axis is a downward vector normal to the FH plane.

In step 3, the hard tissue cephalometric landmarks required to perform McNamara's cephalometric analysis were marked on the reconstructed skull (Fig. 2). The 3D definition shown in Table 1 was used, where unpaired landmarks are located in the midsagittal plane and paired landmarks lie on either side of this plane.

In step 4, McNamara's cephalometric analysis was performed on the midsagittal plane by orthogonally projecting the landmarks. For paired landmarks, the midpoint between the two was projected orthogonally onto the midsagittal plane. Cephalometric reference lines and planes used in McNamara's cephalometric analysis are

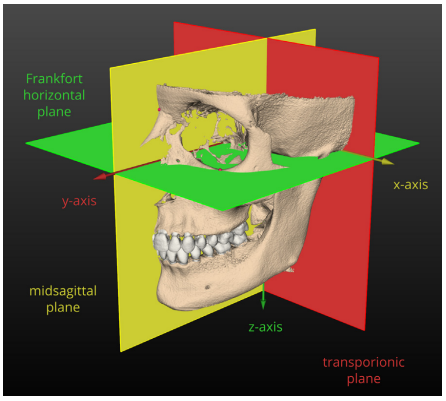

Fig. 1. A reconstructed skull placed in a standardized position oriented to the midsagittal, transporionic, and Frankfort horizontal planes. Three-dimensional hard tissue cephalometric landmarks are represented by magenta spheres of 1-mm radius; only the nasion and left porion are visible in this view of the skull.

Table 1. Three-dimensional definition of the cephalometric landmarks used in McNamara's cephalometric analysis.

	Name	Definition
Unpaired		
1.	Nasion (N)	The point where the frontonasal and internasal sutures intersect
2.	Anterior nasal spine (ANS)	The point on the tip of the anterior nasal spine
3.	Point A (A)	The most posterior point on the intermaxillary suture
4.	Pogonion (Pog)	The most anterior point on the mandibular symphysis
5.	Gnathion (Gn)	The most antero-inferior point on the mandibular symphysis
6.	Menton (Me)	The lowermost point on the mandibular symphysis
7.	Basion (Ba)	The lowermost point on the midline of the anterior rim of the foramen magnum
Paired		
8.	Orbitale (Or)	The lowermost point on the margin of each orbit
9.	Pterygomaxillary fissure (Pt)	The most posterosuperior point on the margin of each pterygomaxillary fissure
10.	Upper incisor (UI)	The most anterior point on the midline of the labial surface of each upper central incisor
11.	Lower incisor (LI)	The most anterior point on the midline of the labial surface of each lower central incisor
12.	Gonion (Go)	The point where the line bisecting the angle formed by extending the posterior ramus border and the inferior body border intersect the gonial angle of each mandibular ramus
13.	Condylion (Cd)	The most posterosuperior point on the midline of each mandibular condyle
14.	Porion (Po)	The uppermost point on the margin of each external acoustic meatus

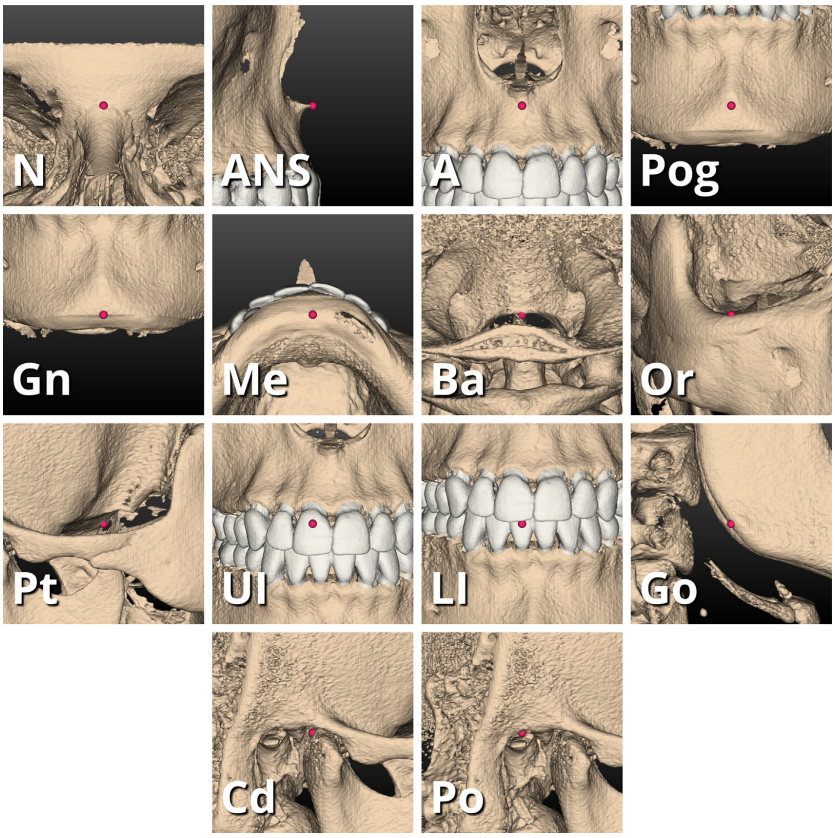

Fig. 2. Three-dimensional hard tissue cephalometric landmarks marked on a reconstructed skull. They are represented by magenta spheres of 1-mm radius. For paired landmarks, only that located on the right side of the skull is shown.

Table 2. Cephalometric reference lines and planes used in McNamara's cephalometric analysis.

	Name	Definition
Planes		
1.	Frankfort horizontal plane	The line crossing the Po and Or landmarks
2.	Mandibular plane	The line crossing the Go and Me landmarks
3.	Facial plane	The line crossing the N and Pog landmarks
4.	Facial axis	The line crossing the Pt landmark and the point where the mandibular and facial planes intersect (named constructed gnathion)
Lines		
5.	Nasion perpendicular	The line crossing the N landmark and orthogonal to the Frankfort horizontal plane
6.	Basion–nasion line	The line crossing the Ba and N landmarks
7.	Point A vertical	The line crossing the A landmark and orthogonal to the Frankfort horizontal plane
8.	Point A–pogonion line	The line crossing the A and Pog landmarks

defined in Table 2, and the cephalometric measurements used in McNamara's analysis are listed in Table 3.

Statistical analysis

The mean value of the two observations was used to calculate the cephalometric norms. Welch's *t*-test, an adaptation of Student's *t*-test for comparing two independent normal samples with unknown and unequal variances, was applied to calculate the probability (*p*-value) of sexual dimorphism for each of the hard tissue cephalometric measurements[23]. Dahlberg's formula was applied to estimate the TEM introduced by the observer[20]. The R (version 3.1.0; R Foundation for Statistical Computing, Vienna, Austria) statistical computing environment was used to perform the statistical analyses.

Results

A total of 1200 hard tissue cephalometric measurements were performed for this study (60 subjects × 10 measurements × 2 observations). CBCT-based cephalometric norms for Brazilian adults are presented in Tables 4 and 5. Only four out of 10 hard tissue cephalometric measurements indicated sexual dimorphism: effective mandibular length, effective midfacial length, maxillomandibular difference, and lower anterior facial height (Table 6). This assessment considered a significance level of 0.01.

The TEM of the hard tissue cephalometric measurements is shown in Table 7. Linear measurements had error of $\leq$0.78 mm, and angular measurements had error of $\leq$1.24°.

Discussion

CBCT-based cephalometric norms for Brazilian adults were established in the current study (Tables 4 and 5). McNamara's cephalometric analysis was performed to generate these normative values. Orthogonal projection of 3D hard tissue cephalometric landmarks onto the midsagittal reference plane and the midpoints between paired landmarks were used to perform this analysis. Sexual dimorphism was also assessed.

The statistical analysis of the cephalometric norms revealed that males and females have similar craniofacial mor-

Table 3. Cephalometric measurements used in McNamara's cephalometric analysis.

Name	Definition
Maxilla to cranial base	
1. Nasion perpendicular to point A (NpA)	The distance (in millimetres) from the A landmark to the nasion perpendicular If the point is more posteriorly positioned than the reference line, a negative sign is required
Mandible to maxilla	
2. Effective mandibular length (EML)	The distance (in millimetres) between the Cd and Gn landmarks
3. Effective midfacial length (EMdL)	The distance (in millimetres) between the A and Cd landmarks
4. Maxillomandibular difference (MD)	The difference (in millimetres) between EML and EMdL
5. Lower anterior face height (LAFH)	The distance (in millimetres) between the Me and ANS landmarks
6. Mandibular plane angle (MPA)	The antero-inferior angle (in degrees) between the Frankfort horizontal and mandibular planes
7. Facial axis angle (FAA)	The postero-inferior angle (in degrees) between the basion–nasion line and the facial axis
Mandible to cranial base	
8. Pogonion to nasion perpendicular (PogNp)	The distance (in millimetres) from the Pog landmark to the nasion perpendicular If the point is more posteriorly positioned than the reference line, a negative sign is required
Dentition	
9. Upper incisor to point A vertical (UIAv)	The distance (in millimetres) from the UI landmark to the point A vertical If the point is more posteriorly positioned than the reference line, a negative sign is required
10. Lower incisor to point A–pogonion line (LIAPog)	The distance (in millimetres) from the LI landmark to the point A–pogonion line If the point is more posteriorly positioned than the reference line, a negative sign is required

Table 4. CBCT-based cephalometric norms for Brazilian adults—males.

	Name	Mean	SD	SEM	95% CI		Range				
					Lower	Upper	Min	Q1	Q2	Q3	Max
1.	NpA (mm)	2.23	4.01	0.73	0.74	3.73	−5.24	−0.94	1.93	4.12	10.33
2.	EML (mm)	118.55	5.57	1.02	116.47	120.63	108.72	115.33	117.30	122.69	133.87
3.	EMdL (mm)	88.21	4.59	0.84	86.49	89.92	78.77	85.21	88.30	91.07	96.90
4.	MD (mm)	30.34	4.24	0.77	28.76	31.92	21.97	28.51	30.31	31.73	42.64
5.	LAFH (mm)	68.93	6.99	1.28	66.32	71.54	54.33	62.52	69.70	73.90	83.45
6.	MPA (°)	23.19	6.02	1.10	20.94	25.44	10.38	19.34	23.87	27.83	32.92
7.	FAA (°)	89.52	5.26	0.96	87.55	91.48	81.04	85.44	89.93	92.75	98.35
8.	PogNp (mm)	1.45	6.44	1.18	−0.95	3.86	−9.87	−3.98	2.31	6.51	13.77
9.	UIAv (mm)	5.57	1.94	0.35	4.85	6.29	1.99	4.25	5.34	6.78	9.47
10.	LIAPog (mm)	2.69	2.51	0.46	1.75	3.62	−2.04	0.95	3.13	4.50	8.28

CBCT, cone beam computed tomography; SD, standard deviation; SEM, standard error of the mean; 95% CI, 95% confidence interval of the mean; Min, minimum value; Q1, lower quartile; Q2, median; Q3, upper quartile; Max, maximum value.

Table 5. CBCT-based cephalometric norms for Brazilian adults—females.

	Name	Mean	SD	SEM	95% CI		Range				
					Lower	Upper	Min	Q1	Q2	Q3	Max
1.	NpA (mm)	1.76	2.75	0.50	0.73	2.79	−5.28	0.04	1.24	4.10	6.89
2.	EML (mm)	110.48	3.16	0.58	109.30	111.66	102.91	108.42	110.82	112.39	116.60
3.	EMdL (mm)	83.51	2.52	0.46	82.57	84.45	78.65	82.01	83.19	84.83	89.07
4.	MD (mm)	26.97	3.30	0.60	25.74	28.20	19.87	24.34	27.12	29.04	33.25
5.	LAFH (mm)	64.31	5.80	1.06	62.15	66.48	52.66	60.17	65.33	67.64	75.41
6.	MPA (°)	24.88	4.10	0.75	23.35	26.41	16.35	21.58	24.48	27.92	34.69
7.	FAA (°)	88.54	4.67	0.85	86.80	90.29	78.26	86.51	88.79	92.16	97.90
8.	PogNp (mm)	−0.05	5.81	1.06	−2.22	2.12	−11.99	−5.15	1.20	4.05	9.03
9.	UIAv (mm)	5.88	1.60	0.29	5.28	6.48	3.43	4.64	5.45	6.63	9.70
10.	LIAPog (mm)	3.84	1.51	0.28	3.28	4.40	1.06	2.92	3.88	4.71	6.97

CBCT, cone beam computed tomography; SD, standard deviation; SEM, standard error of the mean; 95% CI, 95% confidence interval of the mean; Min, minimum value; Q1, lower quartile; Q2, median; Q3, upper quartile; Max, maximum value.

phology; however males have larger jaws than females (Table 6). Other studies have also detected sexual dimorphism in CBCT-based cephalometric measurements performed on samples of other populations[13–15,17,24]. These studies also show that adult males have craniofacial dimensions larger than those of females.

The statistical analysis of TEM indicated no clinically relevant differences between the two observations, considering that errors in linear measurements of ≤1 mm and angular measurements of ≤1.5° are clinically acceptable (Table 7). Therefore, the cephalometric measurements are reliable for use by researchers and clinicians. However, the normative values suggested in this paper should be used with discretion, as the total number of patients involved in this study was small and consequently the statistical power is weak.

Table 6. CBCT-based cephalometric norms for Brazilian adults—difference between males and females.

	Name	Difference[a]	*P*-value
1.	NpA (mm)	0.47	0.599
2.	EML (mm)	8.07	≤0.0001
3.	EMdL (mm)	4.70	≤0.0001
4.	MD (mm)	3.37	≤0.01
5.	LAFH (mm)	4.62	≤0.01
6.	MPA (°)	−1.69	0.21
7.	FAA (°)	0.98	0.451
8.	PogNp (mm)	1.50	0.347
9.	UIAv (mm)	−0.31	0.507
10.	LIAPog (mm)	−1.15	≤0.05

In CBCT-based 3D cephalometry, both the FH and midsagittal reference planes are usually defined by three points[8,13,14,16,17]. The FH plane is created either from both porions and one of the two orbitales or the midpoint between them; or from both orbitales and one of the two porions or the midpoint between them. Altogether, there are six different ways of setting up the FH plane. In order to minimize error caused by different setups of the FH plane, an alternative and more robust method was used in this study: the least-squares best-fit plane to both pairs of porions and orbitales[22]. The midsagittal plane is created from two unpaired landmarks located on the cranial bones and one unpaired landmark located on the upper or lower jaw. However, these three landmarks do not necessarily produce a midsagittal plane orthogonal to the FH plane. Moreover, the landmarks located on the jaws are subject to changes in position following orthognathic surgery. Considering these problems, only two unpaired landmarks located on the cranial bones – basion and nasion – were used in this study. These were chosen because they are postero-anterior far apart from each other and are in McNamara's analysis.

Table 7. Technical error of measurement (TEM) for the cephalometric measurements.

	Name	Dahlberg's formula
1.	NpA (mm)	0.31
2.	EML (mm)	0.32
3.	EMdL (mm)	0.69
4.	MD (mm)	0.78
5.	LAFH (mm)	0.50
6.	MPA (°)	0.84
7.	FAA (°)	1.24
8.	PogNp (mm)	0.20
9.	UIAv (mm)	0.34
10.	LIAPog (mm)	0.18

The hard tissue cephalometric landmarks of McNamara's analysis were originally identified on cephalometric radiographs and not on CBCT scans, where depth and accurate information about the 3D anatomical structures are available. Therefore, the

definitions of these landmarks had to be adapted accordingly for the 3D analysis, as presented in Table 1. These definitions are based on the craniometric and 3D cephalometric definitions presented by Swennen et al.[8], White et al.[25], and Phulari[26]. As the skull is not quite symmetric, the unpaired landmarks were not identified on the midline of the skull (midsagittal reference plane), but on the midline of the bone where they are located. The basion, pterygomaxillary fissures, and porions are difficult to identify. The postero-inferior view of the skull is useful for identifying the basion. The pterygomaxillary fissures are identified in the lateral view of the skull, but they are hidden behind the zygomatic process of the temporal bone. The porions are also identified in the lateral view of the skull, but the inferior view is required to determine the margin of the external acoustic meatus, i.e. the depth of these points in the cranium.

Wong et al.[14] and Liang et al.[15] also applied McNamara's cephalometric analysis to CBCT datasets in order to establish cephalometric norms. These studies, however, present the following deficiencies: (1) The reconstructed skulls were positioned relative to the FH and midsagittal reference planes in the first study. However, a coronal plane, required to set up a 3D Cartesian reference system, was not considered by the authors. In the second study, information about the standard position of the skull was not provided. (2) In the first study, the FH plane was defined from two orbitales and one porion (either left or right), and the midsagittal plane was defined from the nasion, sella, and anterior nasal spine. Standardization of the FH plane is required, otherwise it may produce different measurement outcomes[27]. The anterior nasal spine is not recommended for setting up the midsagittal plane, because it is situated on a breakable bone of the maxilla. Moreover, the landmarks used hardly ever produce planes orthogonal to each other. In the second study, the FH plane was defined from the porion and orbitale in the right lateral view. Inadequate frontal orientation of the skull was not addressed in that paper. (3) Conventional and 3D definitions were adopted for the hard tissue cephalometric landmarks in the first and second studies, respectively. The 3D definitions established by Swennen et al.[8] were adopted in the first study. However, the pterygomaxillary fissure was not mentioned, and the upper and lower incisors were not equivalent to McNamara's analysis. In the second study, the gnathion, gonion, and upper incisor landmarks were incorrectly defined, and the gonion, pterygomaxillary fissure, and lower incisor landmarks were not defined. (4) According to the authors, 3D hard tissue cephalometric measurements were performed in the first study. However, it is not clear whether these measurements were truly in 3D. Hard tissue cephalometric measurements, similar to those presented in this paper, were performed in the second study. However, maxillomandibular difference, mandibular plane angle, facial axis angle, and lower incisor to point A–pogonion line were not calculated. These shortcomings were carefully addressed in the current study.

Cephalometric radiography inherently produces two-dimensional (2D) craniofacial images with size and shape distortions, superimposition, and misrepresentation of the anatomical structures[3]. On the other hand, CBCT produces 3D craniofacial images, which naturally overcomes these undesirable effects[5–7]. CBCT also presents the advantage of allowing the generation of the traditional images used in clinical orthodontics, such as lateral and postero-anterior cephalometric and panoramic radiographs. Additionally, CBCT images enable clinicians to position the patient's virtual head after image acquisition, to obtain 3D coordinates of cephalometric landmarks, to carry out 3D cephalometric measurements, and to perform other useful applications that are not possible using radiographs[8]. However, CBCT has not replaced radiographs mainly because it exposes the patient to more doses of radiation than radiography for standard orthodontic documentation. Therefore, CBCT has just been used for cases in which 3D visualization is necessary, such as the diagnosis and treatment planning of patients with severe craniofacial problems.

Size distortion is an artefact of radiography caused by the emission of X-rays from the source in increasing divergent angles passing through the patient's head until reaching the X-ray detector, where the 2D craniofacial image is created. In the present study, to avoid such distortion, cephalometric measurements were performed based on orthogonal projection instead of the typical perspective projection of cephalometric radiography. As a result, normative values without enlargement were produced. The cephalometric measurements were also performed on the midsagittal reference plane, because the magnification factor of cephalometric radiography is measured on this plane.

This study used CBCT datasets of subjects with normal facial asymmetry, meaning that the measurement differences between the two sides of the subjects' skulls are not statistically significant or clinically relevant[17]. Therefore, individual cephalometric measurements on each side of the skull were not performed, as has been done by other researchers[14,15]. It is important to note that maxillofacial surgeons rectify problems of craniofacial asymmetry based on the midsagittal plane and not on normative values.

It is also important to observe that 3D cephalometric measurements were not performed as done by Wong et al.[14], firstly because McNamara's cephalometric analysis is 2D and it was not a goal to change this analysis. The objective was to take advantage of CBCT-based 3D cephalometry to produce accurate and reliable cephalometric norms. Secondly, since CBCT is not currently the standard craniofacial imaging technique in routine clinical practice, norms compatible with both cephalometric radiography and CBCT were established. For radiography, the magnification factor needs to be considered.

Cephalometric measurements performed on CBCT images are more accurate and reliable than those performed on radiographic images[28]. Moreover, cephalometric analysis of CBCT images using orthogonal projection avoids the size distortion inherently associated with perspective projection of radiographs. However, studies show that cephalometric measurements performed on CBCT images using orthogonal projection are different from those performed on radiographic images[9–11]. Therefore to take full advantage of the analysis of CBCT images using orthogonal projection, it is necessary to define appropriate CBCT cephalometric norms. The current study seeks to contribute to the definition of such norms.

Since McNamara's composite norms were derived from the analysis of almost 1000 X-ray images, and recent studies have used fewer than 100 CBCT images[13–18], it is argued that, for now, cephalometric norms originated from cephalometric radiographs should continue to be used by clinicians for CBCT-based cephalometric analysis. In order to compare the cephalometric norms from the present study with McNamara's composite norms, it is necessary to resize the norms of the present study using the magnification factor reported by McNamara[19]. When the magnification factor is considered, the differences in the measurements performed on radiographic and CBCT images are not statistically significant[9,29].

McNamara identified a geometric relationship between the upper and lower jaws that is not directly related to the age or sex of a person[19]. According to McNamara, people with well-balanced faces and good occlusions have a mandible of 113–116 mm in length and lower face of 63–64 mm in height when the midface is 90 mm in length; and a mandible of 122–125 mm in length and lower face of 67–69 mm in height when the midface is 95 mm in length. Considering the 8% magnification factor reported by McNamara applied to the means presented in Tables 4 and 5, the gold standard for males has a midface 95 mm in length, a mandible 128 mm in length, and a lower face 74 mm in height, and the gold standard for females has a midface 90 mm in length, a mandible 119 mm in length, and a lower face 69 mm in height. Consequently, both gold standards have a length of the mandible (3 mm) and a height of the lower face (5 mm) higher than McNamara's upper limits. The results suggest that McNamara's composite norms (relating the mandible to the maxilla) are not appropriate to the population sample considered in this study. In conclusion, orthognathic surgeons should consider the above differences to preserve the ethnic features of Brazilian adult patients. However, it is recognized that a more extensive study, considering a larger sample size, is required to confirm this hypothesis.

Statistically significant and clinically relevant differences between the Brazilian adult males and females in the effective length of the midface and mandible, in the difference in length between the two, and in the height of the lower face were also identified (Table 6; p-values ≤ 0.01). The means of these cephalometric measurements were found to be higher in males than in females. The results indicate that males have larger jaws than females, but similar craniofacial morphology, since only the size measurements that relate the jaws one to another were found to be subject to sexually dimorphism. Therefore, maxillofacial surgeons should consider the measurement differences to preserve the sexual features of Brazilian adult patients. Once again, it is recognized that a study with a larger sample size is required to confirm this hypothesis.

In conclusion, the results show that (1) the CBCT-based cephalometric norms established in this study are reliable for use by researchers and clinicians, and (2) Brazilian adult males and females have similar craniofacial morphology, with males possessing larger jaws than females.

Funding

The first author has received financial support from the Coordination for the Improvement of Higher Education (Capes), a foundation within the Ministry of Education in Brazil.

Competing interests

There are no relationships/conditions/circumstances that present a potential conflict of interest.

Ethical approval

The Human Research Ethics Committee of the School of Medical Sciences (FCM) at the University of Campinas (Unicamp) reviewed and approved this study. It was registered with the National Health Council of Brazil under protocol number 27917314.0.0000.5404.

Patient consent

Francisco Haiter Neto, co-author of this paper, provided access to a cone beam computed tomography database belonging to the Piracicaba Dental School (FOP) at the University of Campinas (Unicamp), where he is professor.

References

1. Broadbent BH. A new X-ray technique and its application to orthodontia. *Angle Orthod* 1931;**1**:45–66. http://dx.doi.org/10.1043/0003-3219(1931)001<0045:ANXTAI>2.0.CO;2.
2. Mozzo P, Procacci C, Tacconi A, Martini PT, Andreis IAB. A new volumetric CT machine for dental imaging based on the cone-beam technique: preliminary results. *Eur Radiol* 1998;**8**:1558–64. http://dx.doi.org/10.1007/s003300050586.
3. Kapila SD. Contemporary concepts of cone beam computed tomography in orthodontics. In: Kapila SD, editor. *Cone beam computed tomography in orthodontics: indications, insights, and innovations*. Danvers: John Wiley & Sons; 2014. p. 5–42.
4. Damstra J, Slater JJRH, Fourie Z, Ren Y. Reliability and the smallest detectable differences of lateral cephalometric measurements. *Am J Orthod Dentofac Orthop* 2010;**138**:546. http://dx.doi.org/10.1016/j.ajodo.2010.05.013. e1–546. e8.
5. Gribel BF, Gribel MN, Frazão DC, McNamara Jr JA, Manzi FR. Accuracy and reliability of craniometric measurements on lateral cephalometry and 3D measurements on CBCT scans. *Angle Orthod* 2011;**81**:26–35. http://dx.doi.org/10.2319/032210-166.1.
6. Berco M, Rigali PH, Miner RM, DeLuca S, Anderson NK, Will LA. Accuracy and reliability of linear cephalometric measurements from cone-beam computed tomography scans of a dry human skull. *Am J Orthod Dentofac Orthop* 2009;**136**:17. http://dx.doi.org/10.1016/j.ajodo.2008.08.021. e1–17. e9.
7. Kamburoğlu K, Kolsuz E, Kurt H, Kılıç C, Özen T, Paksoy CS. Accuracy of CBCT measurements of a human skull. *J Digit Imaging* 2011;**24**:787–93. http://dx.doi.org/10.1007/s10278-010-9339-9.
8. Swennen GR, Schutyser F, Hausamen JE. *Three-dimensional cephalometry: a color atlas and manual*. New York: Springer; 2006
9. Kumar V, Ludlow JB, Mol A, Cevidanes L. Comparison of conventional and cone beam CT synthesized cephalograms. *Dentomaxillofac Radiol* 2007;**36**:263–9. http://dx.doi.org/10.1259/dmfr/98032356.
10. van Vlijmen OJC, Maal T, Bergé SJ, Bronkhorst EM, Katsaros C, Kuijpers-Jagtman AM. A comparison between two-dimensional and three-dimensional cephalometry on frontal radiographs and on cone beam computed tomography scans of human skulls. *Eur J Oral Sci* 2009;**117**:300–5. http://dx.doi.org/10.1111/j.1600-0722.2009.00633.x.
11. van Vlijmen OJC, Maal T, Bergé SJ, Bronkhorst EM, Katsaros C, Kuijpers-Jagtman AM. A comparison between 2D and 3D cephalometry on CBCT scans of human skulls. *Int J Oral Maxillofac Surg* 2010;**39**:156–60. http://dx.doi.org/10.1016/j.ijom.2009.11.017.
12. Garib DG, Calil LR, Leal CR, Janson G. Is there a consensus for CBCT use in orthodontics? *Dent Press J Orthod* 2014;**19**:136–49. http://dx.doi.org/10.1590/2176-9451.19.5.136-149.sar.
13. Cheung LK, Chan YM, Jayaratne YSN, Lo J. Three-dimensional cephalometric norms of Chinese adults in Hong Kong with balanced facial profile. *Oral Surg Oral Med Oral Pathol Oral Radiol Endod* 2011;**112**:e56–73. http://dx.doi.org/10.1016/j.tripleo.2011.02.045.
14. Wong RW, Chau AC, Hägg U. 3D CBCT McNamaraäs cephalometric analysis in an adult southern Chinese population. *Int J Oral Maxillofac Surg* 2011;**40**:920–5. http://dx.doi.org/10.1016/j.ijom.2011.03.011.
15. Liang C, Liu S, Liu Q, Zhang B, Li Z. Norms of McNamara's cephalometric analysis on lateral view of 3D CT imaging in adults from Northeast China. *J Hard Tissue Biol* 2014;**23**:249–54. http://dx.doi.org/10.2485/jhtb.23.249.
16. Devanna R. Two-dimensional to three-dimensional: a new three-dimensional cone-beam computed tomography cephalometric analysis. *J Orthod Res* 2015;**3**:30–7. http://dx.doi.org/10.4103/2321-3825.146356.
17. Bayome M, Park JH, Kook YA. New three-dimensional cephalometric analyses among adults with a skeletal class I pattern and

normal occlusion. *Korean J Orthod* 2013;**43**:62–73. http://dx.doi.org/10.4041/kjod.2013.43.2.62.
18. Vahdettin L, Aksoy S, Öz U, Orhan K. Three-dimensional cephalometric norms of Turkish Cypriots using CBCT images reconstructed from a volumetric rendering program in vivo. *Turk J Med Sci* 2016;**46**:841–61. http://dx.doi.org/10.3906/sag-1409-21.
19. McNamara Jr JA. A method of cephalometric evaluation. *Am J Orthod* 1984;**86**:449–69. http://dx.doi.org/10.1016/S0002-9416(84)90352-X.
20. Harris EF, Smith RN. Accounting for measurement error: a critical but often overlooked process. *Arch Oral Biol* 2009;**54**:S107–17. http://dx.doi.org/10.1016/j.archoralbio.2008.04.010.
21. Lorensen WE, Cline HE. Marching cubes: a high resolution 3D surface construction algorithm. *Comp Graph (ACM)* 1987;**21**:163–9. http://dx.doi.org/10.1145/37402.37422.
22. Pearson K. On lines and planes of closest fit to systems of points in space. *Philos Mag* 1901;**2**:559–72. http://dx.doi.org/10.1080/14786440109462720.
23. Welch BL. The generalization of Student's problem when several different population variances are involved. *Biometrika* 1947;**34**:28–35. http://dx.doi.org/10.1093/biomet/34.1-2.28.
24. Gamba TO, Alves MC, Haiter-Neto F. Mandibular sexual dimorphism analysis in CBCT scans. *J Forensic Leg Med* 2016;**38**:106–10. http://dx.doi.org/10.1016/j.jflm.2015.11.024.
25. White TD, Black MT, Folkens PA. *Human osteology.* Third edition. Burlington: Elsevier; 2012.
26. Phulari BS. *An atlas on cephalometric landmarks.* New Delhi: JB Medical; 2013.
27. Santos RMG, De Martino JM, Haiter Neto F, Passeri LA. Influence of different setups of the Frankfort horizontal plane on 3-dimensional cephalometric measurements. *Am J Orthod Dentofac Orthop* 2017;**152**:242–9. http://dx.doi.org/10.1016/j.ajodo.2016.12.023.
28. Adams GL, Gansky SA, Miller AJ, Harrell Jr WE, Hatcher DC. Comparison between traditional 2-dimensional cephalometry and a 3-dimensional approach on human dry skulls. *Am J Orthod Dentofac Orthop* 2004;**126**:397–409. http://dx.doi.org/10.1016/j.ajodo.2004.03.023.
29. van Vlijmen OJC, Bergé SJ, Swennen GRJ, Bronkhorst EM, Katsaros C. Comparison of cephalometric radiographs obtained from cone-beam computed tomography scans and conventional radiographs. *J Oral Maxillofac Surg* 2009;**67**:92–7. http://dx.doi.org/10.1016/j.joms.2008.04.025.

Address:
José Mario De Martino
Universidade Estadual de Campinas
Faculdade de Engenharia Elétrica e de Computação
Av. Albert Einstein
400
Cidade Universitária ''Zeferino Vaz'' Barão Geraldo
CEP 13083-852
Campinas
SP
Brazil
Tel.: +55 19 3521 3794
Fax: +55 19 3521 3845
E-mail: martino@fee.unicamp.br

2.4 Publicação 4

Automatic Repositioning of Jaw Segments for Three-Dimensional Virtual Treatment Planning of Orthognathic Surgery

Rodrigo Mologni Gonçalves dos Santos
José Mario De Martino
Luis Augusto Passeri
Romis Ribeiro de Faissol Attux
Francisco Haiter Neto

Journal of Cranio-Maxillo-Facial Surgery

Setembro de 2017

Journal of Cranio-Maxillo-Facial Surgery 45 (2017) 1399–1407

Contents lists available at ScienceDirect

Journal of Cranio-Maxillo-Facial Surgery

journal homepage: www.jcmfs.com

Automatic repositioning of jaw segments for three-dimensional virtual treatment planning of orthognathic surgery

Rodrigo Mologni Gonçalves dos Santos [a], José Mario De Martino [a, *], Luis Augusto Passeri [b], Romis Ribeiro de Faissol Attux [a], Francisco Haiter Neto [c]

[a] Department of Computer Engineering and Industrial Automation, School of Electrical and Computer Engineering, University of Campinas, Campinas, SP, Brazil
[b] Department of Surgery, School of Medical Sciences, University of Campinas, Campinas, SP, Brazil
[c] Department of Oral Diagnosis, Piracicaba Dental School, University of Campinas, Piracicaba, SP, Brazil

ARTICLE INFO

Article history:
Paper received 22 February 2017
Accepted 27 June 2017
Available online 4 July 2017

Keywords:
Orthognathic surgery
Treatment planning
Three-dimensional
Multi-objective optimization

ABSTRACT

Purpose: To develop a computer-based method for automating the repositioning of jaw segments in the skull during three-dimensional virtual treatment planning of orthognathic surgery. The method speeds up the planning phase of the orthognathic procedure, releasing surgeons from laborious and time-consuming tasks.
Materials and methods: The method finds the optimal positions for the maxilla, mandibular body, and bony chin in the skull. Minimization of cephalometric differences between measured and standard values is considered. Cone-beam computed tomographic images acquired from four preoperative patients with skeletal malocclusion were used for evaluating the method.
Results: Dentofacial problems of the four patients were rectified, including skeletal malocclusion, facial asymmetry, and jaw discrepancies.
Conclusions: The results show that the method is potentially able to be used in routine clinical practice as support for treatment-planning decisions in orthognathic surgery.

1. Introduction

The introduction of cone-beam computed tomography (CBCT) in the field of oral and maxillofacial radiology, in the late 1990s (Mozzo et al., 1998), has led to the emergence of new clinical applications for orthodontics and orthognathic surgery (Ahmad et al., 2012; Kau and Richmond, 2010; Quereshy et al., 2008; Sarment, 2014; Scarfe et al., 2006). Three-dimensional (3D) virtual treatment planning of orthognathic surgery is one of these new applications (Cevidanes et al., 2010, 2014; Edwards, 2014; Popat and Richmond, 2010; Swennen and Schutyser, 2007; Swennen et al., 2009). In contrast to standard treatment planning (Proffit et al., 2003), it enables surgeons to plan corrective jaw surgery, making use of an accurate and reliable 3D virtual representation of the patient's head, comprising skull, face, and teeth surface models (Fig. 1). The 3D virtual treatment planning is a powerful approach that provides greater convenience to surgeons. It can be considered a major breakthrough in the field of oral and maxillofacial surgery. The replacement of routine clinical protocols by others based on this new clinical application is foreseen as inevitable in the near future (Swennen et al., 2009).

Currently, there are different protocols for 3D virtual treatment planning of orthognathic surgery. They all share the same basic workflow, composed of the following stages: 1) reconstructing the patient's head, in which a 3D virtual representation of the head is generated; 2) setting up a reference system, in which the virtual head is oriented to a standardized position; 3) identifying cephalometric landmarks, in which anatomical key points are marked on the virtual head; 4) performing cephalometric measurements, in which a cephalometric analysis is performed; 5) performing osteotomies, in which osteotomies of the jaws are simulated; 6) repositioning jaw segments, in which the osteotomized segments are repositioned in the skull of the virtual head; 7) predicting the patient's face, in which the postsurgical result is predicted; and 8)

* Corresponding author. Av. Albert Einstein 400, Cidade Universitária, Campinas, SP, 13083-852, Brazil. Fax: +55 (19) 3521 3845.
E-mail address: martino@fee.unicamp.br (J.M. De Martino).

http://dx.doi.org/10.1016/j.jcms.2017.06.017
1010-5182/

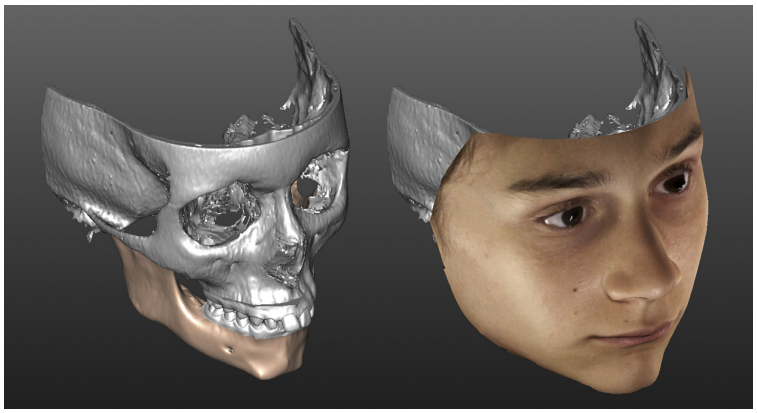

Fig. 1. Three-dimensional virtual representation of a subject's head. The facial surface model is hidden at the left and shown at the right. The virtual head is a demonstration sample included in the SimPlant O&O Viewer (version 2.5.1.1; Materialise Dental NV; Leuven, Belgium).

manufacturing surgical splints, in which splints are produced by rapid prototyping.

Orthognathic surgery can be used to solve dentofacial deformities and other related problems, such as sleep apnea and temporomandibular joint disorders, by repositioning one or both jaws in the skull (Proffit et al., 2003). In this context, Stage 6 of the aforementioned workflow is essential. However, the execution of this stage is as time-consuming and nontrivial as the conventional procedure carried out on cephalometric tracing. It is time-consuming because the virtual movement of the jaw segments is manually performed by the surgeon. In addition, it is nontrivial, because this task has multi-objective in nature, meaning that the surgeon repositions the jaw segments trying to simultaneously reach standard values for all cephalometric measurements. The execution of this stage strongly depends on medical expertise and is challenging, because some measurements are correlated so that changing one may affect the others.

Various methods have been developed to support surgeons. Currently, there are semi-automatic and fully automatic methods for segmentation of jaw (Brandariz et al., 2014; Chang et al., 2013; Gollmer and Buzug, 2012; Kainmueller et al., 2009; Wang et al., 2014); segmentation and classification of teeth (Duy et al., 2012; Gao and Chae, 2010; Ji et al., 2014; Keustermans et al., 2012; Naumovich et al., 2015; Zhang et al., 2016); registration of skull, face, and teeth surface models (Rangel et al., 2012); identification of reference planes, as Frankfurt horizontal and midsagittal planes (Cheng et al., 2012; Van Cauter et al., 2010); identification of anatomical landmarks (Gupta et al., 2015; Keustermans et al., 2011; Makram and Kamel, 2012; Shahidi et al., 2014); and prediction of facial soft tissue deformation (Kim et al., 2012; Mazza and Barbarino, 2011; Mollemans et al., 2007; Pan et al., 2012; Zhang et al., 2015). To the best of our knowledge, only one published approach has dealt with the automation of Stage 6, but focused on the re-establishment of dental occlusion. Both Chang et al. (2010) and Xia et al. (2010) described this approach for virtually repositioning the upper and lower dental arches in maximum intercuspation.

This article introduces a novel computer-based method for automatic repositioning of jaw segments in the skull, in which the maxilla, mandibular body and bony chin are placed in their suitable positions in the skull, aiming to correct skeletal malocclusion, facial asymmetry, and jaw discrepancies. The presented method could be applied to the following: 1) training of residents in oral and maxillofacial surgery, allowing the comparison of treatment planning developed by the resident, with another produced by software; 2) confirmation of more complex treatment planning, which requires significant clinical experience and therefore is especially useful for beginner surgeons; and 3) elaboration of treatment planning for subsequent surgeon's approval, releasing expert surgeons from a laborious and time-consuming task.

2. Materials and methods

The method for automating the repositioning of jaw segments of a patient's head requires as preparation the following: the identification of the 3D hard tissue cephalometric landmarks described in Table 1; and the osteotomy of the maxilla, mandibular body, and bony chin. The automatic method itself is performed in three steps: 1) correcting skeletal malocclusion; 2) correcting facial asymmetry; and 3) correcting jaw discrepancies. These steps are presented below in a simplified form to facilitate the understanding of nontechnical readers.

In Step 1, the skeletal abnormal relationship between the upper and lower dental arches is corrected. A skeletal Class I malocclusion is established in three substeps. First, the maxilla is moved until the midpoint between the left and right upper molars (UML and UMR,

Table 1
The 3D hard tissue cephalometric landmarks required to reposition the jaw segments in the skull.

On the maxilla	
Left/right upper incisor (UIL/UIR)	The most occlusal points on the midline of each upper central incisor.
Left/right upper molar (UML/UMR)	The points on the mesiobuccal cusp of each upper first molar.
On the mandibular body without the bony chin	
Left/right lower incisor (LIL/LIR)	The most occlusal points on the midline of each lower central incisor.
Left/right lower molar (LML/LMR)	The points on the mesiobuccal groove of each lower first molar.
On the bony chin	
Pogonion (Pog)	The most anterior point on the mandibular symphysis.
Gnathion (Gn)	The most anteroinferior point on the mandibular symphysis.
Menton (Me)	The lowermost point on the mandibular symphysis.

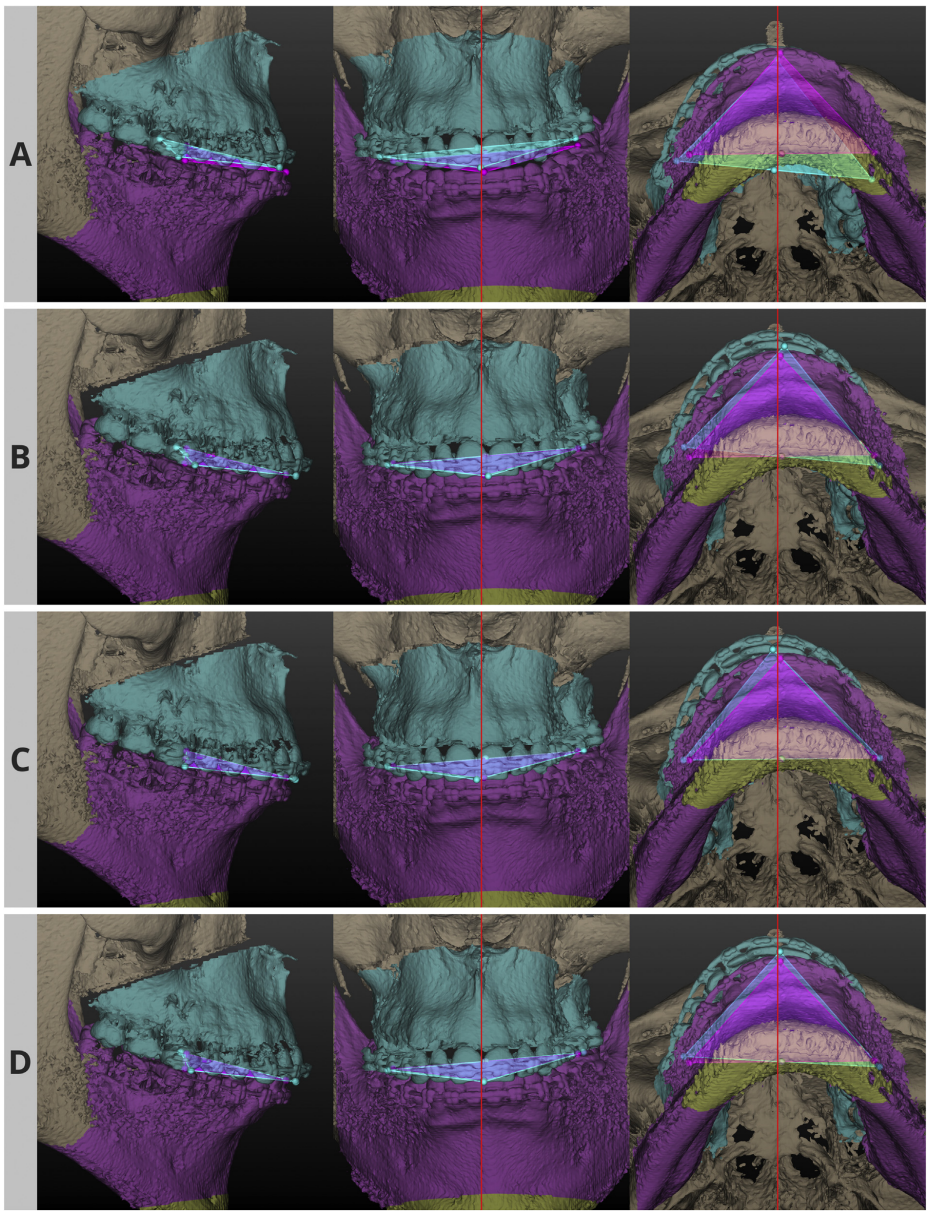

Fig. 2. Results of each one of the three substeps performed in Step 1 of the new method: **A** shows the preoperative positions of the jaw segments, **B** shows the result of the first substep, **C** shows the result of the second substep, and **D** shows the result of the third substep. The superior (cyan) and inferior (magenta) triangles represent the upper and lower mandibular planes. The vertical line (red) represents the midsagittal plane. A same skull surface model is presented in three views: right lateral (at the left), frontal (at the center), and bottom (at the right).

Table 2
The 3D hard tissue cephalometric landmarks required for calculating the lateral hard tissue cephalometric measurements.

On the maxilla	
A-point (A)	The most posterior point on the intermaxillary suture.
Anterior nasal spine (ANS)	The point on the tip of the anterior nasal spine.
On the cranium without the maxilla	
Basion (Ba)	The lowermost point on the midline of the anterior rim of the foramen magnum.
Left/right condylion (CdL/CdR)	The most posterosuperior points on the midline of each mandibular condyle.
Left/right gonion (GoL/GoR)	The points where the line bisecting the angle formed by extending the posterior ramus border and the inferior body border intersect the gonial angle of each mandibular ramus.
Nasion (N)	The point where the frontonasal and internasal sutures intersect.
Left/right pterygomaxillary fissure (PtL/PtR)	The most posterosuperior points on margin of each pterygomaxillary fissure.

respectively) overlaps the midpoint between the left and right lower molars (LML and LMR, respectively). Fig. 2A shows the pre-operative positions of the jaw segments and Fig. 2B shows the positions of the jaw segments after this substep. Second, the maxilla is rotated until the line connecting the UML and UMR overlaps the line connecting the LML and LMR. Fig. 2B and C show the positions of the jaw segments before and after this substep. The axis of rotation is a vector mutually orthogonal to these lines. The center of rotation is the midpoint between the LML and LMR. Third, the maxilla is rotated until the midpoint between the left and right upper incisors (UIL and UIR, respectively) is positioned on the median plane of the mandibular body. Fig. 2C and D show the positions of the jaw segments before and after this substep. The axis of rotation is a normal vector to the occlusal plane. The center of rotation is the same as the before. The median plane of the mandibular body intersects the midpoint between the LML and LMR, the midpoint between the left and right lower incisors (LIL and LIR, respectively), and is orthogonal to the occlusal plane. The occlusal plane intersects the LML, LMR, and the midpoint between the LIL and LIR.

In Step 2, the frontal abnormal relationship of the maxilla, mandibular body, and bony chin in relation to the cranial base is corrected. The facial asymmetry is decreased in four substeps. First, the three jaw segments are rotated until the occlusal plane is at 8° with the Frankfurt horizontal reference plane and the median plane of the mandibular body is parallel to the midsagittal plane. Figs. 2D and 3A show the positions of the jaw segments before and after this substep. The center of rotation is the midpoint between the LML and LMR. Second, the three jaw segments are orthogonally moved so that the center of rotation is on the midsagittal plane. Fig. 3A and B show the positions of the jaw segments before and after this substep. Third, the bony chin is rotated until its median plane is parallel to midsagittal plane. Fig. 4A and B show the positions of the jaw segments before and after this substep. The center of rotation is the midpoint between the pogonion (Pog), gnathion (Gn), and menton (Me). The median plane of the bony chin intersects these three points. Fourth, the bony chin is orthogonally moved to the midsagittal plane so that its center of rotation is on this plane. Fig. 4B and C show the positions of the jaw segments before and after this substep.

In Step 3, the lateral abnormal relationship of the maxilla, mandibular body, and bony chin in relation to the cranial base is

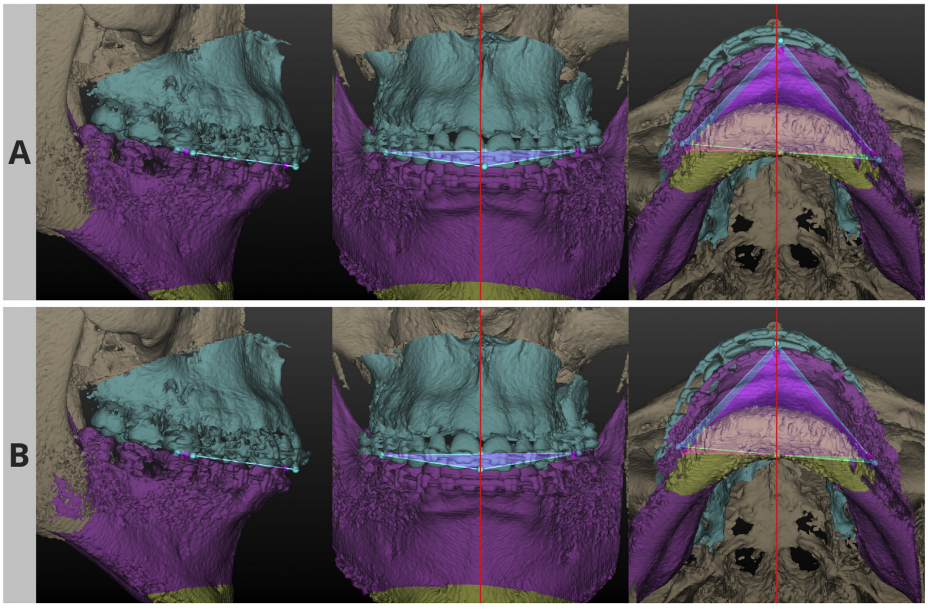

Fig. 3. Results of the first two substeps performed in the Step 2 of the new method: **A** shows the result of the first substep, and **B** shows the result of the second substep. The superior (cyan) and inferior (magenta) triangles represent the upper and lower mandibular planes. The vertical line (red) represents the midsagittal plane. A same skull surface model is presented in three views: right lateral (at the left), frontal (at the center), and bottom (at the right).

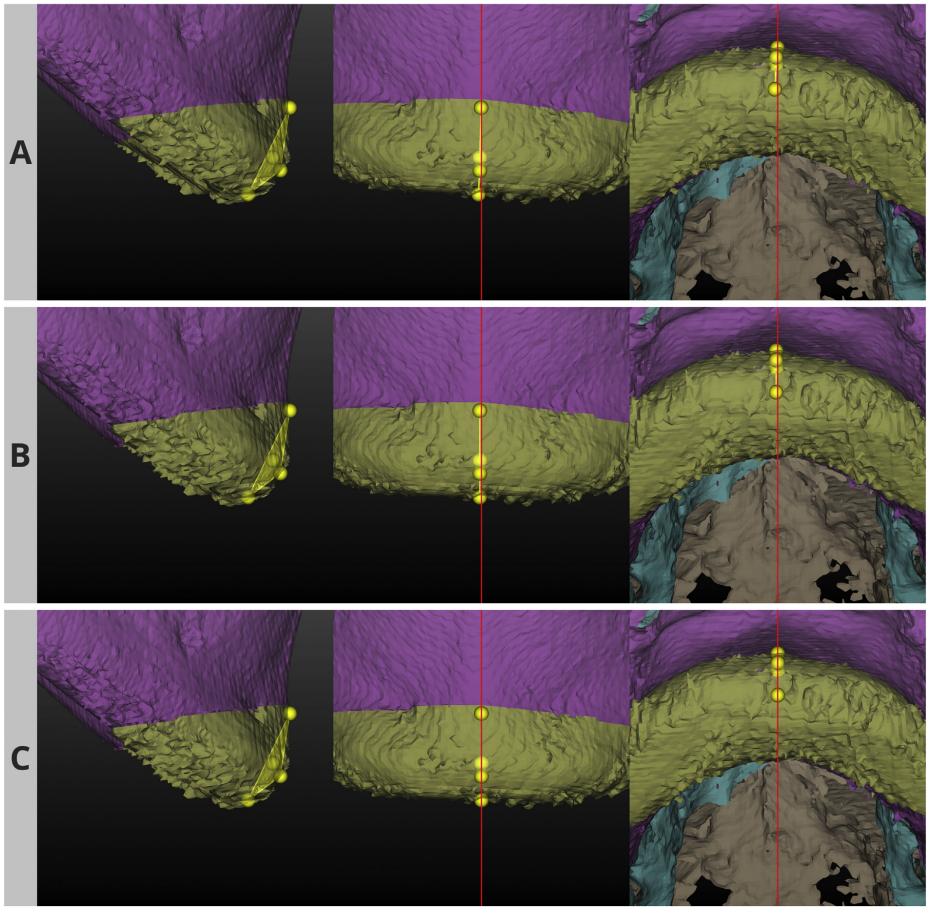

Fig. 4. Results of the last three substeps performed in the Step 2 of the new method: **A** shows the result of the second substep, **B** shows the result of the third substep, and **C** shows the result of the fourth substep. The triangle (yellow) represent the median plane of the bony chin. The vertical line (red) represents the midsagittal plane. A same skull surface model is presented in three views: right lateral (at the left), frontal (at the center), and bottom (at the right).

corrected. The differential evolution algorithm (Storn and Price, 1997) is applied to solve the multi-objective optimization problem described in four substeps. First, the maxilla, mandibular body, and bony chin are rotated θ degrees around a normal vector to the midsagittal plane. The center of rotation is the midpoint between the LML and LMR. Second, the three jaw segments are moved parallel to the midsagittal plane: v_1 mm in vertical and h_1 mm in horizontal. Third, the bony chin is moved parallel to the midsagittal plane: v_2 mm in vertical and h_2 mm in horizontal. Fourth, the cephalometric measurements are recalculated based on the new coordinates of the cephalometric landmarks situated on the jaw segments. These substeps are redone until the minimization of following composite function:

$$\sum_{i=1}^{n} w_i \exp\left[-\frac{1}{2}\left(\frac{x_i-\mu_i}{\sigma_i}\right)^2\right], \quad (1)$$

where n is the number of cephalometric measurements, w_i is the weight for the i-th cephalometric measurement, x_i is the result of the i-th cephalometric measurement, μ_i is the mean for the i-th cephalometric measurement, and σ_i is the standard deviation for the i-th cephalometric measurement. The bounds of the optimization variables and the weights, means, and standard deviations for the cephalometric measurements are provided by the surgeon. Summarizing Step 3, the jaw segments are repeatedly repositioned in the skull until the lowest differences between the measured and standard cephalometric values are obtained.

2.1. Evaluation of the method

This study was conducted in full accordance with the international ethical guidelines for medical research involving human subjects. The ethical aspects were approved by an institutional review board at the University of Campinas in Brazil (protocol number: 27917314.0.0000.5404). Four CBCT datasets acquired from

Table 3
Lateral hard tissue cephalometric measurements relating the jaw elements and cranial base structures one to another.

Maxilla to cranial base	
A-point to nasion perpendicular (A-Np)	The horizontal difference (in millimeters) between the A* and N*.
Mandible to maxilla	
Effective mandibular length (EML)	The distance (in millimeters) from the Gn* to midpoint between the CdL* and CdR*.
Effective midfacial length (EMdL)	The distance (in millimeters) from the Pog* to midpoint between the CdL* and CdR*.
Maxillomandibular differential (MD)	The difference (in millimeters) between the EML and EMdL.
Lower anterior facial height (LAFH)	The distance (in millimeters) from the Me* to ANS*.
Mandibular plane angle (MPA)	The angle (in degrees) between the following lines: the line where the Frankfurt horizontal and midsagittal planes intersect and the line connecting the Me* to midpoint between the GoL* and GoR*.
Facial axis angle (FAA)	The angle (in degrees) between the following lines: the line connecting the N* to Ba* and the line connecting the constructed gnathion to midpoint between the PtL* and PtR*. The constructed gnathion is the intersection point between the line connecting the N* to Pog* and the line connecting the Me* to midpoint between the GoL* and GoR*.
Mandible to cranial base	
Pogonion to nasion perpendicular (Pog-Np)	The horizontal difference (in millimeters) between the Pog* and N*.

X^* is the orthogonal projection of X onto the midsagittal plane.

preoperative white adult patients were used as case studies: 1) a male with skeletal Class II malocclusion; 2) a female with skeletal Class II malocclusion; 3) a male with skeletal Class III malocclusion; and 4) a female with skeletal Class III malocclusion. The datasets were selected from the clinical archive of the Dental School at the University of Campinas. A custom software toolkit was developed by the first author to perform 3D virtual treatment planning of orthognathic surgery. The Python programming environment (Rossum, 2011) and its NumPy (Walt et al., 2011), PyGMO (Biscani et al., 2010), PyQt (Summerfield, 2007), and VTK (Schroeder et al., 2006) extension packages were used for this.

The tasks described ahead were performed for each case study. First, a high-resolution 3D model representing the anatomical surface of the patient's skull was virtually built. Second, a 3D Cartesian coordinate system was set up based on the Frankfurt horizontal and midsagittal planes. Third, the 3D hard tissue cephalometric landmarks described in Tables 1 and 2 were identified onto the virtual skull. Fourth, Le Fort I segmental, bilateral sagittal split, and advancement sliding osteotomies were simulated in the virtual skull. The MeshLab software (Cignoni et al., 2008) was used for this task. Fifth, the lateral hard tissue cephalometric measurements presented in Table 3 were calculated. The orthogonal projection of the landmarks onto the midsagittal plane and the midpoints between bilateral landmarks were used to perform these measurements. Sixth, the new method for automatic repositioning of jaw segments in the skull was applied with the following arguments for a) the bounds: $-10 \leq \theta \leq 10$, $-5 \leq v_1 \leq 5$, $-10 \leq h_1 \leq 10$, $-5 \leq v_2 \leq 5$, and $-8 \leq h_2 \leq 8$; b) the means and standard deviations: CBCT-based lateral hard tissue cephalometric standards for white adult subjects presented in Table 4 (Santos et al., 2017); and c) the weights:

$$w_i = \frac{1}{\sigma_i \sqrt{2\pi}}, \tag{2}$$

in order to benefit the cephalometric measurements of lower dispersion.

The case studies were qualitatively and quantitatively assessed by the third author, an expert oral and maxillofacial surgeon. The statuses before and after the automatic repositioning of jaw segments were considered. The right lateral and frontal views of the virtual skulls were used for the qualitative assessment. The cephalometric measurements and levels of craniofacial normality were used for the quantitative assessment. The level of craniofacial normality is calculated by:

$$\frac{1}{n}\sum_{i=1}^{n} \exp\left[-\frac{1}{2}\left(\frac{x_i - \mu_i}{\sigma_i}\right)^2\right]. \tag{3}$$

It quantifies the degree of craniofacial perfection of the patient by a real number ranging from 0 to 1. The closer to 1, the closer the cephalometric measurement results are to the population mean values.

Table 4
CBCT-based lateral hard tissue cephalometric standards for white adult subjects.

	Male	Female
A-Np (mm)	2.23 ± 4.01	1.76 ± 2.75
EML (mm)	118.55 ± 5.57	110.48 ± 3.16
EMdL (mm)	88.21 ± 4.59	83.51 ± 2.52
MD (mm)	30.34 ± 4.24	26.97 ± 3.30
LAFH (mm)	68.93 ± 6.99	64.31 ± 5.80
MPA (°)	23.19 ± 6.02	24.88 ± 4.10
FAA (°)	89.52 ± 5.26	88.54 ± 4.67
Pog-Np (mm)	1.45 ± 6.44	−0.05 ± 5.81

$\mu \pm \sigma$, μ is the mean and σ is the standard deviation.

Table 5
Preoperative and postoperative results of the lateral hard tissue cephalometric measurements performed on the four case studies.

	Case study 1				Case study 2				Case study 3				Case study 4			
	Before		After		Before		After		Before		After		Before		After	
A-Np (mm)	−1.8	(−4.1)	2.1	(−0.1)	2.9	(1.1)	−0.5	(−2.2)	0.8	(−1.5)	2.1	(−0.1)	3.2	(1.5)	3.4	(1.6)
EML (mm)	110.0	(−8.6)	118.7	(0.2)	110.3	(−0.2)	111.0	(0.5)	117.8	(−0.8)	118.6	(0.1)	102.4	(−8.1)	109.8	(−0.7)
EMdL (mm)	85.4	(−2.9)	88.4	(0.2)	89.1	(5.6)	84.6	(1.1)	88.7	(0.5)	88.4	(0.2)	81.3	(−2.2)	82.5	(−1.0)
MD (mm)	24.6	(−5.7)	30.3	(0.0)	21.2	(−5.8)	26.4	(−0.6)	29.0	(−1.3)	30.3	(−0.1)	21.1	(−5.8)	27.3	(0.3)
LAFH (mm)	75.4	(6.5)	69.1	(0.2)	67.4	(3.1)	68.5	(4.2)	79.1	(10.2)	72.9	(3.9)	54.8	(−9.5)	58.5	(−5.8)
MPA (°)	30.8	(7.6)	20.9	(−2.3)	26.9	(2.0)	23.9	(−1.0)	33.7	(10.5)	22.5	(−0.7)	22.4	(−2.5)	27.4	(2.5)
FAA (°)	75.1	(−14.4)	86.2	(−3.3)	87.9	(−0.7)	90.4	(1.9)	80.3	(−9.3)	88.5	(−1.0)	89.9	(1.3)	88.8	(−0.2)
Pog-Np (mm)	−16.0	(−17.5)	3.1	(1.6)	−5.7	(−5.7)	−2.5	(−2.5)	−9.9	(−11.4)	1.9	(0.5)	2.6	(2.6)	4.8	(4.9)
LCN	0.410		0.964		0.698		0.898		0.608		0.978		0.593		0.859	

LCN, level of craniofacial normality; x (y), x is the measured value and y is the difference between x and the standard mean value.

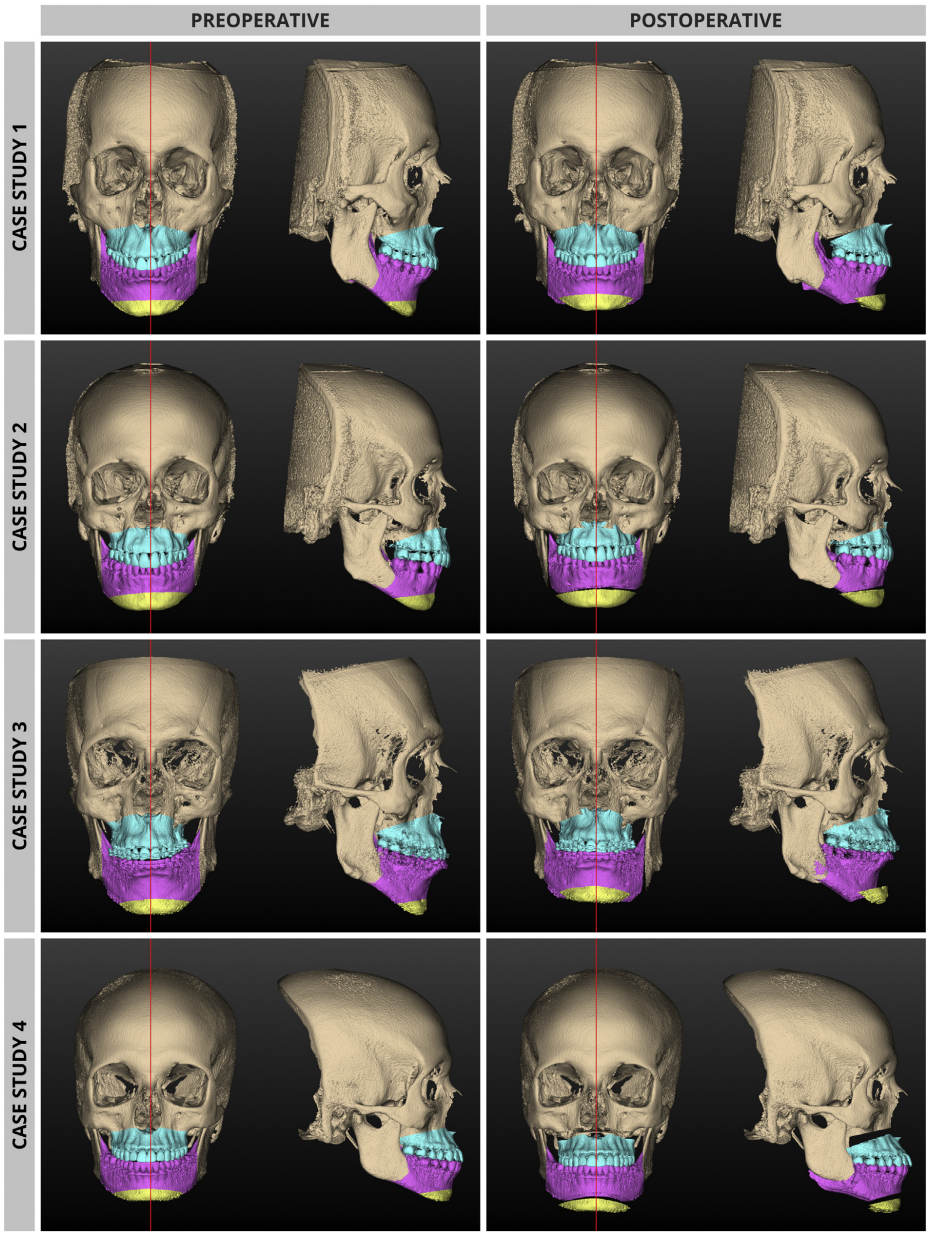

Fig. 5. Skull surface model of each case study before and after the automatic repositioning of jaw segments. The skulls are presented in two views: frontal (at the left), and right lateral (at the right).

3. Results

The results of the cephalometric measurements performed before and after the automatic repositioning of jaw segments in the skull are shown in Table 5. The associated levels of craniofacial normality are also shown in this table. The right lateral and frontal views of each patient are presented in Fig. 5.

The patient in Case Study 1 displays the following skeletal problems: bilateral Class II malocclusion; steep occlusal plane; poor mandible and chin projection; facial asymmetry; and coincident upper and lower dental midlines, but both deviated to the right. The treatment planning proposed by the automatic method corrected these problems and improved all the cephalometric measurements. A-Np, EML, EMdL, MD, and LAFH were on target, since measurement differences <1 mm or <1° are clinically negligible. The level of craniofacial normality increased by 0.554 (greater than its preoperative result) and reached 0.964, only 0.036 below the cephalometric standard.

The patient in Case Study 2 exhibits the following skeletal problems: bilateral Class II malocclusion; poor mandibular projection; vertical maxillary excess; and noncoincident upper and lower dental midlines, both deviated to the right. The treatment planning proposed by the automatic method rectified these problems, but created a new, unwanted superior repositioning of maxilla. Although the level of craniofacial normality has increased, half of the measurements were improved (EMdL, MD, MPA, and Pog-Np) and the other half worsened (A-Np, EML, LAFH, and FAA).

The patient in Case Study 3 shows the following skeletal problems: right Class II malocclusion; left Class III malocclusion; facial asymmetry; maxilla rotated to the right; mandible rotated to the left; vertical inferior facial excess; and poor chin projection. The treatment planning proposed by the automatic method solved these problems and improved all cephalometric measurements. Only LAFH did not reach a perfect result. The level of craniofacial normality increased by 0.37 and reached 0.978, just 0.022 below the cephalometric standard.

The patient in Case Study 4 displays the following skeletal problems: bilateral Class III malocclusion; vertical maxillary deficiency; and coincident upper and lower dental midlines, but both deviated to the right. The treatment planning proposed by the automatic method corrected these problems, but the occlusal plane became too flat. Five of eight cephalometric values (EML, EMdL, MD, LAFH, and FAA) were improved. The level of craniofacial normality increased by 0.266 and reached 0.859.

4. Discussion

The presented method requires the previous identification of eleven 3D hard tissue cephalometric landmarks, of which four are the UIL, UIR, LIL, and LIR (Table 1). These four landmarks are used to calculate the midpoint between the UIL and UIR and the midpoint between the LIL and LIR. In turn, these midpoints are used to create the median plane of the maxilla, the median plane of the mandibular body, and the occlusal plane. Therefore, alternatively, the UIL and UIR can be replaced by the midpoint between both or by any point in the contact surface between the left and right upper central incisors (upper dental midline). Similarly, the LIL and LIR can be replaced by the midpoint between both or by the most occlusal point in the contact surface between the left and right lower central incisors (lower dental midline).

The establishment of a skeletal Class I malocclusion is the goal of Step 1 of the automatic method. However, it is not always perfectly possible to reach this objective. In the second substep of this step, when the UML-UMR and LML-LMR lines overlap, a perfect skeletal Class I malocclusion is established for both the sides of the skull. Later, the upper and lower dental midlines are aligned to rectify the dental asymmetry. As a result, a Class II malocclusion can be produced on one side of the skull and a Class III malocclusion on the other. An alternative is not to apply the third substep of Step 1, which performs this alignment. Another alternative is to use the algorithm developed by Chang et al. (2010) and Xia et al. (2010). This algorithm is able to position the upper and lower dental arches in maximum intercuspation.

The problem addressed in this paper is a multi-objective optimization problem. We used a preference-based approach to solve this problem (Deb, 2014). The problem is reduced to a single-objective optimization problem, by the composite objective function given by Eq. (1). The differential evolution algorithm (Storn and Price, 1997), a simple and efficient heuristic optimization algorithm, was applied in Step 3 of the method to solve this problem.

The automatic method is not restricted to the lateral hard tissue cephalometric measurements in Table 3, other cephalometric measurements can be used, even soft tissue measurements. For the latter case, the facial soft tissue deformations have been considered in the fourth substep of Step 3.

Despite the fact that the patient's skeletal problems in Case Study 2 have been solved, a new problem emerged. The maxilla excessively moved upward. This problem did not arise by error of the automatic method, but due to the particular values provided for the parameters of the method. This problem can be tackled by decreasing the bounds of the optimization variable v_1, which regulates the vertical movement of the jaws, in Step 3. Another strategy is to change the weights or standards of the cephalometric measurements.

In Case Study 4, the inclination of the occlusal plane became lower than normal, which is not acceptable. The occlusal plane should be approximated 8° below the Frankfurt horizontal plane, as was the case in Step 2. This problem can be addressed by decreasing the bounds of the optimization variable θ, which regulates the rotation of the jaws. Another solution is to include the occlusal plane angle in the set of cephalometric measurements. In this case, the weight of this measurement probability would need to be increased.

5. Conclusions

This study aimed to automate an important stage of the 3D virtual treatment planning of orthognathic surgery: the repositioning of jaw segments to their suitable positions in the skull, a laborious and time-consuming task if manually performed by surgeon. The case study results strongly suggest that this aim was fulfilled. The described computer-based method is automatically able to generate treatment plans that can be used to correct dentofacial problems, including skeletal malocclusion, facial asymmetry, and jaw discrepancies.

Source of support

This study was supported by the Coordination for the Improvement of Higher Education Personnel (CAPES), a foundation within the Brazilian Ministry of Education, and the National Council of Technological and Scientific Development (CNPq), an agency of the Brazilian Ministry of Science, Technology, Innovations, and Communications (MCTIC).

References

Ahmad M, Jenny J, Downie M: Application of cone beam computed tomography in oral and maxillofacial surgery. Aust Dent J 57: 82–94. http://dx.doi.org/10.1111/j.1834-7819.2011.01661.x, 2012

Biscani F, Izzo D, Yam CH: A global optimisation toolbox for massively parallel engineering optimisation. In: International conference on astrodynamics tools and techniques – ICATT 2010. Madrid; 2010, 1–13, 2010

Brandariz M, Barreira N, Penedo MG: Automatic segmentation of the mandible in cone-beam computer tomography images. In: International symposium on computer-based medical systems – CBMS 2014. New York; 2014, 467–468. http://dx.doi.org/10.1109/CBMS.2014.93, 2014

Cevidanes LHC, Tucker S, Styner M, Kim H, Chapuis J, Reyes M, et al: Three-dimensional surgical simulation. Am J Orthod Dentofacial Orthop 138: 361–371. http://dx.doi.org/10.1016/j.ajodo.2009.08.026, 2010

Cevidanes LHS, Styner M, Paniagua B, Gonçalves JR: Orthodontic and orthognathic planning using cone beam computed tomography. In: Sarment D (ed.), Cone beam computed tomography: oral and maxillofacial diagnosis and applications. Danvers: Wiley-Blackwell, 91–107, 2014

Chang TB, Xia JJ, Gateno J, Xiong Z, Zhou X, Wong ST: An automatic and robust algorithm of reestablishment of digital dental occlusion. IEEE Trans Med Imag 29: 1652–1663. http://dx.doi.org/10.1109/TMI.2010.2049526, 2010

Chang YB, Xia JJ, Yuan P, Kuo TH, Xiong Z, Gateno J, et al: 3D segmentation of maxilla in cone-beam computed tomography imaging using base invariant wavelet active shape model on customized two-manifold topology. J Xray Sci Technol 21: 251–282. http://dx.doi.org/10.3233/XST-130369, 2013

Cheng Y, Leow WK, Lim TC: Automatic identification of Frankfurt plane and mid-sagittal plane of skull. In: IEEE workshop on applications of computer vision – WACV 2012. Breckenridge; 2012, 233–238. http://dx.doi.org/10.1109/WACV.2012.6162994, 2012

Cignoni P, Callieri M, Corsini M, Dellepiane M, Ganovelli F, Ranzuglia G: MeshLab: an open-source mesh processing tool. In: Scarano V, De Chiara R, Erra U (eds), Eurographics Italian chapter conference 2008. Eurographics association; 2008, 129–136. http://dx.doi.org/10.2312/LocalChapterEvents/ItalChap/ItalianChapConf2008/129-136, 2008

Deb K: Multi-objective optimization. In: Burke EK, Kendall G (eds), Search methodologies: introductory tutorials in optimization and decision support techniques. New York: Springer, 403–449. http://dx.doi.org/10.1007/978-1-4614-6940-7_15, 2014

Duy NT, Lamecker H, Kainmueller D, Zachow S: Automatic detection and classification of teeth in CT data. In: Ayache N, Delingette H, Golland P, Mori K (eds), Medical image computing and computer assisted intervention – MICCAI 2012. Lecture notes in comput sci 7510; 2012, 609–616. http://dx.doi.org/10.1007/978-3-642-33415-3_75, 2012

Edwards SP: Applications of cone beam computed tomography to orthognathic surgery treatment planning. In: Kapila SD (ed.), Cone beam computed tomography in orthodontics: indications, insights, and Innovations. Chichester: Wiley-Blackwell, 437–452, 2014

Gao H, Chae O: Individual tooth segmentation from CT images using level set method with shape and intensity prior. Pattern Recogn 43: 2406–2417. http://dx.doi.org/10.1016/j.patcog.2010.01.010, 2010

Gollmer ST, Buzug TM: Fully automatic shape constrained mandible segmentation from cone-beam CT data. In: Proc IEEE int symp biomed imaging 2012. Barcelona; 2012, 1272–1275. http://dx.doi.org/10.1109/ISBI.2012.6235794, 2012

Gupta A, Kharbanda OP, Sardana V, Balachandran R, Sardana HK: A knowledge-based algorithm for automatic detection of cephalometric landmarks on CBCT images. Int J Comput Assist Radiol Surg 10: 1737–1752. http://dx.doi.org/10.1007/s11548-015-1173-6, 2015

Ji DX, Ong SH, Foong KWC: A level-set based approach for anterior teeth segmentation in cone beam computed tomography images. Comput Biol Med 50: 116–128. http://dx.doi.org/10.1016/j.compbiomed.2014.04.006, 2014

Kainmueller D, Lamecker H, Seim H, Zinser M, Zachow S: Automatic extraction of mandibular nerve and bone from cone-beam CT data. In: Yang GZ, Hawkes D, Rueckert D, Noble A, Taylor C (eds), Medical image computing and computer assisted intervention – MICCAI 2009. Lecture notes in comput sci 5762; 2009, 76–83. http://dx.doi.org/10.1007/978-3-642-04271-3_10, 2009

Kau CH, Richmond S (eds), Three-dimensional imaging for orthodontics and maxillofacial surgery. Chichester, West Sussex: Wiley-Blackwell, 2010

Keustermans J, Smeets D, Vandermeulen D, Suetens P: Automated cephalometric landmark localization using sparse shape and appearance models. In: Suzuki K, Wang F, Dinggang S, Yan P (eds), Machine learning in med imag – MLMI 2011. Lecture notes in comput sci 7009; 2011, 249–256. http://dx.doi.org/10.1007/978-3-642-24319-6_31, 2011

Keustermans J, Vandermeulen D, Suetens P: Integrating statistical shape models into a graph cut framework for tooth segmentation. In: Suzuki K, Wang F, Shen D, Yan P (eds), Machine learning in medical imaging – MLMI 2012. Lecture notes in comput sci 7588; 2012, 242–249. http://dx.doi.org/10.1007/978-3-642-35428-1_30, 2012

Kim H, Jürgens P, Reyes M: Soft-tissue simulation for cranio-maxillofacial surgery: clinical needs and technical aspects. In: Gefen A (ed.), Patient-specific modeling in tomorrow's medicine. Heidelberg: Springer-Verlag Berlin, 413–440, 2012

Makram M, Kamel H: Reeb graphs for automatic localization of 3D craniofacial landmarks: application in 3D cephalometry. In: 15ème Compression et Représentation des Signaux Audiovisuels – CORESA 2012. Lille; 2012, 197–204, 2012

Mazza E, Barbarino GG: 3D mechanical modeling of facial soft tissue for surgery simulation. Facial Plast Surg Clin N Am 19: 623–637. http://dx.doi.org/10.1016/j.fsc.2011.07.006, 2011

Mollemans W, Schutyser F, Nadjmi N, Maes F, Suetens P: Predicting soft tissue deformations for a maxillofacial surgery planning system: from computational strategies to a complete clinical validation. Med Image Anal 11: 282–301. http://dx.doi.org/10.1016/j.media.2007.02.003, 2007

Mozzo P, Procacci C, Tacconi A, Martini PT, Andreis IAB: A new volumetric CT machine for dental imaging based on the cone-beam technique: preliminary results. Eur Radiol 8: 1558–1564. http://dx.doi.org/10.1007/s003300050586, 1998

Naumovich SS, Naumovich SA, Goncharenko VG: Three-dimensional reconstruction of teeth and jaws based on segmentation of CT images using watershed transformation. Dentomaxillofac Radiol 44: 1–6. http://dx.doi.org/10.1259/dmfr.20140313, 2015

Pan B, Xia JJ, Yuan P, Gateno J, Ip HH, He Q, et al: Incremental kernel ridge regression for the prediction of soft tissue deformations. In: Ayache N, Delingette H, Golland P, Mori K (eds), Med image comput comput assist interv – MICCAI 2012. Lecture notes in comput sci 7510; 2012, 99–106. http://dx.doi.org/10.1007/978-3-642-33415-3_13, 2012

Popat H, Richmond S: New developments in: three-dimensional planning for orthognathic surgery. J Orthod 37: 62–71. http://dx.doi.org/10.1179/14653121042885, 2010

Proffit WR, White RP, Sarver DM: Contemporary treatment of dentofacial deformities. St. Louis: Mosby, 2003

Quereshy FA, Savell TA, Palomo JM: Applications of cone beam computed tomography in the practice of oral and maxillofacial surgery. J Oral Maxillofac Surg 66: 791–796. http://dx.doi.org/10.1016/j.joms.2007.11.018, 2008

Rangel FA, Maal TJJ, Bergé SJ, Kuijpers-Jagtman AM: Integration of digital dental casts in cone-beam computed tomography scans. ISRN Dent 1–6. http://dx.doi.org/10.5402/2012/949086, 2012 2012

Rossum G: The Python language reference manual: revised and updated for Python 3.2. In: Drake FL (ed.), Eastbourne: network theory; 2011, 2011

Santos RMG, De Martino JM, Haiter Neto F, Passeri LA: Cone beam computed tomography-based cephalometric norms for Brazilian adults. Int J Oral Maxillofac Surg 2017. http://dx.doi.org/10.1016/j.ijom.2017.06.030, 2017

Sarment D (ed.), Cone beam computed tomography: oral and maxillofacial diagnosis and applications. Chichester: Wiley-Blackwell, 2014

Scarfe WC, Farman AG, Sukovic P: Clinical applications of cone-beam computed tomography in dental practice. J Can Dent Assoc 72: 75–80, 2006

Schroeder W, Martin K, Lorensen B: The visualization toolkit: an object-oriented approach to 3D graphics, 4th ed. Clifton Park: Kitware, 2006

Shahidi S, Bahrampour E, Soltanimehr E, Zamani A, Oshagh M, Moattari M, et al: The accuracy of a designed software for automated localization of craniofacial landmarks on CBCT images. BMC Med Imag 14: 1–8. http://dx.doi.org/10.1186/1471-2342-14-32, 2014

Storn R, Price K: Differential evolution: a simple and efficient Heuristic for global optimization over continuous spaces. J Glob Optim 11: 341–359. http://dx.doi.org/10.1023/A:1008202821328, 1997

Summerfield M: Rapid GUI programming with Python and Qt: the definitive guide to PyQt programming. Upper Saddle River: Pearson Education, 2007

Swennen GRJ, Schutyser F: Three-dimensional virtual approach to diagnosis and treatment planning of maxillofacial deformity. In: Bell WH, Guerrero CA (eds), Distraction osteogenesis of the facial skeleton. Hamilton: BC Decker, 55–79, 2007

Swennen GRJ, Mollemans W, Schutyser F: Three-dimensional treatment planning of orthognathic surgery in the era of virtual imaging. J Oral Maxillofac Surg 67: 2080–2092. http://dx.doi.org/10.1016/j.joms.2009.06.007, 2009

Van Cauter S, Okkerse W, Brijs G, De Beule M, Braem M, Verhegghe B: A new method for improved standardisation in three dimensional computed tomography cephalometry. Comput Meth Biomech Biomed Eng 13: 59–69. http://dx.doi.org/10.1080/10255840903014967, 2010

Walt S, Colbert SC, Varoquaux G: The NumPy array: a structure for efficient numerical computation. Comput Sci Eng 13: 22–30. http://dx.doi.org/10.1109/MCSE.2011.37, 2011

Wang L, Chen KC, Gao Y, Shi F, Liao S, Li G, et al: Automated bone segmentation from dental CBCT images using patch-based sparse representation and convex optimization. Med Phys 41: 1–14. http://dx.doi.org/10.1118/1.4868455, 2014

Xia JJ, Chang YB, Gateno J, Xiong Z, Zhou X: Automated digital dental articulation. In: Jiang T, Navab N, Pluim JPW, Viergever MA (eds), Medical image computer assisted intervention – MICCAI 2010. Lecture notes in comput sci 6363; 2010, 278–286. http://dx.doi.org/10.1007/978-3-642-15711-0_35, 2010

Zhang X, Tang Z, Liebschner MA, Kim D, Shen S, Chang CM, et al: An eFace-template method for efficiently generating patient-specific anatomically-detailed facial soft tissue FE models for craniomaxillofacial surgery simulation. Ann Biomed Eng 44: 1–16. http://dx.doi.org/10.1007/s10439-015-1480-7, 2015

Zhang X, Chen X, Liu Y, Han B, Zhuang T, Zuo W: An effective approach of teeth segmentation within the 3D cone beam computed tomography image based on deformable surface model. Math Probl Eng 2016: 1–10. http://dx.doi.org/10.1155/2016/9505217, 2016

Capítulo 3

Discussão

O Capítulo 2 apresentou os quatro artigos publicados como parte deste trabalho de doutorado e que trataram os problemas apresentados no Capítulo 1. Os resultados de cada publicação são discutidos resumidamente a seguir, uma vez que os artigos já contém discussões aprofundadas.

3.1 Publicação 1

A primeira publicação, intitulada "*Influence of Different Setups of the Frankfort Horizontal Plane on 3-Dimensional Cephalometric Measurements*", trata do problema descrito na Seção 1.2. O foco do artigo é a verificação da validade da hipótese de que a mudança de definição do plano horizontal de Frankfort não produz diferenças de medição clinicamente relevantes ao se considerar indivíduos normais. A abordagem utilizada para testar a hipótese contabiliza as ocorrências cuja diferença de medição apresentou valor maior do que o clinicamente aceito para uma determinada medida cefalométrica. Esta contagem foi realizada para 82 indivíduos adultos, considerando todas as 21 combinações pareadas das definições do plano horizontal de Frankfort e seis medidas cefalométrica dependentes deste plano.

Os resultados, apresentados na Tabela 2 da publicação (ver Seção 2.1), indicam que a hipótese posta à prova é falsa, pois diferenças de medição clinicamente relevantes foram identificadas em todas as seis medidas cefalométricas (A–Np, Pog–Np, UI–Av, FA, YAA e MPA) em função da mudança de definição do plano horizontal de Frankfort (FH1–FH2, FH1–FH3, FH1–FH4 e assim sucessivamente até FH6–FH7). Apenas as comparações pareadas FH3–FH6, FH3–FH7 e FH6–FH7 das definições dos planos horizontal de Frankfort não tiverem nenhuma ocorrência. Isto significa dizer que a mudança de definição exclusivamente realizada entre estas combinações não produz diferenças de medição clinicamente relevantes. A–Np é a distância orientada do ponto A ao násio per-

pendicular, Pog–Np é a distância orientada do pogônio ao násio perpendicular, UI–Av é a distância orientada do incisivo superior ao ponto A vertical, FA é o ângulo facial, YAA é o ângulo do eixo Y e MPA é o ângulo do plano mandibular (ver Figura 5 da publicação). FH1 é o plano que intersecta os dois pórios e o orbital esquerdo, FH2 é o plano que intersecta os dois pórios e o orbital direito, FH3 é o plano que intersecta os dois pórios e o ponto médio entre os dois orbitais, FH4 é o plano que intersecta os dois orbitais e o pório esquerdo, FH5 é o plano que intersecta os dois orbitais e o pório direito, FH6 é o plano que intersecta os dois orbitais e o ponto médio entre os dois pórios, e FH7 é o plano de melhor encaixe entre os pórios e os orbitais.

A não confirmação da validade da hipótese implica que as diferentes definições do plano horizontal de Frankfort podem influenciar negativamente na análise e comparação das medidas cefalométricas e, assim, aumentar a probabilidade de ocorrência de resultados clínicos diferentes ou errôneos. Para reduzir ao máximo a chance destes problemas ocorrerem, recomenda-se fortemente que a definição padrão do plano horizontal de Frankfort seja usada, para desta forma, aumentar a precisão das medidas cefalométricas.

3.2 Publicação 2

A segunda publicação, intitulada "*Cone-Beam Computed Tomography-Based Three-Dimensional McNamara Cephalometric Analysis*", trata do problema descrito na Seção 1.3. Este artigo apresenta uma proposta de adequação da análise de McNamara, ou mais especificamente de suas medidas cefalométricas, para que sejam produzidos valores 3D, sem apresentar os problemas e inconsistências identificados em trabalhos anteriores. Nesta adaptação 3D do método de análise cefalométrica de McNamara, *a*) os pontos cefalométricos têm três coordenadas, pois são identificados no crânio virtual e não sobre o plano de uma telerradiografia; *b*) os pontos cefalométricos bilaterais são identificados dos dois lados do crânio; *c*) o násio perpendicular, o ponto A vertical, a linha ponto A-pogônio e o plano facial são representados por linhas 3D ao invés de linhas 2D; *d*) o plano horizontal de Frankfort, o plano mandibular e o eixo facial são representados por planos ao invés de linhas 2D; *e*) o comprimento efetivo da mandíbula, o comprimento efetivo da maxila, a altura facial anteroinferior são calculados por distância entre dois pontos 3D ao invés de distância entre dois pontos 2D; *f*) o ponto A ao násio perpendicular, o pogônio ao násio perpendicular, o incisivo superior ao ponto A vertical e o incisivo inferior à linha ponto A-pogônio são calculados como componentes de um vetor ao invés de uma distância orientada de um ponto 2D a uma linha 2D; *g*) o ângulo do eixo facial é calculado como um ângulo entre uma linha 3D e um plano ao invés de

um ângulo entre duas linhas 2D; *h*) o ângulo do plano mandibular é calculado como um ângulo entre dois planos ao invés de um ângulo entre duas linhas 2D; e *i*) o comprimento efetivo da mandíbula, o comprimento efetivo da maxila, o incisivo superior ao ponto A vertical e o incisivo inferior à linha ponto A-pogônio são calculados de ambos os lados do crânio virtual.

Em comparação com o método original de McNamara, o método estendido fornece os comprimentos efetivos reais da maxila e da mandíbula de ambos os lados do crânio; a altura real da face anteroinferior; as distâncias orientadas do ponto A ao násio perpendicular, do pogônio ao násio perpendicular, dos incisivos superiores esquerdo e direito ao ponto A vertical e dos incisivos inferiores esquerdo e direito à linha ponto A-pogônio para as vistas lateral e posteroanterior do crânio; e os ângulos reais do eixo facial e do plano mandibular. Em comparação com os métodos de análise cefalométrica 3D, o método criado realiza as medidas que envolvem o cálculo da distância orientada entre um ponto e uma linha cefalométrica de forma diferenciada, com uso de vetor, que fornece duas distâncias, uma para a vista lateral do crânio e outra para a vista frontal. A última vista possibilita a identificação de assimetrias craniofaciais.

3.3 Publicação 3

A terceira publicação, intitulada "*Cone Beam Computed Tomography-Based Cephalometric Norms for Brazilian Adults*", trata do problema descrito na Seção 1.4. O objetivo desta publicação foi estabelecer normas cefalométricas para brasileiros adultos, de ambos os sexos, com ascendência europeia, a partir de imagens de TCFC. O método de análise cefalométrica de McNamara foi aplicado sobre imagens craniofaciais adquiridas de 60 indivíduos, sendo 30 homens e 30 mulheres, todos com oclusão normal. As normas cefalométricas são apresentadas nas Tabelas 4 e 5 da publicação (ver Seção 2.3). Elas mostraram-se confiáveis, pois todas as medidas cefalométricas apresentaram um erro técnico de medição inferior ao erro de medição clinicamente aceitável. Dimorfismo sexual também foi avaliado neste trabalho (ver Tabela 6 da publicação). Diferenças clinicamente relevantes foram encontradas nas seguintes medidas cefalométricas: comprimento efetivo da mandíbula (EML), comprimento efetivo da maxila (EMdL), diferença maxilomandibular (MD) e altura facial anteroinferior (LAFH). Isto mostra que homens têm os maxilares maiores do que mulheres, apesar de ambos terem o mesmo formato craniofacial, dado que as medidas cefalométricas angulares não apresentaram diferença significativa.

Ao contrário das normas cefalométricas convencionais para brasileiros, as normas cefalométricas estabelecidas neste trabalho são isentas de erros de precisão inerentes da

telerradiografia, o que torna estas normas mais fiéis às medidas reais desta população. Em relação à avaliação de dimorfismo sexual, os resultados mostram que as diferenças entre homens e mulheres devem ser consideradas pelos cirurgiões, com o propósito de preservar ou enaltecer as características anatômicas de seus pacientes.

3.4 Publicação 4

A quarta e última publicação, intitulada "*Automatic Repositioning of Jaw Segments for Three-Dimensional Virtual Treatment Planning of Orthognathic Surgery*", aborda o problema descrito na Seção 1.5. Neste artigo é apresentado um método para automatizar a principal etapa do planejamento virtual 3D de cirurgia ortognática: o reposicionamento de segmentos ósseos maxilares no crânio. O método foi projetado para tratar problemas dentofaciais relacionados à maloclusão esquelética, assimetria facial e discrepância de maxilares. Porém, limitando-se ao tratamento de pacientes portadores de deformidades dentofaciais passíveis de correção, exclusivamente, por meio do reposicionamento ósseo da maxila, do corpo da mandíbula e do mento no crânio. Quatro estudos de caso foram usados para a avaliar a eficácia do método. As avaliações clínica e técnica são discutidas abaixo, com base na Tabela 5 e na Figura 5 da publicação (ver Seção 2.4).

Estudo de Caso 1. O paciente é um homem de 22 anos com os seguintes problemas esqueléticos: maloclusão do tipo Classe II bilateral, plano oclusal acentuado, projeção deficiente de mandíbula e mento, assimetria facial e linhas médias das arcadas superior e inferior coincidentes, com ambas desviadas para a direita. O método tratou estes problemas, com melhora de todas as medidas cefalométricas. As medidas de ponto A ao násio perpendicular (A-Np), de comprimento efetivo da mandíbula (EML), de comprimento efetivo da maxila (EMdL), de diferença maxilomandibular (MD) e de altura facial anteroinferior (LAFH) tornaram-se clinicamente perfeitas, considerando que diferenças de medição $< 1\,\text{mm}$ ou $< 1{,}5^{\text{o}}$ são desprezíveis. O nível de normalidade craniofacial — função criada para quantificar o nível de perfeição craniofacial do paciente — aumentou 55,4 pontos percentuais e atingiu 96,4 pontos; apenas 3,6 pontos abaixo do padrão cefalométrico.

Estudo de Caso 2. O paciente é uma mulher de 31 anos com os seguintes problemas esqueléticos: maloclusão do tipo Classe II bilateral, projeção deficiente de mandíbula, excesso vertical de maxila e linhas médias coincidentes das arcadas superior e inferior, com ambas desviadas para a direita. O método tratou estes problemas, porém produziu um novo: o reposicionamento superior indesejado da maxila. Ou seja, a maxila foi excessivamente deslocada para cima. Este problema não surgiu por

um erro do método, mas devido aos argumentos passados a ele. O problema pode ser solucionado diminuindo os limites da componente vertical do primeiro vetor de deslocamento (v_1), que regula o movimento vertical da maxila. Embora o nível de normalidade tenha aumentado, metade dos valores das medidas melhoraram e outra metade piorou.

Estudo de Caso 3. O paciente é um homem de 23 anos com os seguintes problemas esqueléticos: maloclusão do tipo Classe II do lado direito, maloclusão do tipo Classe III do lado esquerdo, assimetria facial, maxila girada para a direita, mandíbula girada para a esquerda, excesso vertical inferior da face e projeção deficiente de mento. O método tratou estes problemas e melhorou os valores das medidas cefalométrica. Apenas a altura facial anteroinferior (LAFH) não tornou-se clinicamente perfeita. O nível de normalidade aumentou 37 pontos percentuais e atingiu 97,8 pontos; apenas 2,2 pontos abaixo do padrão cefalométrico.

Estudo de Caso 4. O paciente é uma mulher de 25 anos com os seguintes problemas esqueléticos: maloclusão do tipo Classe III bilateral, deficiência vertical de maxila e linhas médias das arcadas dentárias superior e inferior coincidentes, com ambas desviadas para a direita. O método tratou estes problemas, porém produziu um novo: o plano oclusal tornou-se muito horizontal. O ideal é que este plano esteja 8^o abaixo do plano horizontal de Frankfort. Este problema pode ser solucionado alterando os argumentos do método, de duas formas: reduzindo os limites do ângulo de rotação dos maxilares (θ) ou definindo o ângulo do plano oclusal como uma medida cefalométrica e aumentando o seu peso (w_i). Apesar do problema criado, os valores de cinco das oito medidas cefalométrica foram melhorados e o nível de normalidade aumentou 26,6 pontos percentuais e atingiu 85,9 pontos.

Os resultados apresentados atestam a eficácia do método para a correção dos problemas dentofaciais mais comuns tratados pela Cirurgia Ortognática. Ao contrário do método estabelecido por Chang, Xia, Gateno et al. (2010) e Xia et al. (2010), que promove apenas o restabelecimento da oclusão dentária, o método criado neste trabalho vai além e promove também a correção de problemas dentofaciais relacionados à assimetria facial e discrepância de maxilares.

Capítulo 4

Conclusões

O Capítulo 1 apresentou os problemas identificados no contexto do planejamento virtual 3D de cirurgia ortognática e que este trabalho de doutorado se propôs a tratar como forma de contribuir para o aprimoramento desta tecnologia.

4.1 Problema 1

O problema relatado na Seção 1.2 foi tratado no artigo intitulado "*Influence of Different Setups of the Frankfort Horizontal Plane on 3-Dimensional Cephalometric Measurements*", disponível no Capítulo 2. O estudo relatado neste artigo objetivou verificar a validade da hipótese de que a mudança de definição do plano horizontal de Frankfort não produz diferenças de medição clinicamente relevantes quando sob indivíduos com crânios consideravelmente simétricos. Os resultados do estudo indicam que a hipótese é falsa, pois foram consideradas todas as possibilidades de definição do plano horizontal de Frankfort e encontradas diferenças de medição clinicamente relevantes em todas as medidas cefalométricas. O artigo disponibiliza uma tabela com todas as combinações pareadas entre as sete definições do plano horizontal de Frankfort para cada uma das seis medidas cefalométricas analisadas. Por meio desta tabela, o leitor pode verificar se suas medidas estão sujeitas à diferença de medição clinicamente relevante em caso de alteração da definição do plano horizontal de Frankfort.

O estudo em questão limitou-se ao uso de: *a*) o método de cefalometria 3D por TCFC criado por Swennen, Schutyser e Hausamen (2006); *b*) seis medidas cefalométricas dependentes do plano horizontal de Frankfort, sendo três medidas cefalométricas lineares — ponto A ao násio perpendicular, pogônio ao násio perpendicular e incisivo superior ao ponto A vertical — e outras três medidas cefalométricas angulares — ângulo facial, ângulo do eixo Y e ângulo do plano mandibular; *c*) medidas cefalométricas realizadas sobre o perfil craniofacial do paciente; e *d*) um único observador e apenas duas obser-

vações para o cálculo da variabilidade de medição clinicamente aceitável. Todas estas limitações podem ser exploradas em trabalhos futuros. Porém, a principal delas seria um estudo envolvendo mais observadores e observações. Isto possibilitaria o cálculo e a comparação da variabilidade de medição intra ou interobservador com a variabilidade de medição entre duas definições do plano horizontal de Frankfort.

4.2 Problema 2

O problema relatado na Seção 1.3 foi tratado no artigo intitulado "*Cone-Beam Computed Tomography-Based Three-Dimensional McNamara Cephalometric Analysis*", disponível no Capítulo 2. Este artigo apresenta uma extensão do método de análise cefalométrica de (MCNAMARA, 1984) que explora a tridimensionalidade das imagens de TCFC. As medidas cefalométricas deste método foram adaptadas para produzir valores verdadeiramente 3D, mas sem perda de informação e com preservação das definições geométricas originais das linhas e planos cefalométricos, que foram justamente os problemas identificados em adaptações realizadas por outros pesquisadores. Ao contrário do método original, o método estendido fornece *a*) os comprimentos efetivos reais da maxila e da mandíbula de ambos os lados do crânio; *b*) a altura real da face anterior inferior; *c*) as distâncias orientadas do ponto A ao násio perpendicular, do pogônio ao násio perpendicular, dos incisivos superiores esquerdo e direito ao ponto A vertical e dos incisivos inferiores esquerdo e direito à linha ponto A-pogônio para as vistas lateral e postero-anterior do crânio; e *d*) os ângulos reais do eixo facial e do plano mandibular. Além disso, o comprimento mandibular efetivo esquerdo e direito, o comprimento maxilar efetivo esquerdo e direito, a componente X do násio perpendicular ao ponto A e a componente X do pogônio ao násio perpendicular possibilitam a identificação de assimetrias craniofaciais.

A análise da extensão do método consistiu na comparação das adaptações das medidas cefalométricas deste trabalho com de outros trabalhos relacionados e na comparação das informações adquiridas por meio da extensão com o método original. Ambas as comparações foram puramente teóricas. Por isso, sugere-se como trabalho futuro, comparações experimentais. A primeira comparação poderia ser realizada por análise estatística dos resultados das diferentes adaptações de uma mesma medida cefalométrica. A segunda comparação, por sua vez, poderia ser realizada por análise clínica de estudos de caso. Neste último caso, realizada obrigatoriamente por especialistas em Cirurgia e Traumatologia Bucomaxilofacial.

4.3 Problema 3

O problema relatado na Seção 1.4 foi tratado no artigo intitulado "*Cone Beam Computed Tomography-Based Cephalometric Norms for Brazilian Adults*", disponível no Capítulo 2. Este artigo fornece normas cefalométricas para brasileiros adultos, de ambos os gêneros, com ascendência europeia. Estas normas são especialmente úteis para o diagnóstico e planejamento de tratamento de pacientes da Cirurgia Ortognática, pois foram estabelecidas a partir do método de análise cefalométrica de McNamara; e podem ser utilizadas tanto no planejamento virtual 3D de cirurgia ortognática quanto no planejamento convencional da Cirurgia Ortognática. Dimorfismo sexual também foi avaliado neste trabalho. A avaliação constatou que homens tem os maxilares maiores do que as mulheres, muito embora ambos tenham a mesma morfologia craniofacial. Portanto, os pacientes masculino e femininos desta população possuem características fisiológicas diferentes que devem ser levadas em consideração pelo cirurgião.

O trabalho limitou-se ao uso: *a*) de 60 imagens de TCFC, sendo 30 imagens adquiridas de homens e outras 30 imagens adquiridos de mulheres; e *b*) das medidas cefalométricas presentes no método de análise cefalométrica de McNamara. Considerando estas limitações, propõe-se como trabalhos futuros: *a*) envolver mais imagens de TCFC para aumentar o poder estatístico das normas cefalométricas já estabelecidas; *b*) estabelecer normas cefalométricas por meio da extensão do método de análise cefalométrica de McNamara apresentado no artigo anterior; e *c*) estabelecer normas cefalométricas para outras medidas cefalométricas.

4.4 Problema 4

O problema relatado na Seção 1.5 foi tratado no artigo intitulado "*Automatic Repositioning of Jaw Segments for Three-Dimensional Virtual Treatment Planning of Orthognathic Surgery*", disponível no Capítulo 2. Este artigo apresenta um método capaz de tratar problemas dentofaciais relacionados à maloclusão esquelética, assimetria facial e discrepância de maxilar, por meio do reposicionamento automático dos ossos da maxila, do corpo da mandíbula e do mento no crânio. O método contribui para: *a*) a redução do tempo dedicado pelo cirurgião na execução do reposicionamento de segmentos ósseos maxilares no crânio; *b*) a redução da complexidade desta etapa, que envolve um procedimento multiobjetivo; e, consequentemente, *c*) o aperfeiçoamento da principal etapa do planejamento virtual 3D de cirurgia ortognática. Potenciais aplicações do método incluem: *a*) o ensino e treinamento de cirurgiões-dentistas residentes em Cirurgia e Traumatologia Bucomaxilofacial, permitindo que os planos de tratamento cirúrgicos

elaborados por eles possam ser comparados aos gerados pelo método; *b*) a confirmação de planos de tratamentos de casos mais complexos, que exigem vasta experiência clínica — sendo especialmente útil para cirurgiões bucomaxilofaciais recém-formados; e *c*) a elaboração de planos de tratamento para posterior aprovação do especialista, desonerando o profissional experiente de tarefas laboriosas e demoradas.

O trabalho em questão limitou-se previamente ao desenvolvimento de um método de apoio ao tratamento de indivíduos não portadores de assimetria facial esquelética grave ou portadores de deformidades dentofaciais passíveis de correção por meio de osteotomias tipo Le Fort I da maxila, sagital bilateral do ramo mandibular e horizontal basilar do mento, que possibilitam o reposicionamento dos ossos da maxila, do corpo da mandíbula e do mento, mas não de suas frações. A validação do método consistiu no uso de quatro estudos de casos, sendo um casal com maloclusão esquelética do tipo Classe II e outro casal com maloclusão esquelética do tipo Classe III. Considerando a limitação de escopo e os estudos de caso do presente trabalho, é sugerido como trabalhos futuros: *a*) aplicar o método criado sobre uma quantidade maior de estudos de caso, visando melhorar a validação do método; *b*) aprimorar o método para que ele possa tratar outras deformidades dentofaciais além das limitações pré-estabelecidas, que envolvem, por exemplo, a expansão da maxila; e *c*) usar medidas cefalométricas de tecido mole, que não foram utilizadas.

4.5 Considerações Finais

Este trabalho identificou e tratou quatro problemas no contexto do planejamento virtual 3D de cirurgia ortognática, com o propósito de contribuir para o aperfeiçoamento desta tecnologia. Na etapa de reorientação da cabeça (ver Seção 1.1), o cirurgião reposiciona a cabeça virtual do paciente para que ela fique disposta com maior precisão na posição padrão da Cefalometria. Como diferentes definições do plano horizontal de Frankfort — que compõe este padrão — têm sido utilizadas por pesquisadores, fica a dúvida se essas diferenças poderiam interferir negativamente nas medidas cefalométricas. Uma vez que nenhum trabalho verificou tal questão na sua integralidade, este trabalho se propôs a fazê-la (ver Seção 2.1). Na etapa de análise cefalométrica (ver Seção 1.1), o cirurgião realiza as medidas cefalométricas do paciente, que o auxiliarão no diagnóstico e planejamento da cirurgia ortognática. Devido à relevância dos métodos de análise cefalométrica convencionais, pesquisadores têm estendido suas medidas para produzir valores 3D, explorando assim a tridimensionalidade da cabeça virtual. Como forma de contribuir com a comunidade científica, este trabalho estendeu o método de McNamara, explorando não só a tridimensionalidade como também os pontos

falhos encontrados em outros métodos de análise cefalométrica 3D (ver Seção 2.2). Na etapa de reposicionamento de segmentos ósseos maxilares no crânio (ver Seção 1.1), o cirurgião reposiciona os segmentos ósseos maxilares no crânio buscando encontrar as posições mais adequadas para estes segmentos. Para tal, ele usa como referência normas cefalométricas, que descrevem as medidas padrão de uma determinada população. Com o propósito de fornecer normas cefalométricas sem os erros de precisão presentes em telerradiografias, este trabalho estabeleceu normas cefalométricas para brasileiros adultos de ascendência europeia, de ambos os gêneros, por meio imagens craniofaciais adquiridas por TCFC (ver Seção 2.3). Ainda na etapa de reposicionamento de segmentos ósseos maxilares no crânio, o reposicionamento é realizado de forma manual pelo cirurgião, demandando dele um esforço desnecessário, uma vez que o computador poderia realizar tal procedimento. Considerando a importância desta etapa e a ausência de um método automático completo, este trabalho se propôs a automatizar o reposicionamento de segmentos ósseos maxilares no crânio (ver Seção 2.4).

Referências

ADAMS, G. L. et al. Comparison between traditional 2-dimensional cephalometry and a 3-dimensional approach on human dry skulls. **American Journal of Orthodontics Dentofacial Orthopedics**, v. 126, n. 4, p. 397–409, out. 2004. DOI: 10.1016/j.ajodo.2004.03.023.

AHMAD, M.; JENNY, J.; DOWNIE, M. Application of cone beam computed tomography in oral and maxillofacial surgery. **Australian Dental Journal**, v. 57, s1, p. 82–94, fev. 2012. DOI: 10.1111/j.1834-7819.2011.01661.x.

AHN, S. J. **Least squares orthogonal distance fitting of curves and surfaces in space**. Berlin: Springer, 2004. (Lecture Notes in Computer Science, 3151). ISBN 978-3-540-23966-6.

BAYOME, M.; PARK, J. H.; KOOK, Y. A. New three-dimensional cephalometric analyses among adults with a skeletal Class I pattern and normal occlusion. **Korean Journal of Orthodontics**, v. 43, n. 2, p. 62–73, abr. 2013. DOI: 10.4041/kjod.2013.43.2.62.

BERCO, M. et al. Accuracy and reliability of linear cephalometric measurements from cone-beam computed tomography scans of a dry human skull. **American Journal of Orthodontics and Dentofacial Orthopedics**, v. 136, n. 1, 17.e1–17.e9, jul. 2009. DOI: 10.1016/j.ajodo.2008.08.021.

BISCANI, F.; IZZO, D.; YAM, C. H. A global optimisation toolbox for massively parallel engineering optimisation, 23 abr. 2010. arXiv: 1004.3824 [cs.DC].

BRANDARIZ, M. et al. Automatic segmentation of the mandible in cone-beam computer tomography images. In: IEEE International Symposium Computer-Based Medical Systems. [S.l.]: IEEE, maio 2014. DOI: 10.1109/cbms.2014.93.

BROADBENT, B. H. A new x-ray technique and its application to orthodontia: The Introduction of cephalometric radiography. **Angle Orthodontics**, v. 1, n. 2, p. 45–66,

abr. 1931. DOI: 10.1043/0003-3219(1931)001<0045:ANXTAI>2.0.CO;2.

CAUTER, S. et al. A new method for improved standardisation in three-dimensional computed tomography cephalometry. **Computer Methods in Biomechanics and Biomedical Engineering**, v. 13, n. 1, p. 59–69, fev. 2010. DOI: 10.1080/10255840903014967.

CENTENERO, S. A.-H.; HERNÁNDEZ-ALFARO, F. 3D planning in orthognathic surgery: CAD/CAM surgical splints and prediction of the soft and hard tissues results — our experience in 16 cases. **Journal of Cranio-Maxillofacial Surgery**, v. 40, n. 2, p. 162–168, fev. 2012. DOI: 10.1016/j.jcms.2011.03.014.

CEVIDANES, L. H. S.; STYNER, M. et al. Orthodontic and orthognathic planning using cone beam computed tomography. In: SARMENT, D. (Ed.). **Cone beam computed tomography**: Oral and maxillofacial diagnosis and applications. [S.l.]: Wiley-Blackwell, out. 2013. p. 91–107. DOI: 10.1002/9781118769027.ch5.

CEVIDANES, L. H. S.; TUCKER, S. et al. Three-dimensional surgical simulation. **American Journal of Orthodontic Dentofacial Orthopedics**, v. 138, n. 3, p. 361–371, set. 2010. DOI: 10.1016/j.ajodo.2009.08.026.

CHANG, Y.-B.; XIA, J. J.; GATENO, J. et al. An automatic and robust algorithm of reestablishment of digital dental occlusion. **IEEE Transactions on Medical Imaging**, v. 29, n. 9, p. 1652–1663, set. 2010. DOI: 10.1109/tmi.2010.2049526.

CHANG, Y.-B.; XIA, J. J.; YUAN, P. et al. 3D segmentation of maxilla in cone-beam computed tomography imaging using base invariant wavelet active shape model on customized two-manifold topology. **Journal of X-Ray Science and Technology**, v. 21, n. 2, p. 251–282, 2013. DOI: 10.3233/XST-130369.

CHENG, Y.; LEOW, W. K.; LIM, T. C. Automatic identification of Frankfurt plane and mid-sagittal plane of skull. In: IEEE Workshop on Applications of Computer Vision. [S.l.]: IEEE, jan. 2012. DOI: 10.1109/wacv.2012.6162994.

CHEUNG, L. K. et al. Three-dimensional cephalometric norms of Chinese adults in Hong Kong with balanced facial profile. **Oral Surgery, Oral Medicine, Oral Pathology and Oral Radiology**, v. 112, n. 2, e56–e73, ago. 2011. DOI: 10.1016/j.tripleo.2011.02.045.

CIGNONI, P. et al. MeshLab. In: _____. **Eurographics Italian Chapter Conference**: An open-source mesh processing tool. [S.l.]: Eurographics Association, 2008. DOI: 10.2312/LocalChapterEvents/ItalChap/ItalianChapConf2008/129-136.

DAMSTRA, J.; FOURIE, Z. et al. Reliability and the smallest detectable difference of measurements on 3-dimensional cone-beam computed tomography images. **American**

Journal of Orthodontics and Dentofacial Orthopedics, v. 140, n. 3, e107–e114, set. 2011. DOI: 10.1016/j.ajodo.2011.02.020.

DAMSTRA, J.; SLATER, J. J. R. H. et al. Reliability and the smallest detectable differences of lateral cephalometric measurements. **American Journal of Orthodontics and Dentofacial Orthopedics**, v. 138, n. 5, 546.e1–546.e8, nov. 2010. DOI: 10.1016/j.ajodo.2010.05.013.

DEB, K. Multi-objective optimization. In: BURKE, E. K.; KENDALL, G. (Ed.). **Search methodologies**: Introductory tutorials in optimization and decision support techniques. [S.l.]: Springer Nature, 2014. cap. 15, p. 403–449. ISBN 978-1-4614-6939-1. DOI: 10.1007/978-1-4614-6940-7_15.

DEVANNA, R. Two-dimensional to three-dimensional: A new three-dimensional cone-beam computed tomography cephalometric analysis. **Journal of Orthodontic Research**, v. 3, n. 1, p. 30–37, 7 out. 2015. DOI: 10.4103/2321-3825.146356.

DUY, N. T. et al. Automatic detection and classification of teeth in CT data. In: AYACHE, N. et al. (Ed.). **Medical Image Computing and Computer-Assisted Intervention**. [S.l.]: Springer Nature, 2012. p. 609–616. DOI: 10.1007/978-3-642-33415-3_75.

EDWARDS, S. P.; CONLEY, R. S. Applications of cone beam computed tomography to orthognathic surgery treatment planning. In: KAPILA, S. D. (Ed.). **Cone beam computed tomography in orthodontics**: Indications, insights, and innovations. [S.l.]: John Wiley e Sons, out. 2014. p. 437–452. DOI: 10.1002/9781118674888.ch20.

GAMBA, T. O.; ALVES, M. C.; HAITER-NETO, F. Mandibular sexual dimorphism analysis in CBCT scans. **Journal of Forensic and Legal Medicine**, v. 38, p. 106–110, fev. 2016. DOI: 10.1016/j.jflm.2015.11.024.

GAO, H.; CHAE, O. Individual tooth segmentation from CT images using level set method with shape and intensity prior. **Pattern Recognit**, v. 43, n. 7, p. 2406–2417, jul. 2010. DOI: 10.1016/j.patcog.2010.01.010.

GARIB, D. G. et al. Is there a consensus for CBCT use in orthodontics? **Dental Press Journal of Orthodontics**, v. 19, n. 5, p. 136–149, out. 2014. DOI: 10.1590/2176-9451.19.5.136-149.sar.

GARSON, J. G. The Frankfort Craniometric Agreement, with critical remarks thereon. **Journal of the Anthropological Institute of Great Britain and Ireland**, v. 14, p. 64–83, 1885. DOI: 10.2307/2841484.

GATENO, J.; XIA, J. J.; TEICHGRAEBER, J. F. New 3-dimensional cephalometric analysis for orthognathic surgery. **Journal of Oral and Maxillofacial Surgery**, v. 69, n. 3, p. 606–622, mar. 2011. DOI: 10.1016/j.joms.2010.09.010.

GOLLMER, S. T.; BUZUG, T. M. Fully automatic shape constrained mandible segmentation from cone-beam CT data. In: IEEE International Symposium on Biomedical Imaging. [S.l.]: IEEE, maio 2012. DOI: 10.1109/isbi.2012.6235794.

GRAYSON, B. et al. The three-dimensional cephalogram: Theory, techniques, and clinical application. **American Journal of Orthodontics and Dentofacial Orthopedics**, v. 94, n. 4, p. 327–337, out. 1988. DOI: 10.1016/0889-5406(88)90058-3.

GRIBEL, B. F. et al. Accuracy and reliability of craniometric measurements on lateral cephalometry and 3D measurements on CBCT scans. **Angle Orthodontics**, v. 81, n. 1, p. 26–35, jan. 2011. DOI: 10.2319/032210-166.1.

GUPTA, A. et al. A knowledge-based algorithm for automatic detection of cephalometric landmarks on CBCT images. **International Journal of Computer Assisted Radiology and Surgery**, v. 10, n. 11, p. 1737–1752, abr. 2015. DOI: 10.1007/s11548-015-1173-6.

HAFFNER, C. L. et al. A technique for three-dimensional cephalometric analysis as an aid in evaluating changes in the craniofacial skeleton. **Angle Orthodontist**, v. 69, n. 4, p. 345–348, ago. 1999. DOI: 10.1043/0003-3219(1999)069<0345:ATFTDC>2.3.CO;2.

HARRIS, E. F.; SMITH, R. N. Accounting for measurement error: A critical but often overlooked process. **Archives of Oral Biology**, v. 54, s1, s107–s117, dez. 2009. DOI: 10.1016/j.archoralbio.2008.04.010.

JI, D. X.; ONG, S. H.; FOONG, K. W. C. A level-set based approach for anterior teeth segmentation in cone beam computed tomography images. **Computers in Biology and Medicine**, v. 50, p. 116–128, jul. 2014. DOI: 10.1016/j.compbiomed.2014.04.006.

KAINMUELLER, D. et al. Automatic extraction of mandibular nerve and bone from cone-beam CT data. In: YANG, G.-Z. et al. (Ed.). **Medical Image Computing and Computer-Assisted Intervention**. [S.l.]: Springer Nature, 2009. p. 76–83. DOI: 10.1007/978-3-642-04271-3_10.

KAMBUROĞLU, K. et al. Accuracy of CBCT measurements of a human skull. **Journal of Digital Imaging**, v. 24, n. 5, p. 787–793, out. 2011. DOI: 10.1007/s10278-010-9339-9.

KAPILA, S. D. Contemporary concepts of cone beam computed tomography in orthodontics. In: _____. **Cone beam computed tomography in orthodontics**: Indications, insights, and innovations. Edição: S. D. Kapila. [S.l.]: Wiley-Blackwell, out. 2014. p. 3–42. DOI: 10.1002/9781118674888.ch1.

KAU, C. H.; RICHMOND, S. (Ed.). **Three-dimensional imaging for orthodontics and maxillofacial surgery**. [S.l.]: Wiley-Blackwell, 2010. ISBN 978-1-4051-6240-1.

KEUSTERMANS, J.; SMEETS, D. et al. Automated cephalometric landmark localization using sparse shape and appearance models. In: SUZUKI, K. et al. (Ed.). **Machine**

Learning in Medical Imaging. [S.l.]: Springer Nature, 2011. p. 249–256. DOI: 10.1007/978-3-642-24319-6_31.

KEUSTERMANS, J.; VANDERMEULEN, D.; SUETENS, P. Integrating statistical shape models into a graph cut framework for tooth segmentation. In: WANG, F. et al. (Ed.). **Machine Learning in Medical Imaging**. [S.l.]: Springer Nature, 2012. p. 242–249. DOI: 10.1007/978-3-642-35428-1_30.

KIM, E.-J. et al. Maxillofacial characteristics affecting chin deviation between mandibular retrusion and prognathism patients. **Angle Orthodontist**, v. 81, n. 6, p. 988–993, nov. 2011. DOI: 10.2319/112210-681.1.

KIM, H.; JÜRGENS, P.; REYES, M. Soft-tissue simulation for cranio-maxillofacial surgery: Clinical needs and technical aspects. In: GEFEN, A. (Ed.). **Patient-Specific Modeling in Tomorrow's Medicine**. [S.l.]: Springer Nature, out. 2011. p. 413–440. DOI: 10.1007/8415_2011_105.

KIM, Y.-I. et al. Cone-beam computerized tomography evaluation of condylar changes and stability following two-jaw surgery: Le Fort I osteotomy and mandibular setback surgery with rigid fixation. **Oral Surgery, Oral Medicine, Oral Pathology, Oral Radiology**, v. 111, n. 6, p. 681–687, jun. 2011. DOI: 10.1016/j.tripleo.2010.08.001.

KUMAR, V. et al. Comparison of conventional and cone beam CT synthesized cephalograms. **Dentomaxillofacial Radiology**, v. 36, n. 5, p. 263–269, jul. 2007. DOI: 10.1259/dmfr/98032356.

LIANG, C. et al. Norms of McNamara's cephalometric analysis on lateral view of 3D CT imaging in adults from Northeast China. **Journal of Hard Tissue Biology**, v. 23, n. 2, p. 249–254, 2014. DOI: 10.2485/jhtb.23.249.

LIN, H.-H. et al. Comparative validity and reproducibility study of various landmark-oriented reference planes in 3-dimensional computed tomographic analysis for patients receiving orthognathic surgery. **PLOS ONE**, v. 10, n. 2, p. 1–16, 10 fev. 2015. DOI: 10.1371/journal.pone.0117604.

LORENSEN, W. E.; CLINE, H. E. Marching cubes: A high resolution 3D surface construction algorithm. **ACM SIGGRAPH Computer Graphics**, v. 21, n. 4, p. 163–169, jul. 1987. DOI: 10.1145/37402.37422.

MAKRAM, M.; KAMEL, H. Reeb Graphs for automatic localization of 3D craniofacial landmarks: Application in 3D cephalometry. **15ème Compression et Représentation des Signaux Audiovisuels**, 2012.

MAZZA, E.; BARBARINO, G. G. 3D mechanical modeling of facial soft tissue for surgery simulation. **Facial Plastic Surgery Clinics of North America**, v. 19, n. 4, p. 623–637,

nov. 2011. DOI: 10.1016/j.fsc.2011.07.006.

MCNAMARA, J. A. A method of cephalometric evaluation. **American Journal of Orthodontics**, v. 86, n. 6, p. 449–469, dez. 1984. DOI: 10.1016/s0002-9416(84)90352-x.

MOLLEMANS, W. et al. Predicting soft tissue deformations for a maxillofacial surgery planning system: From computational strategies to a complete clinical validation. **Medical Image Analysis**, v. 11, n. 3, p. 282–301, jun. 2007. DOI: 10.1016/j.media.2007.02.003.

MOZZO, P. et al. A new volumetric CT machine for dental imaging based on the cone-beam technique: Preliminary results. **European Radiology**, v. 8, n. 9, p. 1558–1564, nov. 1998. DOI: 10.1007/s003300050586.

NAUMOVICH, S. S.; NAUMOVICH, S. A.; GONCHARENKO, V. G. Three-dimensional reconstruction of teeth and jaws based on segmentation of CT images using watershed transformation. **Dentomaxillofacial Radiology**, v. 44, n. 4, p. 20140313, abr. 2015. DOI: 10.1259/dmfr.20140313.

OH, S. et al. Frankfort horizontal plane is an appropriate three-dimensional reference in the evaluation of clinical and skeletal cant. **Journal of the Korean Association of Oral and Maxillofacial Surgeons**, v. 39, n. 2, p. 71–76, abr. 2013. DOI: 10.5125/jkaoms.2013.39.2.71.

PAN, B. et al. Incremental kernel ridge regression for the prediction of soft tissue deformations. In: AYACHE, N. et al. (Ed.). **Medical Image Computing and Computer-Assisted Intervention**. [S.l.]: Springer Nature, 2012. p. 99–106. DOI: 10.1007/978-3-642-33415-3_13.

PARK, S.-B. et al. Midfacial soft-tissue changes after mandibular setback surgery with or without paranasal augmentation: Cone-beam computed tomography (CBCT) volume superimposition. **Journal of Cranio-Maxillofacial Surgery**, v. 41, n. 2, p. 119–123, mar. 2013. DOI: 10.1016/j.jcms.2012.05.017.

PARK, S.-H. et al. A proposal for a new analysis of craniofacial morphology by 3-dimensional computed tomography. **American Journal of Orthodontics and Dentofacial Orthopedics**, v. 129, n. 5, 600.e23–600.e34, maio 2006. DOI: 10.1016/j.ajodo.2005.11.032.

PEARSON, K. On lines and planes of closest fit to systems of points in space. **Philosophical Magazine**, v. 2, n. 11, p. 559–572, nov. 1901. DOI: 10.1080/14786440109462720.

PHULARI, B. S. **An atlas on cephalometric landmarks**. New Delhi: Jaypee Brothers Medical Publishers, 2008. ISBN 978-93-5090-324-7.

POPAT, H.; RICHMOND, S. New developments in: Three-dimensional planning for orthognathic surgery. **Journal of Orthodontics**, v. 37, n. 1, p. 62–71, mar. 2010. DOI: 10.1179/14653121042885.

PROFFIT, W. R.; WHITE, R. P.; SARVER, D. M. **Contemporary treatment of dentofacial deformity**. [S.l.]: Mosby, 2003. ISBN 978-0323016971.

QUERESHY, F. A.; SAVELL, T. A.; PALOMO, J. M. Applications of cone beam computed tomography in the practice of oral and maxillofacial surgery. **Journal of Oral and Maxillofacial Surgery**, v. 66, n. 4, p. 791–796, abr. 2008. DOI: 10.1016/j.joms.2007.11.018.

R DEVELOPMENT CORE TEAM. **R**: A language and environment for statistical computing. Vienna, AT, 2014. ISBN 3-900051-07-0. Disponível em: <http://www.R-project.org/>.

RANGEL, F. A. et al. Integration of digital dental casts in cone-beam computed tomography scans. **ISRN Dentistry**, v. 2012, p. 1–6, 2012. DOI: 10.5402/2012/949086.

ROSSUM, G. **Python language reference manual**: Revised and updated for Python 3.2. Edição: Fred L. Jr. Drake. Bristol, 2011. ISBN 978-1-906966-14-0.

SANTOS, R. M. G.; DE MARTINO, J. M.; HAITER NETO, F. et al. Influence of different setups of the Frankfort horizontal plane on 3-dimensional cephalometric measurements. **American Journal of Orthodontics and Dentofacial Orthopedics**, v. 152, n. 2, p. 242–249, ago. 2017. DOI: 10.1016/j.ajodo.2016.12.023.

SANTOS, R. M. G.; DE MARTINO, J. M.; PASSERI, L. A. et al. Automatic repositioning of jaw segments for three-dimensional virtual treatment planning of orthognathic surgery. **Journal of Cranio-Maxillo-Facial Surgery**, v. 45, n. 9, p. 1399–1407, set. 2017. DOI: 10.1016/j.jcms.2017.06.017.

SARDANELLI, F.; DI LEO, G. **Biostatistics for radiologists**: Planning, performing, and writing a radiologic study. Milan: Springer, 2009. ISBN 978-88-470-1132-8.

SARMENT, D. (Ed.). **Cone beam computed tomography**: Oral and maxillofacial diagnosis and applications. [S.l.]: Wiley-Blackwell, 2014. ISBN 978-0470961407.

SCARFE, W. C.; FARMAN, A. G.; SUKOVIC, P. Clinical applications of cone-beam computed tomography in dental practice. **Journal of the Canadian Dental Association**, v. 72, n. 1, p. 75–80, fev. 2006.

SCHROEDER, W.; MARTIN, K.; LORENSEN, B. **The visualization toolkit**: An object-oriented approach to 3D graphics. 4. ed. Clifton Park: Kitware, 2006. ISBN 978-1-930934-19-1. Disponível em: <http://www.kitware.com/products/books/VTKTextbook.pdf>.

SHAHIDI, S. et al. The accuracy of a designed software for automated localization of craniofacial landmarks on CBCT images. **BMC Medical Imaging**, v. 14, n. 1, set. 2014. DOI: 10.1186/1471-2342-14-32.

SONG, W.-W. et al. Maxillary yaw as the primary predictor of maxillary dental midline deviation: 3D analysis using cone-beam computed tomography. **Journal of Oral and Maxillofacial Surgery**, v. 71, n. 4, p. 752–762, abr. 2013. DOI: 10.1016/j.joms.2012.07.043.

SPENCER, F. (Ed.). **History of physical anthropology**: An encyclopedia. New York: Garland Publishing, 1997. v. 1. (Garland Reference Library of Social Science, 677). ISBN 978-0-8153-0490-6.

STORN, R.; PRICE, K. Differential evolution: A simple and efficient Heuristic for global optimization over continuous spaces. **Journal of Global Optimization**, v. 11, n. 4, p. 341–359, 1997. DOI: 10.1023/a:1008202821328.

SUMMERFIELD, M. **Rapid GUI programming with Python and Qt**: The definitive guide to PyQt programming. Upper Saddle River: Pearson Education, 2008. ISBN 978-0-13-235418-9.

SWENNEN, G. R. J.; MOLLEMANS, W.; SCHUTYSER, F. Three-dimensional treatment planning of orthognathic surgery in the era of virtual imaging. **Journal of Oral and Maxillofacial Surgery**, v. 67, n. 10, p. 2080–2092, out. 2009. DOI: 10.1016/j.joms.2009.06.007.

SWENNEN, G. R. J.; SCHUTYSER, F. Three-dimensional virtual approach to diagnosis and treatment planning of maxillofacial deformity. In: BELL, W. H. (Ed.). **Distraction Osteogenesis of the Facial Skeleton**. [S.l.]: BC Decker, 2007. cap. 6.

SWENNEN, G. R. J.; SCHUTYSER, F.; BARTH, E.-L. et al. A new method of 3-D cephalometry Part I: The anatomic Cartesian 3-D reference system. **Journal of Craniofacial Surgery**, v. 17, n. 2, p. 314–325, mar. 2006. DOI: 10.1097/00001665-200603000-00019.

SWENNEN, G. R. J.; SCHUTYSER, F.; HAUSAMEN, J.-E. (Ed.). **Three-dimensional cephalometry**: A color atlas and manual. New York: Springer, 2006. ISBN 978-3-540-25440-9.

TERAJIMA, M. et al. A 3-dimensional method for analyzing the morphology of patients with maxillofacial deformities. **American Journal of Orthodontics and Dentofacial Orthopedics**, v. 136, n. 6, p. 857–867, dez. 2009. DOI: 10.1016/j.ajodo.2008.01.019.

VAHDETTIN, L. et al. Three-dimensional cephalometric norms of Turkish Cypriots using CBCT images reconstructed from a volumetric rendering program in vivo. **Turkish Journal of Medical Sciences**, v. 46, p. 848–861, abr. 2016. DOI: 10.3906/sag-1409-21.

VLIJMEN, O. J. C.; BERGÉ, S. J. et al. Comparison of cephalometric radiographs obtained from cone-beam computed tomography scans and conventional radiographs. **Journal of Oral and Maxillofacial Surgery**, v. 67, n. 1, p. 92–97, jan. 2009. DOI: 10.1016/j.joms.2008.04.025.

VLIJMEN, O. J. C.; MAAL, T. J. J. et al. A comparison between 2D and 3D cephalometry on CBCT scans of human skulls. **International Journal of Oral Maxillofacial Surgery**, v. 39, n. 2, p. 156–160, fev. 2010. DOI: 10.1016/j.ijom.2009.11.017.

_____. A comparison between two-dimensional and three-dimensional cephalometry on frontal radiographs and on cone beam computed tomography scans of human skulls. **European Journal of Oral Sciences**, v. 117, n. 3, p. 300–305, jun. 2009. DOI: 10.1111/j.1600-0722.2009.00633.x.

WALT, S.; COLBERT, S. C.; VAROQUAUX, G. The NumPy array: A structure for efficient numerical computation. **Computing in Science and Engineering**, v. 13, n. 2, p. 22–30, 7 mar. 2011. DOI: 10.1109/MCSE.2011.37.

WANG, L. et al. Automated bone segmentation from dental CBCT images using patch-based sparse representation and convex optimization. **Medical Physics**, v. 41, n. 4, p. 043503, mar. 2014. DOI: 10.1118/1.4868455.

WELCH, B. L. The generalization of 'Student's' problem when several different population variances are involved. **Biometrika**, v. 34, n. 1-2, p. 28–35, jan. 1947. DOI: 10.1093/biomet/34.1-2.28.

WHITE, T. D.; BLACK, M. T.; FOLKENS, P. A. **Human osteology**. 3. ed. San Diego: Academic Press, 2012. ISBN 978-0-12-374134-9.

WONG, R. W. K.; CHAU, A. C. M.; HÄGG, U. 3D CBCT McNamara's cephalometric analysis in an adult Southern Chinese population. **International Journal of Oral and Maxillofacial Surgery**, v. 40, n. 9, p. 920–925, set. 2011. DOI: 10.1016/j.ijom.2011.03.011.

XIA, J. J. et al. Automated digital dental articulation. In: JIANG, T. et al. (Ed.). **Medical Image Computing and Computer-Assisted Intervention**. [S.l.]: Springer Nature, 2010. p. 278–286. DOI: 10.1007/978-3-642-15711-0_35.

YOON, K. W. et al. Deviation of landmarks in accordance with methods of establishing reference planes in three-dimensional facial CT evaluation. **Imaging Science in Dentistry**, v. 44, n. 3, p. 207–212, set. 2014. DOI: 10.5624/isd.2014.44.3.207.

ZHANG, X.; CHEN, X. et al. An effective approach of teeth segmentation within the 3D cone beam computed tomography image based on deformable surface model. **Mathematical Problems in Engineering**, v. 2016, p. 1–10, 2016. DOI: 10.1155/2016/9505217.

ZHANG, X.; TANG, Z. et al. An eFace-template method for efficiently generating patient-specific anatomically-detailed facial soft tissue FE models for craniomaxillofacial surgery simulation. **Annals of Biomedical Engineering**, v. 44, n. 5, p. 1656–1671, out. 2015. DOI: 10.1007/s10439-015-1480-7.

Apêndice A

Permissões

Os artigos do autor foram incluídos nesta tese em acordância com a política de reprodução de conteúdo das editoras responsáveis pelas publicações. As permissões das editoras são apresentadas abaixo.

A.1 Elsevier

Informação extraída do endereço eletrônico https://www.elsevier.com/about/our-business/policies/copyright/personal-use, em 13 de outubro de 2017:

> *Authors can use their articles, in full or in part, for a wide range of scholarly, non-commercial purposes as outlined below:*
>
> - *Use by an author in the author's classroom teaching (including distribution of copies, paper or electronic)*
> - *Distribution of copies (including through e-mail) to known research colleagues for their personal use (but not for Commercial Use)*
> - *Inclusion in a thesis or dissertation (provided that this is not to be published commercially)*
> - *Use in a subsequent compilation of the author's works*
> - *Extending the Article to book-length form*
> - *Preparation of other derivative works (but not for Commercial Use)*
> - *Otherwise using or re-using portions or excerpts in other works*
>
> *These rights apply for all Elsevier authors who publish their article as either a subscription article or an open access article. In all cases we require that all Elsevier authors always include a full acknowledgement and, if appropriate, a link to the final published version hosted on Science Direct.*

A.2 Wolters Kluwer

Informação fornecida pelo Wolters Kluwer *Permission Team*, por meio de contato eletrônico realizado em 13 de outubro de 2017:

> *[Wolters Kluwer] will permit the author(s) to deposit for display a "final peer-reviewed manuscript" (the final manuscript after peer-review and acceptance for publication but prior to the publisher's copyediting, design, formatting, and other services) 12 months after publication of the final article on the author's personal web site, university's institutional repository or employer's intranet, subject to the following:*
>
> - *You may only deposit the final peer-reviewed manuscript.*
> - *You may not update the final peer-reviewed manuscript text or replace it with a proof or with the final published version.*
> - *You may not include the final peer-reviewed manuscript or any other version of the article on any commercial site or in any repository owned or operated by any third party. For authors of articles based on research funded by the National Institutes of Health (NIH), Wellcome Trust, Howard Hughes Medical Institute (HHMI), or other funding agency, see below for the services that Lippincott Williams & Wilkins (LWW) will provide on your behalf to comply with "Public Access Policy" guidelines.*
> - *You may not display the final peer-reviewed manuscript until twelve months after publication of the final article.*
> - *You must attach the following notice to the final peer-reviewed manuscript: "This is a non-final version of an article published in final form in (provide complete journal citation)".*
> - *You shall provide a link in the final peer-reviewed manuscript to the journal website.*

Apêndice B

Pareceres

Este capítulo exibe cópia dos pareceres consubstanciados emitidos pelo Comitê de Ética em Pesquisa (CEP) da Universidade Estadual de Campinas, órgão institucional que analisou e aprovou os aspectos éticos do trabalho apresentado nesta tese de doutorado. Os pareceres são referentes às análises do projeto de pesquisa e dos relatórios de acompanhamento do projeto, como listados abaixo.

1. Projeto de Pesquisa
2. Notificação 1 – Relatório Parcial
3. Notificação 2 – Relatório Parcial
4. Notificação 3 – Relatório Parcial
5. Notificação 4 – Relatório Parcial
6. Notificação 5 – Relatório Parcial
7. Notificação 6 – Relatório Parcial
8. Notificação 7 – Relatório Final

B.1 Parecer 1

Projeto de Pesquisa

Cópia do parecer consubstanciado do CEP referente ao projeto de pesquisa submetido para análise em 18 de fevereiro de 2014.

31 de março de 2014

FACULDADE DE CIENCIAS MEDICAS - UNICAMP (CAMPUS CAMPINAS)

PARECER CONSUBSTANCIADO DO CEP

DADOS DO PROJETO DE PESQUISA

Título da Pesquisa: Automatização de Planos de Tratamento em Cirurgia Ortognática e Aprimoramento de Análise Cefalométrica em 3D

Pesquisador: Rodrigo Mologni Gonçalves dos Santos

Área Temática:

Versão: 1

CAAE: 27917314.0.0000.5404

Instituição Proponente: Faculdade de Engenharia Elétrica e de Computação

Patrocinador Principal: Financiamento Próprio

DADOS DO PARECER

Número do Parecer: 574.504

Data da Relatoria: 25/03/2014

Apresentação do Projeto:

A tecnologia em 3D à disposição da Cirurgia Ortognática viabilizou a execução do diagnóstico e planejamento cirúrgico de deformidades dentofaciais sobre um modelo virtual de alta precisão da cabeça do paciente. Por ser muito recente e ainda em desenvolvimento, boas oportunidades de pesquisa concentram-se nesta temática. Buscando contribuir neste sentido, serão analisadas imagens de Tomografia Computadorizada (TC) por feixe cônico (TCFC) de indivíduos adultos caucasianos, buscando identificar pontos cefalométricos, na realização de medidas, na produção de modelos de cabeças e, por fim, na simulação virtual da correção cirúrgica. Espera-se como resultados: (1) o estabelecimento de um padrão cefalométrico em 3D que estenda o padrão em 2D definido por McNamara sem perder a compatibilidade com este; 2) o desenvolvimento de um método computacional que possibilite a elaboração automatizada de planos de tratamento em cirurgia ortognática num ambiente virtual em 3D e (3) a elaboração de uma análise cefalométrica puramente em 3D.

Objetivo da Pesquisa:

Objetivo Primário:

1. Desenvolver um método computacional para a elaboração automatizada de planos de tratamento cirúrgico a indivíduos adultos, portadores de maloclusões esqueléticas;

Endereço: Rua Tessália Vieira de Camargo, 126
Bairro: Barão Geraldo **CEP:** 13.083-887
UF: SP **Município:** CAMPINAS
Telefone: (19)3521-8936 **Fax:** (19)3521-7187 **E-mail:** cep@fcm.unicamp.br

FACULDADE DE CIENCIAS MEDICAS - UNICAMP (CAMPUS CAMPINAS)

Continuação do Parecer: 574.504

2. Estabelecer uma análise cefalométrica com medidas em 3D que explore a terceira dimensão acrescida pela imagem de TC em relação à imagem radiográfica.
TC em relação à imagem radiográfica.

Avaliação dos Riscos e Benefícios:

Riscos:

Não haverá riscos previsíveis aos indivíduos, uma vez que os procedimentos serão realizados sobre imagens de TCFC já existentes, caracterizando estudo retrospectivo. No que se refere à preservação da identidade dos sujeitos, pesquisadores informam que será atribuído um código de identificação exclusivo a cada caso que, por sua vez, dispensará o uso do nome ou de qualquer outra informação que possibilite a identificação dos sujeitos ao longo o da pesquisa.

Benefícios: não haverá benefícios diretos aos indivíduos relacionados ao estudo.

Academicamente, o estudo poderá contribuir favoravelmente para o planejamento e resolução cirúrgica de deformidades dentofaciais.

Comentários e Considerações sobre a Pesquisa:

Trata-se de projeto de pesquisa para doutorado, da área de Engenharia Elétrica da Universidade estadual de Campinas.

Pesquisadores apontam os seguintes critérios de composição da amostra:

Critérios de Inclusão: será reaproveitada uma base de imagens de TCFC de posse da Área de Radiologia Odontológica da Faculdade de Odontologia de Piracicaba (FOP). A base contém 86 imagens de face completa e foi cedida dos arquivos de pesquisa desta área.

Critério de Exclusão: imagens do acervo advindas de indivíduos sob as seguintes condições:

1. já submetidos a intervenção cirúrgica nos ossos da face;
2. portadores de traumatismos, assimetrias ou deformidades craniofaciais severas;
3. portadores de deformidades dentofaciais que não são possíveis de serem corrigidas fazendo uso apenas de osteotomias convencionais;
4. com ausência de dentes. Na presença de implantes dentários, que sejam poucos e não estejam no lugar dos primeiros molares e nem dos incisivos centrais;
5. com características faciais não predominantes da raça caucasiana;
6. com idade fora da faixa etária entre 18 e 29 anos para o sexo masculino e entre 16 e 29 para o sexo feminino.

Considerações sobre os Termos de apresentação obrigatória:

Foram apresentados:

Endereço: Rua Tessália Vieira de Camargo, 126
Bairro: Barão Geraldo **CEP:** 13.083-887
UF: SP **Município:** CAMPINAS
Telefone: (19)3521-8936 **Fax:** (19)3521-7187 **E-mail:** cep@fcm.unicamp.br

FACULDADE DE CIENCIAS MEDICAS - UNICAMP (CAMPUS CAMPINAS)

Continuação do Parecer: 574.504

- Folha de rosto devidamente assinada pelo pesquisador principal e pelo diretor da instituição proponente (Faculdade de Engenharia elétrica da Unicamp).
- Projeto detalhado e formulário de informações básicas do projeto, gerado pela Plataforma Brasil.
- Declaração para uso de arquivos, registros e similares, autorizando o presente estudo, assinada pelo responsável pelo sistema de arquivo da área de Radiologia odontológica da FOP (Faculdade de Odontologia de Piracicaba).

Pesquisadores solicitam dispensa de aplicação de Termo de Consentimento Livre e Esclarecido (TCLE), com a devida justificativa, que foi aceita por este CEP (ver quadro riscos e benefícios).

Recomendações:

--

Conclusões ou Pendências e Lista de Inadequações:

Projeto aprovado com dispensa de apresentação de TCLE.

Situação do Parecer:

Aprovado

Necessita Apreciação da CONEP:

Não

Considerações Finais a critério do CEP:

Projeto aprovado em reunião do colegiado, em 25-03-2014.

CAMPINAS, 31 de Março de 2014

Assinador por:
Fátima Aparecida Bottcher Luiz
(Coordenador)

Endereço: Rua Tessália Vieira de Camargo, 126
Bairro: Barão Geraldo **CEP:** 13.083-887
UF: SP **Município:** CAMPINAS
Telefone: (19)3521-8936 **Fax:** (19)3521-7187 **E-mail:** cep@fcm.unicamp.br

B.2 Parecer 2

Notificação 1 – Relatório Parcial

Cópia do parecer consubstanciado do CEP referente ao relatório parcial de acompanhamento do projeto de pesquisa submetido para análise em 22 de setembro de 2014.

20 de março de 2015

COMITÊ DE ÉTICA EM PESQUISA DA UNICAMP - CAMPUS CAMPINAS

PARECER CONSUBSTANCIADO DO CEP

DADOS DO PROJETO DE PESQUISA

Título da Pesquisa: Automatização de Planos de Tratamento em Cirurgia Ortognática e Aprimoramento de Análise Cefalométrica em 3D

Pesquisador: Rodrigo Mologni Gonçalves dos Santos

Área Temática:

Versão: 1

CAAE: 27917314.0.0000.5404

Instituição Proponente: Faculdade de Engenharia Elétrica e de Computação

Patrocinador Principal: Financiamento Próprio

DADOS DA NOTIFICAÇÃO

Tipo de Notificação: Envio de Relatório Parcial

Detalhe:

Justificativa:

Data do Envio: 22/09/2014

Situação da Notificação: Parecer Consubstanciado Emitido

DADOS DO PARECER

Número do Parecer: 992.892

Data da Relatoria: 20/03/2015

Apresentação da Notificação:

Apresentação do relatório parcial do referido estudo.

Objetivo da Notificação:

Apresentação do relatório parcial do referido estudo.

Avaliação dos Riscos e Benefícios:

Mantidos em relação ao projeto original.

Comentários e Considerações sobre a Notificação:

Relatório apresentado satisfatoriamente, em todos os seus itens.

Considerações sobre os Termos de apresentação obrigatória:

Vide pareceres anteriores.

Endereço: Rua Tessália Vieira de Camargo, 126
Bairro: Barão Geraldo **CEP:** 13.083-887
UF: SP **Município:** CAMPINAS
Telefone: (19)3521-8936 **Fax:** (19)3521-7187 **E-mail:** cep@fcm.unicamp.br

COMITÊ DE ÉTICA EM PESQUISA DA UNICAMP - CAMPUS CAMPINAS

Continuação do Parecer: 992.892

Recomendações:

Conclusões ou Pendências e Lista de Inadequações:

Relatório parcial do estudo aprovado.

Situação do Parecer:

Aprovado

Necessita Apreciação da CONEP:

Não

Considerações Finais a critério do CEP:

CAMPINAS, 20 de Março de 2015

Assinado por:
Renata Maria dos Santos Celeghini
(Coordenador)

Endereço: Rua Tessália Vieira de Camargo, 126
Bairro: Barão Geraldo **CEP:** 13.083-887
UF: SP **Município:** CAMPINAS
Telefone: (19)3521-8936 **Fax:** (19)3521-7187 **E-mail:** cep@fcm.unicamp.br

B.3 Parecer 3

Notificação 2 – Relatório Parcial

Cópia do parecer consubstanciado do CEP referente ao relatório parcial de acompanhamento do projeto de pesquisa submetido para análise em 20 de março de 2015.

16 de junho de 2015

COMITÊ DE ÉTICA EM PESQUISA DA UNICAMP - CAMPUS CAMPINAS

PARECER CONSUBSTANCIADO DO CEP

DADOS DO PROJETO DE PESQUISA

Título da Pesquisa: Automatização de Planos de Tratamento em Cirurgia Ortognática e Aprimoramento de Análise Cefalométrica em 3D

Pesquisador: Rodrigo Mologni Gonçalves dos Santos

Área Temática:

Versão: 1

CAAE: 27917314.0.0000.5404

Instituição Proponente: Faculdade de Engenharia Elétrica e de Computação

Patrocinador Principal: Financiamento Próprio

DADOS DA NOTIFICAÇÃO

Tipo de Notificação: Envio de Relatório Parcial

Detalhe:

Justificativa:

Data do Envio: 20/03/2015

Situação da Notificação: Parecer Consubstanciado Emitido

DADOS DO PARECER

Número do Parecer: 1.109.415

Data da Relatoria: 10/06/2015

Apresentação da Notificação:

Apresentação do relatório parcial do referido estudo.

Objetivo da Notificação:

Apresentação do relatório parcial do referido estudo.

Avaliação dos Riscos e Benefícios:

Mantidos em relação ao projeto original.

Comentários e Considerações sobre a Notificação:

Relatório apresentado satisfatoriamente, em todos os seus itens.

Considerações sobre os Termos de apresentação obrigatória:

Vide pareceres anteriores.

Endereço: Rua Tessália Vieira de Camargo, 126
Bairro: Barão Geraldo **CEP:** 13.083-887
UF: SP **Município:** CAMPINAS
Telefone: (19)3521-8936 **Fax:** (19)3521-7187 **E-mail:** cep@fcm.unicamp.br

COMITÊ DE ÉTICA EM PESQUISA DA UNICAMP - CAMPUS CAMPINAS

Continuação do Parecer: 1.109.415

Recomendações:

Conclusões ou Pendências e Lista de Inadequações:
Relatório parcial do estudo aprovado.

Situação do Parecer:
Aprovado

Necessita Apreciação da CONEP:
Não

Considerações Finais a critério do CEP:
- O sujeito de pesquisa deve receber uma via do Termo de Consentimento Livre e Esclarecido, na íntegra, por ele assinado.

- O sujeito da pesquisa tem a liberdade de recusar-se a participar ou de retirar seu consentimento em qualquer fase da pesquisa, sem penalização alguma e sem prejuízo ao seu cuidado.

- O pesquisador deve desenvolver a pesquisa conforme delineada no protocolo aprovado. Se o pesquisador considerar a descontinuação do estudo, esta deve ser justificada e somente ser realizada após análise das razões da descontinuidade pelo CEP que o aprovou. O pesquisador deve aguardar o parecer do CEP quanto à descontinuação, exceto quando perceber risco ou dano não previsto ao sujeito participante ou quando constatar a superioridade de uma estratégia diagnóstica ou terapêutica oferecida a um dos grupos da pesquisa, isto é, somente em caso de necessidade de ação imediata com intuito de proteger os participantes.

- O CEP deve ser informado de todos os efeitos adversos ou fatos relevantes que alterem o curso normal do estudo. É papel do pesquisador assegurar medidas imediatas adequadas frente a evento adverso grave ocorrido (mesmo que tenha sido em outro centro) e enviar notificação ao CEP e à Agência Nacional de Vigilância Sanitária – ANVISA – junto com seu posicionamento.

- Eventuais modificações ou emendas ao protocolo devem ser apresentadas ao CEP de forma clara e sucinta, identificando a parte do protocolo a ser modificada e suas justificativas. Em caso de projetos do Grupo I ou II apresentados anteriormente à ANVISA, o pesquisador ou patrocinador deve enviá-las também à mesma, junto com o parecer aprovatório do CEP, para serem juntadas ao protocolo inicial.

Endereço: Rua Tessália Vieira de Camargo, 126
Bairro: Barão Geraldo **CEP:** 13.083-887
UF: SP **Município:** CAMPINAS
Telefone: (19)3521-8936 **Fax:** (19)3521-7187 **E-mail:** cep@fcm.unicamp.br

COMITÊ DE ÉTICA EM PESQUISA DA UNICAMP - CAMPUS CAMPINAS

Continuação do Parecer: 1.109.415

- Relatórios parciais e final devem ser apresentados ao CEP, inicialmente seis meses após a data deste parecer de aprovação e ao término do estudo.

-Lembramos que segundo a Resolução 466/2012 , item XI.2 letra e, “cabe ao pesquisador apresentar dados solicitados pelo CEP ou pela CONEP a qualquer momento”.

CAMPINAS, 16 de Junho de 2015

Assinado por:
Renata Maria dos Santos Celeghini
(Coordenador)

Endereço: Rua Tessália Vieira de Camargo, 126
Bairro: Barão Geraldo **CEP:** 13.083-887
UF: SP **Município:** CAMPINAS
Telefone: (19)3521-8936 **Fax:** (19)3521-7187 **E-mail:** cep@fcm.unicamp.br

B.4 Parecer 4

Notificação 3 – Relatório Parcial

Cópia do parecer consubstanciado do CEP referente ao relatório parcial de acompanhamento do projeto de pesquisa submetido para análise em 24 de setembro de 2015.

5 de janeiro de 2016

COMITÊ DE ÉTICA EM PESQUISA DA UNICAMP - CAMPUS CAMPINAS

PARECER CONSUBSTANCIADO DO CEP

DADOS DO PROJETO DE PESQUISA

Título da Pesquisa: Automatização de Planos de Tratamento em Cirurgia Ortognática e Aprimoramento de Análise Cefalométrica em 3D

Pesquisador: Rodrigo Mologni Gonçalves dos Santos

Área Temática:

Versão: 1

CAAE: 27917314.0.0000.5404

Instituição Proponente: Faculdade de Engenharia Elétrica e de Computação

Patrocinador Principal: Financiamento Próprio

DADOS DA NOTIFICAÇÃO

Tipo de Notificação: Envio de Relatório Parcial

Detalhe:

Justificativa:

Data do Envio: 24/09/2015

Situação da Notificação: Parecer Consubstanciado Emitido

DADOS DO PARECER

Número do Parecer: 1.383.753

Apresentação da Notificação:

--

Objetivo da Notificação:

Apresentação de relatório parcial.

Avaliação dos Riscos e Benefícios:

--

Endereço: Rua Tessália Vieira de Camargo, 126
Bairro: Barão Geraldo **CEP:** 13.083-887
UF: SP **Município:** CAMPINAS
Telefone: (19)3521-8936 **Fax:** (19)3521-7187 **E-mail:** cep@fcm.unicamp.br

COMITÊ DE ÉTICA EM PESQUISA DA UNICAMP - CAMPUS CAMPINAS

Continuação do Parecer: 1.383.753

Comentários e Considerações sobre a Notificação:
Formulário do relatório parcial da pesquisa foi preenchido adequadamente. Oitenta e seis participantes foram incluídos no estudo. Não houve intercorrências.

Considerações sobre os Termos de apresentação obrigatória:
Foi anexado formulário do relatório parcial no modelo preconizado pelo CEP, que visa detalhar possíveis intercorrências éticas durante o estudo.

Recomendações:
--

Conclusões ou Pendências e Lista de Inadequações:
Relatório aprovado.

Considerações Finais a critério do CEP:

Este parecer foi elaborado baseado nos documentos abaixo relacionados:

Tipo Documento	Arquivo	Postagem	Autor	Situação
Envio de Relatório Parcial	Relatorio_3.pdf	24/09/2015 13:10:41	Rodrigo Mologni Gonçalves dos Santos	Aceito

Situação do Parecer:
Aprovado

Necessita Apreciação da CONEP:
Não

CAMPINAS, 05 de Janeiro de 2016

Assinado por:
Renata Maria dos Santos Celeghini
(Coordenador)

Endereço: Rua Tessália Vieira de Camargo, 126
Bairro: Barão Geraldo **CEP:** 13.083-887
UF: SP **Município:** CAMPINAS
Telefone: (19)3521-8936 **Fax:** (19)3521-7187 **E-mail:** cep@fcm.unicamp.br

B.5 Parecer 5

Notificação 4 – Relatório Parcial

Cópia do parecer consubstanciado do CEP referente ao relatório parcial de acompanhamento do projeto de pesquisa submetido para análise em 9 de abril de 2016.

23 de maio de 2016

COMITÊ DE ÉTICA EM PESQUISA DA UNICAMP - CAMPUS CAMPINAS

PARECER CONSUBSTANCIADO DO CEP

DADOS DO PROJETO DE PESQUISA

Título da Pesquisa: Automatização de Planos de Tratamento em Cirurgia Ortognática e Aprimoramento de Análise Cefalométrica em 3D

Pesquisador: Rodrigo Mologni Gonçalves dos Santos

Área Temática:

Versão: 1

CAAE: 27917314.0.0000.5404

Instituição Proponente: Faculdade de Engenharia Elétrica e de Computação

Patrocinador Principal: Financiamento Próprio

DADOS DA NOTIFICAÇÃO

Tipo de Notificação: Envio de Relatório Parcial

Detalhe:

Justificativa:

Data do Envio: 09/04/2016

Situação da Notificação: Parecer Consubstanciado Emitido

DADOS DO PARECER

Número do Parecer: 1.556.084

Apresentação da Notificação:

Apresentação do relatório parcial do referido estudo.

Objetivo da Notificação:

Apresentação do relatório parcial do referido estudo.

Avaliação dos Riscos e Benefícios:

Mantidos em relação ao projeto original.

Comentários e Considerações sobre a Notificação:

Segundo informações contempladas no relatório parcial, a pesquisa encontra-se em andamento com previsão de conclusão para 23/10/2015. Foram incluídos 86 participantes de pesquisa e não houve intercorrências. O pesquisador informou que:"Três de quatro artigos previstos foram

Endereço: Rua Tessália Vieira de Camargo, 126
Bairro: Barão Geraldo **CEP:** 13.083-887
UF: SP **Município:** CAMPINAS
Telefone: (19)3521-8936 **Fax:** (19)3521-7187 **E-mail:** cep@fcm.unicamp.br

submetidos para publicação na American Journal of Orthodontics and Dentofacial Orthopedics (AJO-DO). O quarto artigo, um pedido de patente e uma tese de doutorado estão em fase de elaboração."

Considerações sobre os Termos de apresentação obrigatória:
Para avaliação desta notificação foi analisado o relatório parcial anexado no documento intitulado "Relatorio_4.pdf 09/04/2016 11:00:59".

Recomendações:

Conclusões ou Pendências e Lista de Inadequações:
Relatório parcial do estudo aprovado, mas segundo a data prevista para a conclusão da pesquisa, o estudo já foi finalizado. Diante do exposto, solicitamos que o pesquisador encaminhe o relatório final.

Considerações Finais a critério do CEP:
- O sujeito de pesquisa deve receber uma via do Termo de Consentimento Livre e Esclarecido, na íntegra, por ele assinado (quando aplicável).

- O sujeito da pesquisa tem a liberdade de recusar-se a participar ou de retirar seu consentimento em qualquer fase da pesquisa, sem penalização alguma e sem prejuízo ao seu cuidado (quando aplicável).

- O pesquisador deve desenvolver a pesquisa conforme delineada no protocolo aprovado. Se o pesquisador considerar a descontinuação do estudo, esta deve ser justificada e somente ser realizada após análise das razões da descontinuidade pelo CEP que o aprovou. O pesquisador deve aguardar o parecer do CEP quanto à descontinuação, exceto quando perceber risco ou dano não previsto ao sujeito participante ou quando constatar a superioridade de uma estratégia diagnóstica ou terapêutica oferecida a um dos grupos da pesquisa, isto é, somente em caso de necessidade de ação imediata com intuito de proteger os participantes.

- O CEP deve ser informado de todos os efeitos adversos ou fatos relevantes que alterem o curso normal do estudo. É papel do pesquisador assegurar medidas imediatas adequadas frente a evento adverso grave ocorrido (mesmo que tenha sido em outro centro) e enviar notificação ao CEP e à Agência Nacional de Vigilância Sanitária – ANVISA – junto com seu posicionamento.

Endereço: Rua Tessália Vieira de Camargo, 126
Bairro: Barão Geraldo **CEP:** 13.083-887
UF: SP **Município:** CAMPINAS
Telefone: (19)3521-8936 **Fax:** (19)3521-7187 **E-mail:** cep@fcm.unicamp.br

COMITÊ DE ÉTICA EM PESQUISA DA UNICAMP - CAMPUS CAMPINAS

Continuação do Parecer: 1.556.084

- Eventuais modificações ou emendas ao protocolo devem ser apresentadas ao CEP de forma clara e sucinta, identificando a parte do protocolo a ser modificada e suas justificativas e aguardando a aprovação do CEP para continuidade da pesquisa. Em caso de projetos do Grupo I ou II apresentados anteriormente à ANVISA, o pesquisador ou patrocinador deve enviá-las também à mesma, junto com o parecer aprovatório do CEP, para serem juntadas ao protocolo inicial.

- Relatórios parciais e final devem ser apresentados ao CEP, inicialmente seis meses após a data deste parecer de aprovação e ao término do estudo.

-Lembramos que segundo a Resolução 466/2012 , item XI.2 letra e, "cabe ao pesquisador apresentar dados solicitados pelo CEP ou pela CONEP a qualquer momento".

Este parecer foi elaborado baseado nos documentos abaixo relacionados:

Tipo Documento	Arquivo	Postagem	Autor	Situação
Envio de Relatório Parcial	Relatorio_4.pdf	09/04/2016 11:00:59	Rodrigo Mologni Gonçalves dos Santos	Aceito

Situação do Parecer:
Aprovado

Necessita Apreciação da CONEP:
Não

CAMPINAS, 23 de Maio de 2016

Assinado por:
Renata Maria dos Santos Celeghini
(Coordenador)

Endereço: Rua Tessália Vieira de Camargo, 126
Bairro: Barão Geraldo **CEP:** 13.083-887
UF: SP **Município:** CAMPINAS
Telefone: (19)3521-8936 **Fax:** (19)3521-7187 **E-mail:** cep@fcm.unicamp.br

B.6 Parecer 6

Notificação 5 – Relatório Parcial

Cópia do parecer consubstanciado do CEP referente ao relatório parcial de acompanhamento do projeto de pesquisa submetido para análise em 16 de outubro de 2016.

15 de dezembro de 2016

UNICAMP - FACULDADE DE CIÊNCIAS MÉDICAS DA UNIVERSIDADE DE CAMPINAS

PARECER CONSUBSTANCIADO DO CEP

DADOS DO PROJETO DE PESQUISA

Título da Pesquisa: Automatização de Planos de Tratamento em Cirurgia Ortognática e Aprimoramento de Análise Cefalométrica em 3D

Pesquisador: Rodrigo Mologni Gonçalves dos Santos

Área Temática:

Versão: 1

CAAE: 27917314.0.0000.5404

Instituição Proponente: Faculdade de Engenharia Elétrica e de Computação

Patrocinador Principal: Financiamento Próprio

DADOS DA NOTIFICAÇÃO

Tipo de Notificação: Envio de Relatório Parcial

Detalhe:

Justificativa:

Data do Envio: 16/10/2016

Situação da Notificação: Parecer Consubstanciado Emitido

DADOS DO PARECER

Número do Parecer: 1.868.831

Apresentação da Notificação:

Apresentação do relatório parcial do referido estudo.

Objetivo da Notificação:

Apresentação do relatório parcial do referido estudo.

Avaliação dos Riscos e Benefícios:

Mantidos em relação ao projeto original.

Comentários e Considerações sobre a Notificação:

Segundo informações contempladas no relatório parcial: "a parte prática do projeto foi concluída. Não alteramos seu "status", pois as publicações ainda estão em fase de desenvolvimento. Faremos isto após a conclusão definitiva da pesquisa."

Endereço: Rua Tessália Vieira de Camargo, 126
Bairro: Barão Geraldo **CEP:** 13.083-887
UF: SP **Município:** CAMPINAS
Telefone: (19)3521-8936 **Fax:** (19)3521-7187 **E-mail:** cep@fcm.unicamp.br

UNICAMP - FACULDADE DE CIÊNCIAS MÉDICAS DA UNIVERSIDADE DE CAMPINAS

Continuação do Parecer: 1.868.831

Considerações sobre os Termos de apresentação obrigatória:

Para avaliação desta notificação foi analisado o relatório parcial anexado no documento intitulado "Relatorio_5.pdf 16/10/2016 10:23:32 ".

Conclusões ou Pendências e Lista de Inadequações:

O Relatório de acompanhamento da pesquisa informa que a pesquisa está em andamento com previsão de conclusão para 23/10/2015. Esclarecemos que o relatório de acompanhamento visa acompanhar a situação da pesquisa em relação ao participante (participantes incluídos, excluídos e os motivos, intercorrências, etc...). Portanto, se a coleta de dados já foi finalizada e os dados avaliados, o pesquisador deverá encaminhar ao CEP o relatório final da pesquisa e as futuras publicações poderão ser encaminhadas através de notificações.

Considerações Finais a critério do CEP:

Este parecer foi elaborado baseado nos documentos abaixo relacionados:

Tipo Documento	Arquivo	Postagem	Autor	Situação
Envio de Relatório Parcial	Relatorio_5.pdf	16/10/2016 10:23:32	Rodrigo Mologni Gonçalves dos Santos	Aceito

Situação do Parecer:

Não Aprovado

Necessita Apreciação da CONEP:

Não

CAMPINAS, 15 de Dezembro de 2016

Assinado por:
Renata Maria dos Santos Celeghini
(Coordenador)

Endereço: Rua Tessália Vieira de Camargo, 126
Bairro: Barão Geraldo **CEP:** 13.083-887
UF: SP **Município:** CAMPINAS
Telefone: (19)3521-8936 **Fax:** (19)3521-7187 **E-mail:** cep@fcm.unicamp.br

B.7 Parecer 7

Notificação 6 – Relatório Parcial

Cópia do parecer consubstanciado do CEP referente ao relatório parcial de acompanhamento do projeto de pesquisa submetido para análise em 21 de abril de 2017.

18 de maio de 2017

UNICAMP - CAMPUS CAMPINAS

PARECER CONSUBSTANCIADO DO CEP

DADOS DO PROJETO DE PESQUISA

Título da Pesquisa: Automatização de Planos de Tratamento em Cirurgia Ortognática e Aprimoramento de Análise Cefalométrica em 3D

Pesquisador: Rodrigo Mologni Gonçalves dos Santos

Área Temática:

Versão: 1

CAAE: 27917314.0.0000.5404

Instituição Proponente: Faculdade de Engenharia Elétrica e de Computação

Patrocinador Principal: Financiamento Próprio

DADOS DA NOTIFICAÇÃO

Tipo de Notificação: Envio de Relatório Parcial

Detalhe:

Justificativa:

Data do Envio: 21/04/2017

Situação da Notificação: Parecer Consubstanciado Emitido

DADOS DO PARECER

Número do Parecer: 2.070.367

Apresentação da Notificação:

Apresentação de relatório parcial de pesquisa.

Objetivo da Notificação:

Apresentação de relatório parcial de pesquisa.

Avaliação dos Riscos e Benefícios:

--

Comentários e Considerações sobre a Notificação:

No formulário consta a previsão de conclusão da pesquisa 23/10/2015 e, segundo o pesquisador: "A parte prática do projeto está concluída há tempos. Estou mantendo o status do projeto como “em andamento”, pois tenho artigos e uma tese em fase de elaboração. Darei o projeto por

Endereço: Rua Tessália Vieira de Camargo, 126
Bairro: Barão Geraldo **CEP:** 13.083-887
UF: SP **Município:** CAMPINAS
Telefone: (19)3521-8936 **Fax:** (19)3521-7187 **E-mail:** cep@fcm.unicamp.br

UNICAMP - CAMPUS CAMPINAS

Continuação do Parecer: 2.070.367

encerrado somente após a submissão de todos os artigos e a defesa de minha tese." A pesquisa inclui 86 participantes.

Considerações sobre os Termos de apresentação obrigatória:

Foi anexado o formulário no modelo preconizado pelo CEP.

Recomendações:

Vide abaixo.

Conclusões ou Pendências e Lista de Inadequações:

O pesquisador deverá providenciar:

1) Alterar a data de previsão de conclusão para quando a pesquisa estiver finalizada.

Este parecer foi elaborado baseado nos documentos abaixo relacionados:

Tipo Documento	Arquivo	Postagem	Autor	Situação
Envio de Relatório Parcial	Relatorio_6.pdf	21/04/2017 18:48:40	Rodrigo Mologni Gonçalves dos Santos	Aceito

Situação do Parecer:

Não Aprovado

Necessita Apreciação da CONEP:

Não

CAMPINAS, 18 de Maio de 2017

Assinado por:
Renata Maria dos Santos Celeghini
(Coordenador)

Endereço: Rua Tessália Vieira de Camargo, 126
Bairro: Barão Geraldo **CEP:** 13.083-887
UF: SP **Município:** CAMPINAS
Telefone: (19)3521-8936 **Fax:** (19)3521-7187 **E-mail:** cep@fcm.unicamp.br

B.8 Parecer 8

Notificação 7 – Relatório Final

Cópia do parecer consubstanciado do CEP referente ao relatório final de acompanhamento do projeto de pesquisa submetido para análise em 18 de maio de 2017.

11 de julho de 2017

UNICAMP - CAMPUS CAMPINAS

PARECER CONSUBSTANCIADO DO CEP

DADOS DO PROJETO DE PESQUISA

Título da Pesquisa: Automatização de Planos de Tratamento em Cirurgia Ortognática e Aprimoramento de Análise Cefalométrica em 3D

Pesquisador: Rodrigo Mologni Gonçalves dos Santos

Área Temática:

Versão: 1

CAAE: 27917314.0.0000.5404

Instituição Proponente: Faculdade de Engenharia Elétrica e de Computação

Patrocinador Principal: Financiamento Próprio

DADOS DA NOTIFICAÇÃO

Tipo de Notificação: Envio de Relatório Final

Detalhe:

Justificativa:

Data do Envio: 18/05/2017

Situação da Notificação: Parecer Consubstanciado Emitido

DADOS DO PARECER

Número do Parecer: 2.168.141

Apresentação da Notificação:

Apresentação do relatório final do referido estudo.

Objetivo da Notificação:

Apresentação do relatório final do referido estudo.

Avaliação dos Riscos e Benefícios:

Mantidos em relação ao projeto original.

Comentários e Considerações sobre a Notificação:

Segundo informações contempladas no relatório final, a pesquisa foi concluída em 23/10/2015, foram incluídos 86 participantes de pesquisa, não houve intercorrências com o participante de pesquisa. Os resultados foram publicados:

Endereço: Rua Tessália Vieira de Camargo, 126
Bairro: Barão Geraldo **CEP:** 13.083-887
UF: SP **Município:** CAMPINAS
Telefone: (19)3521-8936 **Fax:** (19)3521-7187 **E-mail:** cep@fcm.unicamp.br

UNICAMP - CAMPUS CAMPINAS

Continuação do Parecer: 2.168.141

Artigos completos aceitos para publicação em periódicos especializados internacionais:

• SANTOS, R. M. G.; DE MARTINO, J. M.; HAITER NETO, F.; PASSERI, L. A. Influence of different setups of the Frankfort horizontal plane on 3-dimensional cephalometric measurements. American Journal of Orthodontics and Dentofacial Orthopedics, [s.l.], v. , n. , p. -, 2017. http://dx.doi.org/10.1016/j.ajodo.2016.12.023.

Artigos completos submetidos para publicação em periódicos especializados internacionais:

• SANTOS, R. M. G.; DE MARTINO, J. M.; HAITER NETO, F.; PASSERI, L. A. CBCT-based cephalometric norms for Brazilian adults. International Journal of Oral and Maxillofacial Surgery, [s.l.], v. , n. , p. -, .

• SANTOS, R. M. G.; DE MARTINO, J. M.; HAITER NETO, F.; PASSERI, L. A. CBCT-based 3D McNamara's cephalometric analysis. Journal of Craniofacial Surgery, [s.l.], v. , n. , p. -, .

• SANTOS, R. M. G.; DE MARTINO, J. M.; PASSERI, L. A.; ATTUX, R. R. F.; HAITER NETO, F. Automatic repositioning of jaw segments for three-dimensional virtual treatment planning of orthognathic surgery. Journal of Cranio-Maxillo-Facial Surgery, [s.l.], v. , n. , p. -, .

Pedidos de patente depositados no Instituto Nacional da Propriedade Industrial:

• UNICAMP. De Martino, J. M.; Santos, R. M. G.; Passeri, L. A. Método para reposicionamento automático de segmentos ósseos maxilares em planejamento virtual tridimensional. BR-10-2017-004146-8. 2 mar. 2017.

Participação em congressos especializados nacionais:

• SANTOS, R. M. G.; DE MARTINO, J. M.; PASSERI, L. A.; HAITER NETO, F. Automatização do reposicionamento de segmentos ósseos maxilares para planejamento virtual em três dimensões de cirurgia ortognática. In: SEMANA DE PESQUISA DA FCM, 9., 2016, Campinas.

Considerações sobre os Termos de apresentação obrigatória:

Para avaliação desta notificação foi analisado o relatório final anexado no documento intitulado "Relatorio_7.pdf 18/05/2017 15:02:20".

Conclusões ou Pendências e Lista de Inadequações:

Relatório final do estudo aprovado.

Considerações Finais a critério do CEP:

Endereço: Rua Tessália Vieira de Camargo, 126
Bairro: Barão Geraldo **CEP:** 13.083-887
UF: SP **Município:** CAMPINAS
Telefone: (19)3521-8936 **Fax:** (19)3521-7187 **E-mail:** cep@fcm.unicamp.br

UNICAMP - CAMPUS CAMPINAS

Continuação do Parecer: 2.168.141

Este parecer foi elaborado baseado nos documentos abaixo relacionados:

Tipo Documento	Arquivo	Postagem	Autor	Situação
Envio de Relatório Final	Relatorio_7.pdf	18/05/2017 15:02:20	Rodrigo Mologni Gonçalves dos Santos	Aceito

Situação do Parecer:
Aprovado

Necessita Apreciação da CONEP:
Não

CAMPINAS, 11 de Julho de 2017

Assinado por:
Renata Maria dos Santos Celeghini
(Coordenador)

Endereço: Rua Tessália Vieira de Camargo, 126
Bairro: Barão Geraldo **CEP:** 13.083-887
UF: SP **Município:** CAMPINAS
Telefone: (19)3521-8936 **Fax:** (19)3521-7187 **E-mail:** cep@fcm.unicamp.br